LOW-PROFILE POLYMER ACTUATOR FABRICATION FOR SPASTIC HAND EXOSKELETONS

Sanaz Bahrami

Thesis submitted in partial fulfillment of the requirements for the

MASTER OF APPLIED SCIENCE

Degree in Biomedical Engineering

Ottawa-Carleton Institute for Mechanical and Aerospace Engineering
Faculty of Engineering
University of Ottawa

Abstract

Spasticity is a neurological impairment that presents itself in the form of a continuous muscle contraction, with the key motor deficit being impaired hand function. Hand exoskeleton technologies play a vital role in the therapeutic rehabilitation of this condition. The optimal design of these devices is currently a challenge due to the limited availability of actuation devices that are light weight, portable, and aesthetically pleasing. Natural muscles have many favourable characteristics, such as their high power-to-weight ratio, efficient energy conversion, and fast actuation times. Unfortunately, traditional systems such as pneumatics muscles and electromagnetic motors have yet to attain similar properties. These traditional actuators exhibit hysteretic performance, high manufacturing cost, low stroke, and limited cycle life. In recent years a new category of actuators has been developed from highly twisted and coiled low-cost nylon fibres such as fishing line and conductive sewing thread. These muscles produce a high specific work per cycle with a reversible contraction. This thesis develops and tests these twisted and coiled polymer (TCP) actuators using various nylon and polyethylene polymers in order to establish a foundation for their implementation as a novel actuation device in a spastic hand exoskeleton. An initial comprehensive experimental evaluation of several nylon fibres is completed by attempting to reproduce the work of previous researchers. Subsequently, the information obtained is taken and adapted to the development of UHMWPE TCPs and other types of nylon monofilament. This thesis characterizes the contractility and force output of these novel actuation devices.

Acknowledgments

This Master's thesis is the product of a very difficult and eye opening journey that taught me not only engineering skills, but life skills that will be remembered eternally. It would not have been possible without the love and support of few very special individuals.

Primarily, I would like to take a moment to express my sincerest gratitude to my supervising professor, Patrick Dumond, for being patient with me, always being there when I needed him, and providing me with endless knowledge and support. Without you I would not have been able to achieve my goals and reach this stage, and for that I will always be grateful.

I would also like to thank the Faculty of Mechanical and Biomedical Engineering at the University of Ottawa for taking a chance on me and allowing me to progress in my higher education. I would especially like to thank the guys in the machine shop for always offering a helping hand whenever I was in need. Particularly, I'd like to express my appreciation to Leo Denner and Paul Burberry for the countless times I ran down to the shop whining to you for help.

I would like to thank my amazing family, my mom, dad, and two beautiful sisters for your constant support throughout this challenging process. Without the emotional, financial, and physical support that you have provided, I would not have been able to achieve my goals. Thank you for always believing in me, even when I did not.

And finally, I would like to thank all my awesome office mates, lab mates, and members of my research team for always providing support and humour to enlighten my journey. Without the connection I built with all of you throughout my years in Ottawa this experience would have been much less enjoyable. Thank you for playing a vital role in the progression of my education.

Table of Contents

List of Figures

List of Tables

Chapter 1

Introduction

Spasticity is a neurological impairment which is commonly associated with upper motor neuron (UMN) syndrome. This condition is one of several sensory-motor disorders whose symptoms may be present following an upper motor neuron lesion such as a stroke [1]. Clinical characteristics of the spastic state can be described as a motor disorder which causes an exaggeration of the stretch reflex in the form of continuous muscle contractions as seen in spastic hand syndrome [2]. For operational purposes Lance has come up with the most commonly used definition of spasticity, where he describes it as a *"motor disorder characterized by a velocity dependent increase in the tonic stretch reflex (muscle tone) with exaggerated tendon jerks, resulting from hyper excitability of the stretch reflex, as one component of the upper motor neurone syndrome"* [3]. The disorder presents itself in the form of a continuous muscle contraction, where the hand is stuck in a constant flexed state as seen in Figure 1-1 [1]. Spasticity can be seen in conditions such as stroke, multiple sclerosis (MS), cerebral palsy (CP), and other traumatic brain injuries, as well as other not so common conditions such as meningitis, encephalitis, and adrenoleukosytrophy [4].

Since spasticity in the hand is one of the leading syndromes resulting from stroke and MS, hand exoskeleton technologies play an important role in patient rehabilitation. Although assistive

engineering has been around for years, it has yet to satisfy the specific needs of hand exoskeletons used in the rehabilitation of spastic hand syndrome due to the inherent sensory and motor requirements involved. In fact, none have excelled in rehabilitation or therapeutic environments [5].

Figure 1-1 Patient right hand diagnosed with Spastic Hand Syndrome [5]

The main limitation of currently used therapeutic exoskeletons is their large size and weight typically attributed to their actuation devices and associated mechanisms. Most devices are currently powered by electric motors and hydraulic or pneumatic cylinders. These assistive devices can greatly increase human motion, but they are typically large, heavy, and bulky systems that are often tethered to bulky external devices. This has led researchers to search for novel actuation mechanisms suitable for assistive rehabilitation devices. One such novel alternative actuator, first demonstrated by Haines et al. in 2014, is made of inexpensive polymer fibres such as nylon 6 monofilament or braided polyethylene fishing line, which when twisted and coiled, are capable of hysteresis free thermal contraction [6].

The scope of this thesis is intended to identify important parameters and values and determine procedures which could help in the fabrication of consistent thermo-responsive actuators which could be use in spastic hand exoskeletons, by twisting and coiling fibres embedded with an electrical heating element, thereby building on the work introduced by Haines et al.

1.1 Motivation

Hand injuries as a result of stroke and MS are very common and debilitating conditions that directly affect a patients' quality of life. Patients that experience such injuries are traditionally rehabilitated with the help of occupational and physical therapists, which can be time consuming and costly. In an attempt to create a more patient-friendly method of rehabilitation to regain motor function in the upper limbs, this study considers the direct consumer needs related to the actuation of spastic hand rehabilitation exoskeletons and uses these parameters as best as possible to help improve such actuators.

A thorough interview was conducted with a patient suffering from spasticity in her right hand, alongside her occupational therapist. To address all the patient's needs, the patient and her therapist were asked to indicate on a scale of 1-5 (one being the most important and five being the least) the importance of critical exoskeleton parameters. Based on this feedback from direct patient and occupational therapist interviews, the flow chart shown in Figure 1-2 demonstrates the most important design parameters for a functional spastic hand exoskeleton.

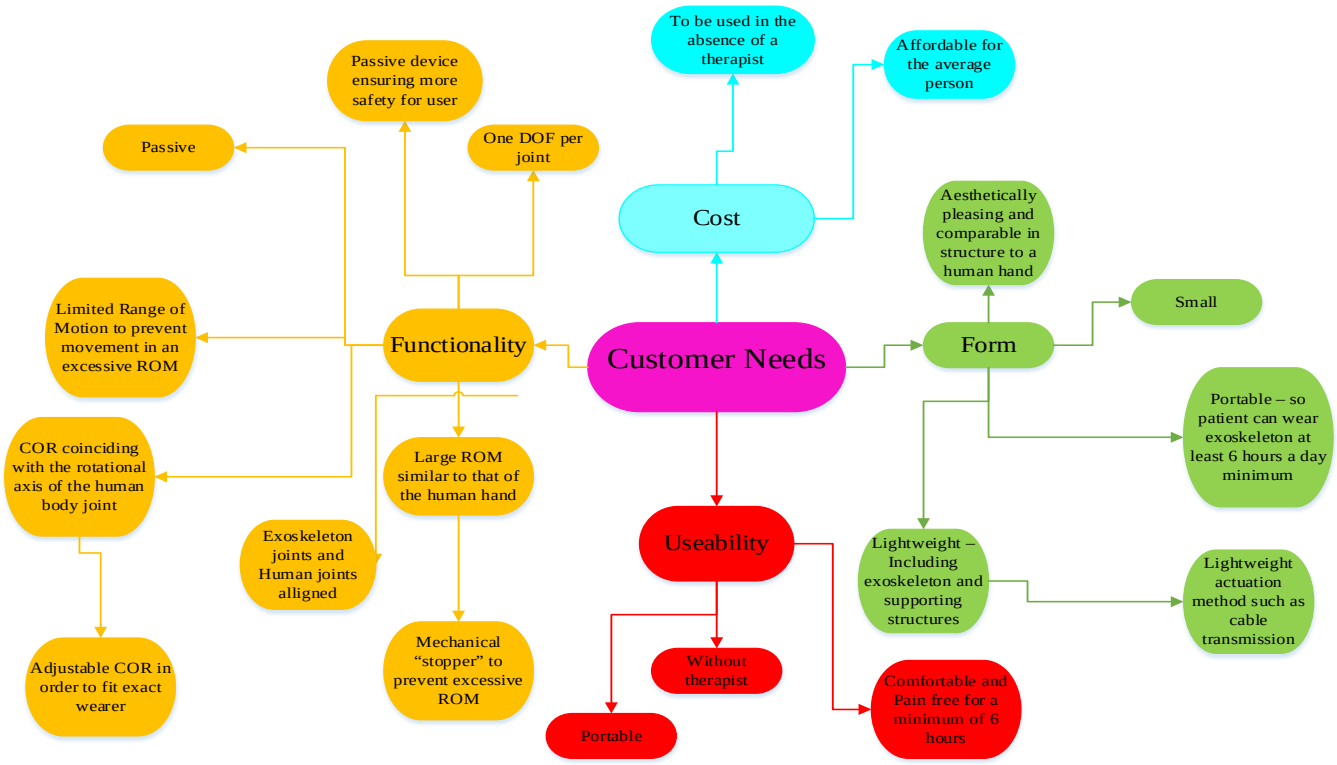

Figure 1-2 Customer needs exoskeleton flow chart

As demonstrated in Figure 1-2, usability, cost, form, and functionality are the main aspects to consider when designing an exoskeleton of this nature. The next step in the design process is to rate the significance of each characteristic within each category and in order to determine which need is the most important based on consumer feedback. From this information, a needs chart is made. This places patients' needs in chronological order based on importance (with 1 being the most important, and 5 being the least important). As shown in Table 1-1, aside from the basic necessary functional components that a good exoskeleton must possess (which were typically associated with a score of 1), the next most important needs are all related to the ergonomics, weight, comfort and aesthetics of the device which are factors that are often overlooked and which are directly affected by the exoskeleton's actuator(s). In particular, the patient emphasized a need for a lightweight, low profile, and aesthetically pleasing exoskeleton. To design a device that can

satisfy all the needs identified in Table 1-1, a literature survey is conducted to characterize the target metrics of each need. This is to ensure that a range of metrics for each need is realistic and suitable for a given exoskeleton design.

Table 1-1 Exoskeleton Needs Table

#	*Exoskeleton Need*	*Imp*
1.	Is lightweight/ low-profile	1
2.	Is aesthetically pleasing and comparable to a human hand	2
3.	Can be comfortably worn for 6 hours	2
4.	Is portable	2
5.	Is affordable for an average person	3
6.	Can be worn in the absence of a therapist	2
7.	Is adjustable with the use of the non-paretic hand	3
8.	Is aligned with the coinciding human joints	1
9.	Is actuated	1
10.	Has at least one DOF per joint for finger extension	1
11.	Has a COR that coincides with the rotational axis of the human body	2
12.	Embodies a stop which prevents motion in an excessive ROM	4
13.	Is adjustable in order to match COR with that of the patient	5
14.	Has a long service life comparable to other devices	5
15.	Is able to overcome spastic hand force in order to extend fingers and thumb	1
16.	Takes less than 2 minutes to attach to the body	3

In Table 1-2, the needs are all characterized by their units of measure. These numbers are very important during design and prototyping. They ensure that all design parameters fit within a realistic range of exoskeleton features. Table 1-2 shows the marginal range for the target metrics, as well as the ideal values of all needs. These values were derived from an extensive literature review and a thorough understanding of previous designs, anthropometric data, as well as user

feedback. With the help of these numbers, as well as previous exoskeleton research, improvements to the design of these exoskeletons, and specifically to their actuators, can now be considered.

Table 1-2 Marginal and Ideal Values of Exoskeleton Parameters

	Metric	*Units*	*Marginal Value*	*Ideal Value*
1.	Minimum continuous force in the tendons of a spastic hand to extend fingers and thumb	N	55±14.7 [7]	40 [7]
2.	Spastic torque in paretic hand	Nm	0.65-0.75 [8]	>0.75 [8]
3.	Total mass of device without actuator (just glove)	kg	<0.5 [9]	0.23 [10]
4.	Total mass of device with actuator	kg	<3 [9]	<1 [9]
5.	Mean finger length (middle finger)	cm	7.82-9.74 [11]	8.57 [11]
6.	CMC range of motion (wrist)	deg	53-67 [10]	60[10]
7.	MCP range of motion (wrist)	deg	53-67 [10]	60 [10]
8.	Maximum displacement of middle finger extension	cm	12 − 13.5 [11]	13 [11]
9.	Aesthetically pleasing	Subj.	1-5	1
10.	Controlled release maximum	cm/s		
11.	Extension velocity maximum	cm/s		
12.	Manufacturing cost	US $	<500 [12]	<250[12]
11.	Comfort level	Subj.	1-5	1
12.	Service Life expectancy	cycles		
13.	Number of parts per finger	#	6	3
14.	Size of entire device (volume)	cm^3	<500	<75
15.	Mean hand breadth	cm	6.5-9.8 [11]	8.96 [11]
16.	Mean hand length	cm	16.9-22.9 [11]	18.07 [11]
17.	Duration of wear	mins	≈240-360	>360
18.	Time to strap into device	mins	<2 [13]	≈1
19.	Degrees of freedom/finger joint	#	1-3	3

The marginal and ideal values from the “Minimum continuous force in the tendons of a spastic hand to extend fingers and thumb” found in the first row of Table 1-2 come from research on tendon extension force in adult patients who suffer from spasticity post stroke. Another important metric value is the spasticity torque in the paretic hand. This was quantified by examining the magnitude of the velocity dependant torque and used to specify torque requirements for the exoskeleton [8]. Moreover, a practical consideration to keep in mind during the design phase is the mass of the device with and without its actuation device. In order to meet customer needs and make the device low profile and lightweight, it must not exceed 0.5kg, while separated from its actuation device [9]. Research also indicates that the device’s power mechanism should weigh no more than the weight of a typical portable consumer electronic product, which can be estimated at 3kg [10]. All anthropometric data regarding hand dimensions were derived from a compiled literature review of hand kinematics and dynamics for exoskeleton design [11]. Furthermore, the human hand is capable of 4 degrees of freedom for each finger. Three of these are the flexion/extension degree of freedom in each joint, with the fourth being the abduction, adduction motion. In order to mimic the extension motion of the finger identically, it would be ideal for improvements to allow for three degrees of freedom. This is because the goal of this work is to extend the fingers of a spastic hand. Extension in each knuckle provides three degrees of freedom whereas the fourth is the abduction/adduction motion which is unnecessary for this application.

Since the actuation device plays an important role in satisfying many of the important needs described above, the remainder of this thesis will focus on improving the actuation device for these therapeutic exoskeletons. In particular, suitable actuators have the potential to significantly

improve the exoskeleton's cost, mass, size, portability and look if innovative solutions are considered.

1.2 Objectives

The main objective of this thesis is to expand on the work by Haines et al. in order to verify the feasibility of using twisted and coiled polymer (TCP) actuators as the sole actuation mechanism in therapeutic spastic hand exoskeletons. While Haines et al. provided the groundwork for this research, TCP actuator fabrication parameters remain unclear. In particular, their work demonstrated that:

- Polymers are capable of reversible thermal fibre contraction
- Coiled fibres have a much higher reversible thermal contraction compared to uncoiled fibres (nylon went from 4% → 34% thermal contraction and polyethylene went from 0.3% → 16% thermal contraction as a result of coiling)
- Tighter coils had smaller max stroke, but produced more contraction force
- Wider coils produced larger stroke at the expense of contraction force
- Work done during contraction increases up to loads that cause the actuator to break
- Maximum force of contraction obtained for a 4lb fishing line was 0.44N

This work first aims use the work of Haines et al. as a baseline for experimentally characterizing the fabrication parameters of successful TCP actuators, such as fibre type, fibre length, load weight and heating method. Once fabrication parameters are clearly set out and capable of reproducing consistent actuators, the aim will then be to study the contractile capabilities of all fibres (nylon 6, nylon 6,6, and polyethylene) that exhibit favorable coiling and twisting traits.

1.3 Methodology

In order to accomplish the goals set out above, a thorough understanding of TCP fabrication parameters is necessary. Firstly, various nylon and polyethylene fibres are cut, twisted, coiled, and heated by way of Joule heating in order to characterize their performance as linear actuators using a range of parameters for each phase of the fabrication and activation processes. Secondly, fibres that demonstrate favorable contractile/heating characteristics without failing are chosen for further testing (contractile and force) using an Instron Universal Test Machine.

1.4 Contribution

This thesis provides a thorough experimental evaluation of TCP actuator development beginning with the precursor fibres (linear fibres prior to twist and coil insertion) and providing a detailed description of their fabrication process. Although there has been previous research on the use of low-cost polymers used in TCP actuators, this thesis is the first to provide a comprehensive outline of the direct fabrication parameters and the basic principles for successful implementation. The thermal and contractile responses were studied to provide a better understanding of which low-cost polymers were capable of providing the largest hysteresis free contraction at peak force without demonstrating signs of failure. These tests illustrate the potential of TCPs as actuation devices to power a hand exoskeleton. The specific unique contributions of this thesis include:

- Providing detailed TCP fabrication procedures.
- Determining ways to increase the force output of low-cost polymer actuators.
- Determining ways of increasing contraction to maximize linear displacement.
- Determining ways of controlling the heating/activation of various polymer actuators.

- Looking at ways of limiting creep in ultra-high molecular weight polyethylene (UHMWPE) fibres.
- Enhancing portability of polymer actuator powered devices.

1.5 Thesis Outline

Chapter 2 presents a literature review subdivided into two parts. This chapter begins by providing background on current commercially used actuation devices, as well as novel twisted and coiled polymer actuators which represent a class of smart materials. This chapter then gives a detailed review of current upper limb, hand exoskeletons and the advantages and limitations of their associated actuation devices. Chapter 3 goes on to demonstrate the characterization of TCP actuators. The chapter begins by attempting to mimic the work done by previous research to validate their results and describe their processes. The TCP fabrication process is then modified to enhance force and maximize linear displacement through contraction. This is done by testing numerous polymers such as braided polyethylene, as well as nylon monofilament to illustrate these polymers' contractile response in the presence of heat. These actuators are then subjected to a series of force tests performed on an Instron Universal Testing Machine to better understand their mechanical capabilities. Chapter 4 describes the results of TCP testing and discusses the advantages and limitations of the various fibres that are tested. Chapter 5 presents the conclusions of this work and suggestions for future work, including changes to the experimental method, and consideration for future TCP fabrication procedures.

Chapter 2

Exoskeleton Actuator Technologies

2.1 Actuator Technologies Currently Used in Upper Limb Exoskeletons

There are numerous actuator technologies currently commercially available to power exoskeletons. The most conventionally used technologies for upper limb exoskeletons can be divided into three main groups: electrical/electrochemical actuators, pneumatic muscle actuators, and hydraulic actuators.

Electrical actuation devices are the most common actuators seen in today's devices. They can be in the form of stepper motors, permanent-magnet DC motors, brushless motors or solenoids [14]. These actuators require small power supplies, and can transmit energy easily from the supply to the device in the form of flexible wires. The major limitation that hinders their use in exoskeleton devices is the small torque or limited linear displacement they are capable of generating relative to their size and weight [15].

Compliant pneumatic muscle actuators (PMA) have recently been favoured in robot-based rehabilitation systems and assistive engineering applications [16]. PMAs are soft and exhibit many physical properties similar to human muscles, making them a more natural option for actuation of robotic rehabilitation systems [15]. These actuators have many benefits such as their low-cost,

lightweight, and compliance, as well as their high power-weight, and power-volume ratios [8],[15]. Therefore, in comparison to their electrical and hydraulic actuator counterparts, PMAs are much safer, more natural, and user friendly. However, the main drawback of these actuation systems is the fact that they can “only be operated in the contractile direction and therefore must be used in antagonistic pairs in order to achieve bi-directional motion of a single joint” [16]. In order to achieve a flexion/extension motion that mimics a human MCP joint (amongst many other joint types), antagonistic pairs must be used, which increase the complexity of the mechanical design, bulkiness, weight and cost of the wearable robotic [16]. They also depend on their non-portable pressure supplies such as pumps or air compressors to pressurize fluids. These systems are often bulky, heavy, and noisy.

Hydraulic actuators are also used on exoskeletons. However, they are more commonly used in lower limb exoskeletons. Hydraulic transmission is beneficial because it can support high specific power and force. These systems are silent, precise, and unaffected by dusty and/or wet environments. They are capable of smooth actuation with no exposed moving components capable of generating both linear and rotary motion. These devices have similar limitations to that of pneumatic muscles due to their need for large and noisy non-portable pressure supplies [17]. A brief summary of the advantages and limitations of these actuator technologies is given in Table 2-1.

Table 2-1 Summary of Advantages and Limitations of Current Actuator Technologies [13]–[15]

Actuator Technology	*Advantages*	*Limitations*
Electric Motors	-high specific power -easily controlled -fast operation	-need for transmission elements -relatively unsafe -noisy -heavy/bulky -low torque to weight ratio
Pneumatic Muscles	- high specific power -flexible and soft -high specific force -inherently compliant -low-cost -low mass	-not capable of bidirectional motion -non-linear actuation -large and noisy air compressor -less accurate motion
Hydraulic Cylinders	- compact -high specific power -lightweight -wide control bandwidth -high force output	-non-portable pressure supplies -pressure supplies bulky, heavy, and non-portable -large amounts of power lost in pressure drops across hydraulic valves

The limitations of conventional actuators mentioned above have resulted in a push towards the development of alternative actuation devices in the field of mechatronics, robotics, and biomedical engineering. Particularly in the field of therapeutic exoskeletons, an alternative mechanism capable of providing a high power-weight ratio, hysteresis free actuation, and lightweight portability is required.

The newest arrivals in actuation devices are commonly referred to as “smart materials” or “shape memory materials”. Their growing popularity can be attributed to their relative simplicity. Shape memory materials (SMM) are materials that can significantly alter their mechanical properties (such as shape, stiffness, and viscosity), or their thermal, optical, or electromagnetic properties in a controlled manner in the presence of an external stimuli. They can be stimulated by heat (thermo-responsive), stress/pressure (mechano-responsive), electrical current/voltage (electro-responsive),

magnetic field (magneto-responsive), pH change, solvent or moisture (chemo-responsive), or light (photo-responsive) [20]. These materials are favorable as actuators because they are lightweight, low-cost, have a large range of operating temperatures, low power consumption, and are capable of high active stresses [21], [22].

SMMs can adapt to the surrounding environment, regulate the transport of ions and molecules or convert (bio)chemical signals into optical, electrical, thermal and mechanical signals, and vice versa [23]. This makes them extremely effective in (biomedical) applications such as drug delivery, medical diagnostics and imaging, tissue engineering and biosensing. “Smart” materials that are of special interest are the ones that can undergo conformational or chemical changes in response to variations in temperature. For this research, only thermo-responsive SMMs will be discussed in further detail [23].

Amongst the several applicable stimuli, temperature is the most typically exploited in the field of actuators used in engineering applications, meaning in the presence of a heat stimulus they are capable of recovering their initial shape after being severely or quasi-plastically distorted [24]. Thermo-responsive technologies most commonly used as actuators in biomedical applications are shape memory alloys, shape memory polymers, and a new emerging class of thermo-responsive highly twisted carbon nanotubes (CNT).

Shape memory alloys (SMA) are alloys that have the ability to return to their original state in the presence of a heat stimulus [25]. Only those that exhibit fully reversible crystal transformations are of interest based on their ability to recover from large strains. They are comprised of two major

types, copper-based (Cu), and nickel-titanium-based (NiTi). NiTi based SMAs are the most suitable for actuation applications based on their stability, biocompatibility, and practicality compared to other alloys. They can either be one way or two way alloys meaning they are either capable of returning to their original shape or remembering two different shapes (one at low temperatures and one at high temperatures). These actuators are able to hold a maximum reversible strain of 8% without demonstrating any permanent damage making them appealing in the field of biomimetics and engineering [23]. Their major limitation is their high manufacturing cost and processing requirements. These alloys cost approximately $3,600/kg and exhibit a large hysteresis loop in their stress-strain curve, making them hard to control [26].

Shape memory polymers (SMP) are polymeric materials that are able to transition from their deformed state (temporary shape) back to their original (permanent) shape under the influence of an external stimulus such as heat [27]. These polymers can retain two, and sometimes three shapes. SMPs are advantageous over SMAs in that they have lower densities, lower cost of raw material and fabrication, their strain recovery rate is an order higher than their counterparts, it is easier to tailor their thermo-mechanical properties, and they possess a larger shape recovery temperature range [24].

In 2011, a novel category of artificial muscles emerged, based on twisted fibres capable of torsional actuation [28]. Carbon Nanotube (CNT) yarn is the earliest demonstration of highly twisted artificial muscles. A year later, in 2012, CNT yarns showed tensile actuation capabilities when twisted to such a high extent that the fibre formed spontaneous coils [29]. These “coils mechanically behave like tight springs and can provide tensile contraction of ~7.3% when pristine

coiled CNT yarns are heated to incandescent temperatures in an inert environment" [29]. These yarns have so far been limited in their application as actuation mechanisms due to their high ($3,000/kg) material and manufacturing costs similar to that of SMAs [26].

More recently, there has been an emerging interest in the fabrication of twisted and coiled polymer (TCP) actuators as a novel thermal driven artificial muscle. Although further research is necessary in using TCPs as practical artificial muscles for biomimetic applications, they have already demonstrated admirable contractile qualities that require further investigation such as their low-cost in comparison to other currently available fibres ($5/kg) [26].

2.2 Introduction to Twisted and Coiled Polymer Actuators

Haines et al. introduced the possibility of using inexpensive high-strength polymer fibres as twisted and coiled polymer (TCP) linear actuation mechanisms in 2014 [6]. Their goal was to take low-cost polymers that cost only $5/kg such as nylon 6 4lb monofilament fishing line, nylon 6,6 sewing thread and braided polyethylene fishing line and convert them to hysteresis free actuators that mimic the performance of human muscles. Haines et al. found that low-cost polymer fibres were capable of reversible thermal fibre contraction. They also demonstrated that if precursor actuator fibres (fibres in their initial state prior to twist and coil insertion) are twisted past a certain threshold using a manufacturing method similar to that used for the fabrication of significantly more expensive carbon nanotube yarn actuators, fibres begin to spontaneously form coils, greatly increasing their capabilities for tensile stroke. The proposed procedure calls for a weight to be attached to one end of the fibre, while the other end is rotated using some form of powered

rotational device. The value of the attached weight was found to be crucial in order to keep the fibre taught. Specifically, their work states that the weight must be heavy enough to prevent the fibre from snarling, while not so heavy to overload the fibre, causing it to break. Once the formation of the coil was complete, a slightly heavier weight was attached to the TCP fibre to separate adjacent coils that were in contact in order to improve the contractile response.

Unfortunately, very little guidance was provided in choosing these weights. As an extra step, to prevent fibres from untwisting, fibres were thermally annealed or torque balanced (the weight is supported in such a way that it does not produce a torque) to maintain their new coiled configuration. Again, no mention of ideal temperatures or heating times is provided for the annealing process.

Since these TCP actuators are thermally activated, Haines et al. briefly describe their methods for hydrothermally and electrothermally activating the coiled fibres using heated water or by using an electrical heating element such as a CNT sheet to wrap the coiled fibre, using Shieldex conductive sewing thread, or by placing a conductor on the inside or outside of the actuator. Hydrothermal actuation occurred by switching between 25°C and 95°C water flowing through a silicon tube containing the coiled fibre and was only used for the polyethylene fibres [6]. Unfortunately, the practicality of heating fibres using water is overlooked and parameters for electrothermally heating fibres and the exact approach they used to include the heating element (other than the conductive sewing thread) remain undefined.

Once the coiled fibres were heated, results showed that nylon 6,6 muscles were capable of delivering over one million cycles during periodic actuation at 1 Hz, while pulling a 10g weight. Throughout the cycling process the TCP actuator did exhibit creep; however it was below 2%. Table 2-2 shows the contractile response of coiled versus uncoiled polymer fibres. The nylon 6,6 monofilament demonstrated an increase in contraction from 1% to 34% as a result of coiling and heating up to 240°C, whereas polyethylene, having a much lower melting temperature than nylon, was limited in its contractile response to 0.3% for the non-coiled fibre, and 16% for the coiled fibre at 130°C, as demonstrated in [6].

Table 2-2 Thermomechanical analysis of various polymers before and after coiling [6]

	Uncoiled			*Coiled*		
Temperature (°C)	20	130	240	20	130	240
Nylon 6	0%	0.7%	-	0%	12%	-
Nylon 6,6	0%	1%	4%	0%	9%	34%
Polyethylene	0%	0.3%	-	0%	16%	-

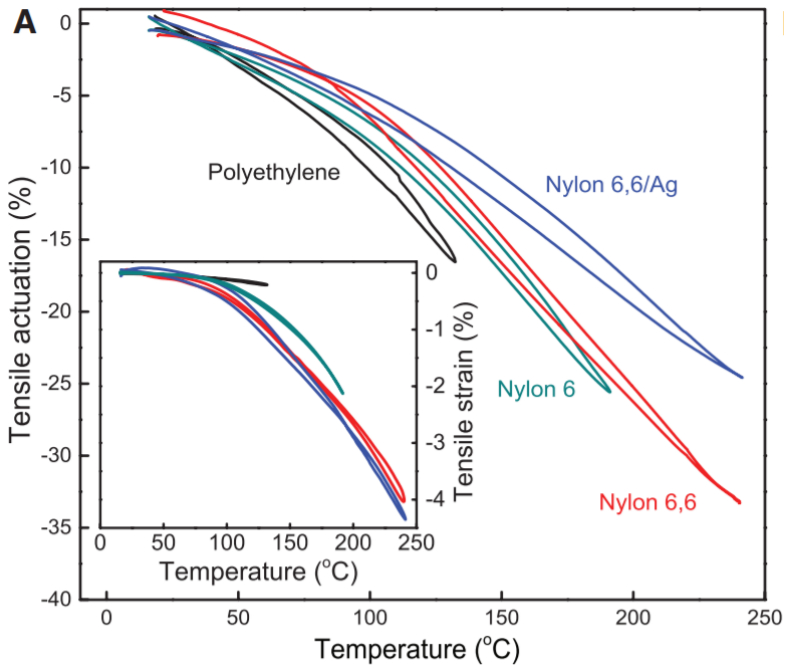

Figure 2-1 Comparison of the negative thermal expansion of braided polyethylene, nylon 6 monofilament, and nylon 6,6 monofilament before twisting (insert) and after coiling by twist insertion [3]

They also concluded that tighter coils had a smaller maximum stroke, thereby producing more force, whereas larger coils had a larger maximum stroke and a smaller force. They went on to indicate that the work done during contraction increases up to loads that cause the actuator to break or fail.

The higher modulus of elasticity and strength of polyethylene did however demonstrate the benefit of being able to lift heavier loads at increased energy efficiency. Unfortunately, the maximum stroke was found to be inversely proportional to the maximum load, due to the differences in coil configurations required for each. The maximum specific work during contraction for a nylon 6,6 actuator was found to be 2.48 kJ/kg compared to 2.63 kJ/kg for polyethylene. This is 64 and 100 times greater than that of mammalian skeletal muscles respectfully. The maximum contractile force obtained from their work for a loaded actuator (127 µm diameter nylon 6,6 4lb monofilament

fibre) that was coiled by twist insertion under a load of 35MPa was found to be 0.44N. The maximum force of 0.44N was obtained by calculating the fibre cross-sectional area as follows (where d represents the fibre diameter):

$$A = \frac{\pi d^2}{4}$$
$$A = \pi\left(\frac{(127\times10^{-6}m)^2}{4}\right) = 1.27 \times 10^{-8}m^2 \quad (1)$$

The maximum force can then be calculated as:

$$F = P \cdot A$$
$$F = (35 \times 10^6 Pa) \cdot (1.27 \times 10^{-8}m^2) = 0.44N \quad (2)$$

This research was the first attempt at understanding the potential performance of TCPs as low-cost linear actuation devices for biomimetic applications. However, there were many limitations in this paper which make this work difficult to reproduce and the results impossible to replicate. The fabrication procedures described are vague. The temperature control methods are not explained and problems with local heating due to the placement of the heating element are ignored. The fibre thermal annealing process is important, but appropriate parameters are undefined. Only fibre diameters are provided, fibre manufacturers for each fibre type or the length of the fibre is never indicated. The length of the fibre would play an important role in the performance of such actuators and were not provided. Finally, the importance of the coiling procedure and the selection of the best weights for each fibre are emphasized, but little guidance is provided for coiling parameters or determining the required weights. In fact, although the researchers make a point of mentioning that the weight attached during manufacturing is crucial and should be different than that which is used to separate the coils, there is no indication of what ideal weights are used for nylon or

polyethylene based on fibre size. A thorough investigation of critical parameters would be required to produce consistent and useful actuators.

2.3 Understanding Polymer Thermal Contraction and Expansion

Polymers such as nylon and polyethylene show promising potential for actuator fabrication due to their remarkable capabilities of exhibiting “reversible-fibre-direction thermal contraction, large volumetric thermal expansion, and large anisotropy in thermally induced dimensional changes to provide enhanced muscle stroke” [6]. Although crystalline regions of highly drawn polymers, such as nylon and polyethylene, can have small negative thermal expansion coefficients, fibre-direction–aligned polymer chains in neighboring noncrystalline regions are less conformationally constrained, so they can provide large reversible contractions as they access conformational entropy when heated [6], [30]. During twist insertion, coils begin to spontaneously form within the fibre due to mechanical instability. Twisted fibres can be coiled to obtain linear actuation. Inserting a large amount of twist in fibres such as nylon and polyethylene can make them chiral, meaning the molecules within the fibre are not superimposable on their own mirror image. Linear actuators can either be homochiral or heterochiral based on the polymer chain direction shown in Figure 2-2. When the chirality of fibre twist is identical to the chirality of the newly formed coils, the twisted actuator produces homochiral coils and is capable of contraction during heating. This is usually a product of a method called ‘autocoiling’, meaning twisting to the point of coil formation [26]. When the coiling and twisting have opposite chirality the fibre is heterochiral. This research uses the autocoiling method and therefore produces homochiral actuators.

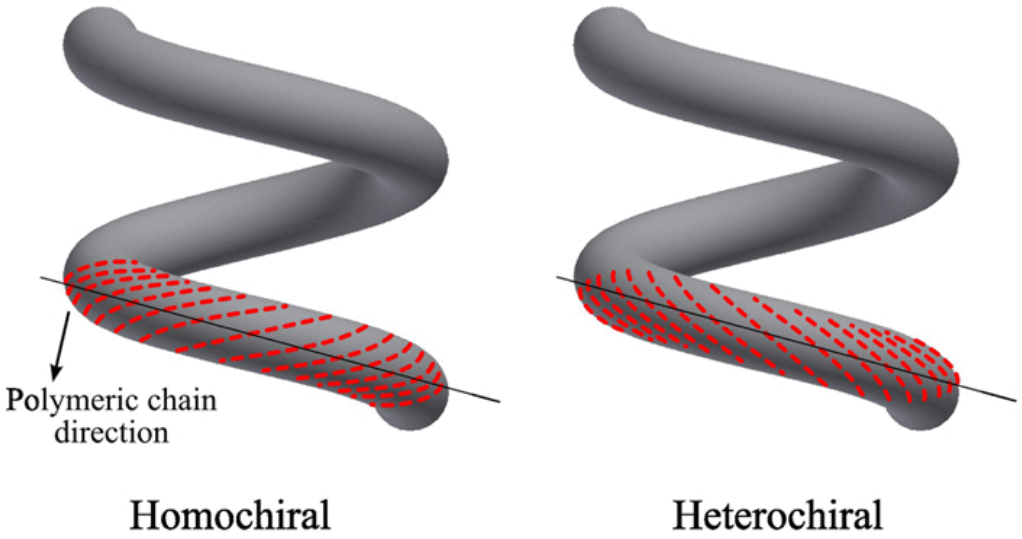

Figure 2-2 Chirality of newly formed coils within a fibre due to mechanical instability during twist insertion [26]

The subsequent mechanical response of the TCP actuator to thermal stimulus is dependent on several factors. These are factors such as weight during preloading, unloaded coil bias angle (α_c), precursor fibre diameter, fibre type, temperature during heating, number of rotations necessary to form coils, etc.

Directly prior to coil formation, parallel polymer chains are twisted into helices that have a bias angle relative to the fibre direction.

$$\alpha_c = tan^{-1}(2\pi r\tau) \quad (3)$$

Where *r* depicts the radial distance from the fibre center and τ is the amount of twists inserted into the fibre per initial fibre length (presented in units of turns per meter). After twisting, both the length contraction of these helically configured polymer chains, and the fibre diameter expansion will cause the fibre to untwist [6]. In an attempt to better understand this untwist phenomenon,

consider an artificial decoupling of these effects, where the polymer chain length contracts while fibre diameter is kept constant, or fibre diameter increases while the polymer chain length is kept constant. In both of these cases, an untwisting of the fibre is the result. Polymers such as nylon are ideal for thermal untwist due to their negative axial expansion and positive radial expansion which together play a role in untwist. The fibre untwist that is thermally induced ($\Delta\tau$ is the change in number of twists per initial fibre length) is responsible for the torsional actuation observed in twisted fibres and drives the length change for coiled fibres by requiring the fibre coil bias angle to change from α_c to $\alpha_c{}'$ as shown by the equation for spring mechanics:

$$\Delta\tau = \frac{sin(\alpha_c')\,cos(\alpha_c')}{\pi D'} - \frac{sin(\alpha_c)\,cos(\alpha_c)}{\pi D} \qquad (4)$$

Where *D* and *D'* are the coil diameter, taken through the centerline before and after heating, and the coil bias angle, α_c, is the angle between the fibre and the coil's cross section [6]. For a coil of *N* turns length *L* made from a fibre of length *l*: $\sin(\alpha_c) = L/l$ and $\cos(\alpha_c) = N\Delta L/l^2$. By assuming that the change in fibre length *l* is negligible, and using these relationships, stretching a coil clamped to prevent end rotation creates a change in the fibre twist of

$$\Delta\tau = \frac{N\Delta L}{l^2} \qquad (5)$$

Equation 5 enables us to predict the changes in stress (expansion and contraction) depending on the change in length of the actuator fibre caused by stress during fibre untwist. Once a homochiral muscle is heated, the TCP generates an untwisting torque which pulls the neighbouring coils together, providing work by contracting in length [3].

Haines et al. introduced the experimental research on the formation of TCP actuators from low-cost polymers. The following chapter attempts to mimic the experimental procedure used by Haines et al. in order to fabricate TCP actuators with various types of nylon fibres, and then expands on these results in order to create consistent and useful actuators for biomimetic applications. These small and lightweight actuators are capable of contraction while producing a linear displacement similar to the linear motion provided by a pneumatic or hydraulic device, making their application opportunities vast. Unlike their conventional counterparts that are limited by their size and weight which compromises their dexterity, work capability and force generation, these actuators are small and lightweight. These TCP devices should have a maximum length of 10cm and a contraction of at least 1.5cm or 15% of the maximum length to be deemed acceptable for this application. This number was measured manually with reference to the anthropometric data of appendix A for the length and range of motion of an average human index finger. It is assumed that potential exoskeletons using TCP actuators would use a mechanism that could provide a mechanical advantage of at least two. They should also be able to overcome the spastic force in a patients “spastic” hand which provided in Table 1-1 as 55±14.7N.

2.4 Review of Current Hand Exoskeletons

Over the last few decades, various novel hand exoskeletons have been developed by research groups for rehabilitation or assistive applications. Exoskeletons that are developed for rehabilitation can provide two different types of exercise for patients to aid with motor recovery of the hand, either active rehabilitation where the patients themselves exercise a muscle or joint without the help of a therapist, or passive rehabilitation where a patient cannot perform the exercise or exert any energy in doing so. There are two major groupings of devices as well. Either passive

devices, where the hand is being moved against the resistive forces created by the exoskeleton, or active devices, which involve the movement of the hand being driven by the exoskeleton [12]. Passive exoskeletons (i.e. non-actuated) use the laws of physics, such as potential or kinetic energy as its main source of energy. From a mechanical point of view these devices are more efficient. However, there is a substantially high amount of metabolic energy required in order to achieve optimal function. Therefore, efficiency is somewhat hindered. Active devices (i.e. actuated) on the other hand need to be powered to work, using an external source of energy such as an electric motor or pneumatic/hydraulic system. These devices provide power in order to move the limb and reduce any extra metabolic energy consumption. Amongst these systems, actuators and sensors are not mandatory, but instead depend on the outcome the exoskeleton is trying to achieve. There are also exoskeletons developed for assistive applications which acquire the patient's motion intention and provides assistance to the patient performing the action. Therefore, this grouping of exoskeletons are required to be equipped with sensors and actuators [12]. Upper limb exoskeletons, specifically hand devices, can be grouped using several different classification variables such as "actuator type, power transmission method, degrees of freedom (DOF), intention sensing method, and control method" [12]. For the purpose of this research, the major classification type of interest is the actuator used to drive the device. This work focuses on actuation devices used in rehabilitation exoskeletons because no ideal actuator has yet been found and there exists a significant gap between actuators that can achieve adequate force output for an upper limb exoskeleton while being low-cost, lightweight, aesthetically pleasing, low-profile and portable.

2.4.1 Electrical/Electrochemical Actuated Exoskeletons

2.4.1.1 MIT-Manus

The MIT-manus was designed and developed over 11 years at the Massachusetts Institute of Technology's Interactive Motion Technologies, Inc. [13]. Hogan et al. were one of the first to develop an exoskeleton that provided assistance in arm reaching motions during simplified target matching games to help patient recovery post stroke. This device is commonly referred to as the "robotic test bed" developed to study the use of neuro rehabilitation for motor function. It enables voluntary motion in a two degree range of motion (ROM) (abduction/adduction) in the horizontal plane, allowing for unrestricted movement in the elbow and shoulder joint. Although the device is effective for the upper arm, the wrist modular component of the MIT-manus is not suitable for wrist motion as it is very complicated and takes too long to secure a patient's spastic hand in place, as seen in Figure 2-3. The device contains an active module that is capable of moving, guiding, or perturbing the movements of a patient's limb. It can also simultaneously record motions and mechanical quantities such as velocity and displacement. This device is powered by brushless motors, with its control implemented into a standard personal computer. A differential mechanism mounted on a parallelogram linkage driven by geared actuators provides three degrees of freedom of wrist motion.

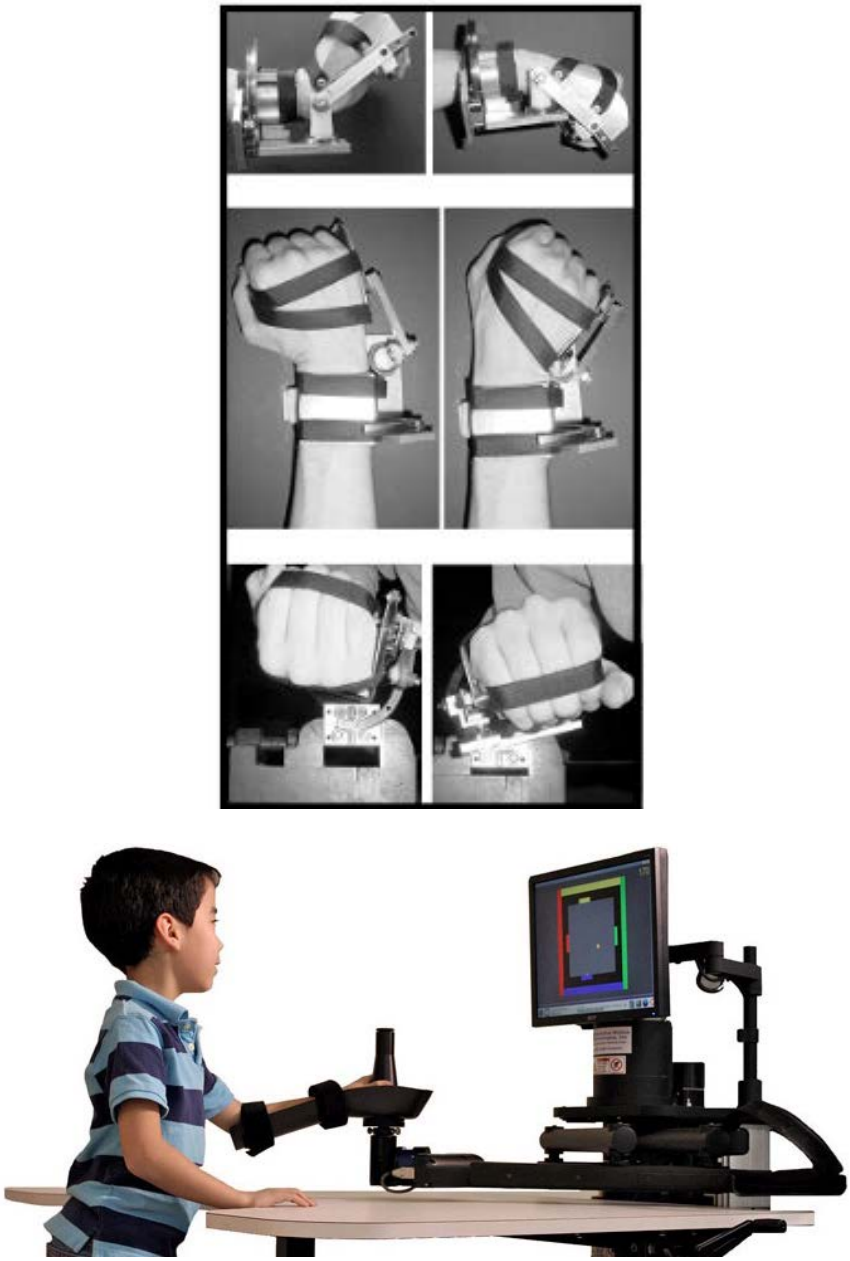

Figure 2-3 MIT-manus proposed wrist module and patient experience with virtual environment [13]

Although this device was one of the initial hand/wrist exoskeletons designed to help stroke patients regain upper limb function, many components of their design are still commonly used today in novel exoskeletons. The main functional aspect that is important to note is that the exoskeleton

enables a 2 DOF motion in abduction and adduction of the wrist. The major limitation of the proposed design is that it does not measure individual joint force/torque in all DOFs, so it is hard to gauge the ability/disability level of the patient and needs of each finger. Finally, another reason this design is ineffective for hand motion is that the wrist modular component takes too long for patients to secure themselves in place. The ideal amount of time recorded for setup is approximately 2 min or less [31].

2.4.1.2 HEXORR - the Hand EXOskeleton Rehabilitation Robot

The Hand EXOskeleton Rehabilitation Robot (HEXORR) developed by Schabowsky et al. is an active rehabilitation device that uses gear trains and electromagnetic motors for both position and torque control therapy. HEXORR is an exoskeleton whose robotic joints are aligned with the joints of the human hand as demonstrated in Figure 2-4 and built of two modular components: one for the digits and another for the thumb. The finger (digit) component is built of a four-bar linkage that enables coupled rotations of the digit joints. This device provides patients with a nearly full ROM for all digits and allows physiologically accurate grasping movements while being powered by only actuators. Each module is driven by an electrical motor and the patient's movement volition is sensed using a torque sensor, with mechanical ROM "stops" implemented to ensure patients are never hyper-flexed or hyper-extended. This design has implemented a 'kill switch' in order for the experimenter to shut down both motors simultaneously if necessary. It is also equipped with a patient specific software ROM 'stop' which assesses individual extension and flexion ranges based on patient needs [32].

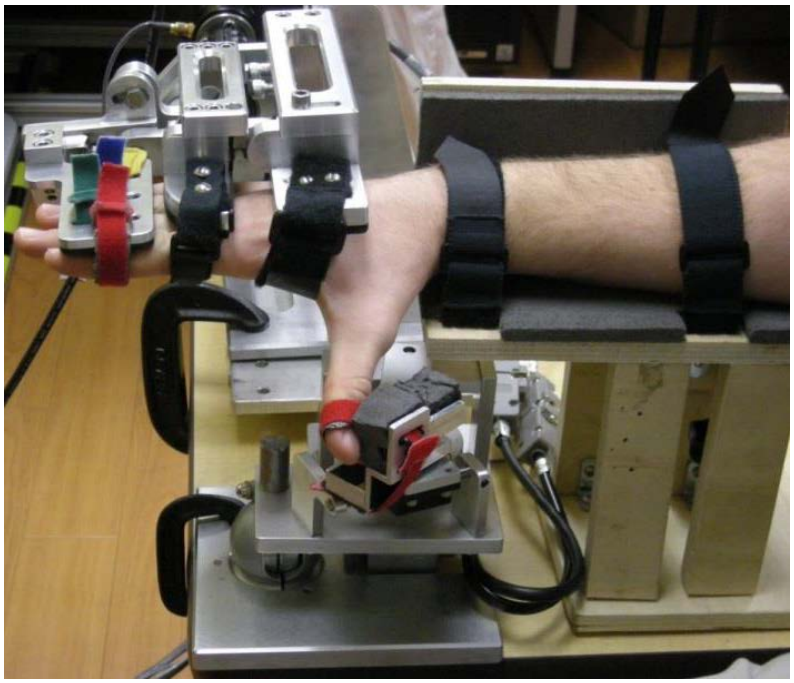

Figure 2-4 HEXORR - Hand EXOskeleton Rehabilitation Robot [32]

This device has three modes of operation: 1) continuous passive movements , 2) active unassisted flexion/extension movement, and 3) active force assisted flexion/extension movement [12]. Throughout the second mode the device compensates for the weight and friction of the device itself while rejecting unintentional movement commands such as flexion [32]. In the third mode the device provides assistance for extension movements. Because the exoskeleton is active and requires a computer station, it remains bulky and non-portable, meaning that a patient would only be able to wear it during exact times of therapy or exercise.

2.4.1.3 HANDEXOS

The HANDEXOS was developed in 2009 by Chiri et al. in St. Louis, Missouri, as a novel hand exoskeleton device for hand rehabilitation [33]. The first experimental prototype was developed as a single finger module for the index finger (seen in Figure 2-5), in order to initially test

wearability and kinematic coupling with the joints of a patient's finger. The actual device concept is composed of five independent finger modules with three links per finger where the center of rotation is matched with the corresponding joint of the human finger, which is demonstrated in Figure 2-6. This device was aimed at simplifying the complexity of the exoskeleton in terms of its actuation, mechanics, and structure, while ensuring full hand mobility with independent actuation for all five fingers. Each finger is actuated by a cable running across idle pulleys placed on each finger joint and fixed to the distal phalanx through a cable stop. The cable is pulled through a linear slider by a DC motor placed extrinsically. The flexion of the finger is passively obtained by means of a set of three (one for each joint) antagonist cables running across the pulleys placed on the other side of the finger, connected to three extrinsic linear compression springs whose elastic torques cause the finger to flex.

It was also intended that the palm and fingertip area remain free for direct interaction with activities of daily living (ADL) objects [34]. The main design concept that separates the HANDEXOS from all previously designed exoskeletons is the use of 5 independent finger modules which are individually activated. This allows patients to not only work on coordination and flexibility, but also achieve more complex movement patterns [33]. This is especially beneficial in a device that will be worn for many hours throughout the day. A major limitation of this exoskeleton is that each finger needs a separate module equipped with its own actuator making it large, bulky, and altogether non-portable. Due to the complexity of the many different pulleys and cables that are included in the design, it is also difficult for a patient to be able to put the glove on without the assistance of a therapist or physician.

Figure 2-5 HANDEXOS - individual finger module [33]

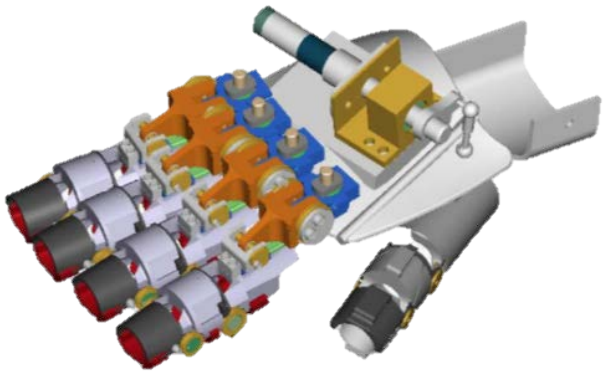

Figure 2-6 Future HANDEXOS full hand concept [33]

2.4.1.4 iHandRehab

The iHandRehab is a therapeutic interactive passive and active hand exoskeleton developed by Li et al. in 2011 in Beijing, China for hand rehabilitation. It is composed of a module for the index finger and a separate module for the thumb. The exoskeleton proposed is lightweight, has low inertia, is capable of independently controlling finger joints and can accommodate different hand

sizes with adjustable joint ROM and phalanx length. It is made up of a mechanism for the index finger and one for the thumb so that they can each move in four possible DOFs simultaneously and independently of one another, with angle and force sensors. The device is actuated by 8 motors (RE25, RE36 Maxon motor) located on the frame of the virtual environment desktop. The actuation module is kept near the desktop, away from the hand in order to decrease the overall weight of the device on the limb. These motors provide force and motion transmitted to the finger joints by a reducer and a cable sheath transmission system. It also has a control system (with controller and driver), and is attached to a virtual environment shown in Figure 2-7. The virtual rehabilitation environment (VRE) can be controlled by a host computer and therapist to set individualized training parameters such as ROM, training time, and speed. All the actuated joints are controlled by cable transmissions where two cables are used for each joint motion to create bidirectional movement [35]. The iHandRehab device is one of the first lightweight (only 250g), low inertia, exoskeletons capable of independently actuating each finger joint. It is also equipped with adjustable finger joint lengths that can accommodate various patient joint lengths using a fastening screw, which can be moved in a slot on the connection slider of the exoskeleton which makes it available to a larger range of patients. The actuation system is located separately from the hand module which is an effective design characteristic for decreasing the overall weight. However, the device cannot function without a virtual environment and host computer which makes it non-portable and difficult to use without the supervision of a therapist.

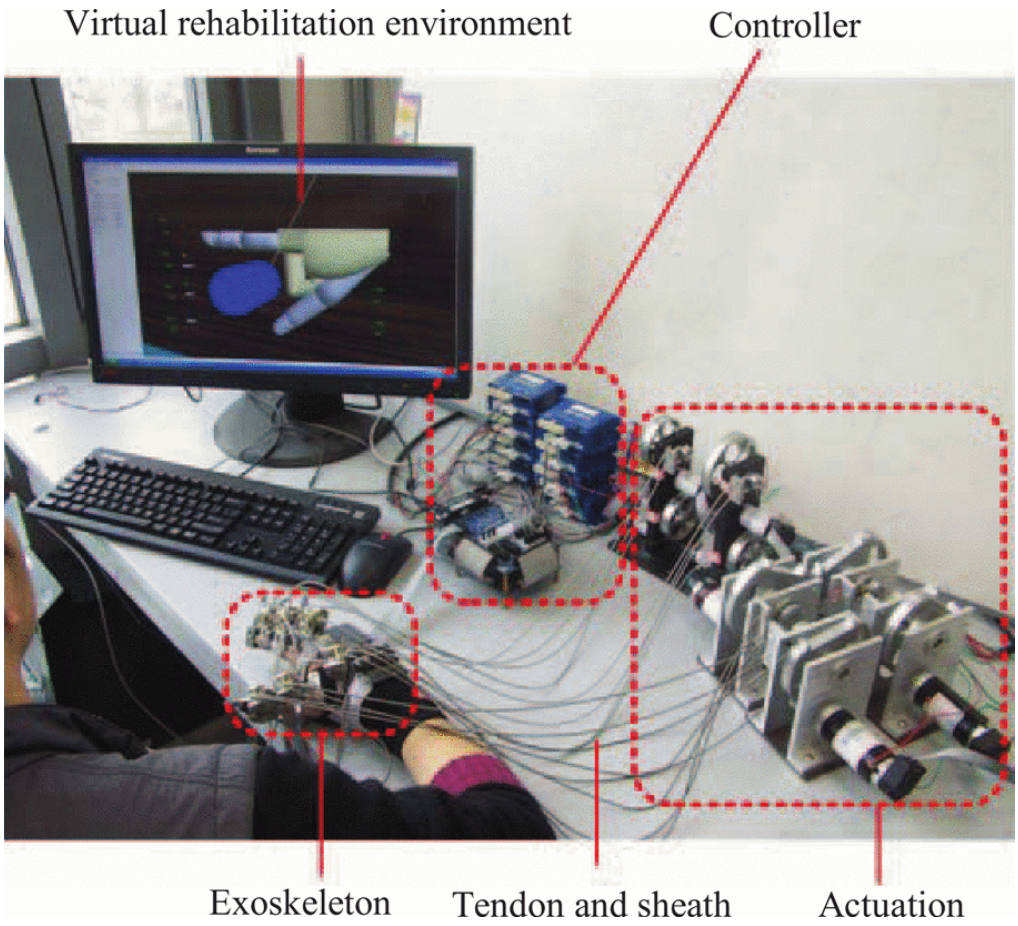

Figure 2-7 iHandRehab device with complete device setup [35]

Another limitation of this design is that it only embodies a thumb and index finger component, therefore, leaving the remaining three fingers untreated. Finally, friction that is generated through the cable and cable sheath are difficult to analyse because the finger displacement changes the curvature of the model. Therefore Li et al. proposed an experimental method to estimate the resistance torque [35]. This is relatively inaccurate and would need to be further developed.

2.4.1.5 IntelliArm

The IntelliArm, designed by Ren et al., is a whole arm grasping training exoskeleton designed to aid patients suffering from spastic hypertonia and other neurological impairments. It is a 7+2

degree of freedom system capable of controlling the shoulder, arm, and wrist individually. However, for the purpose of this study only the one degree of freedom hand and finger system is considered. The exoskeleton is a patient friendly device with a single electric motor drive which attaches to the robotic device [36]. The wrist and hand portion of the system have one active degree of freedom and uses a cable bevel gear mechanism in the form of a 4-bar linkage system to create hand flexion/extension training. The motor is designed to rotate link 1 and open the joints of all four fingers, while link 3 will push the thumb away synchronously as seen in Figure 2-8.

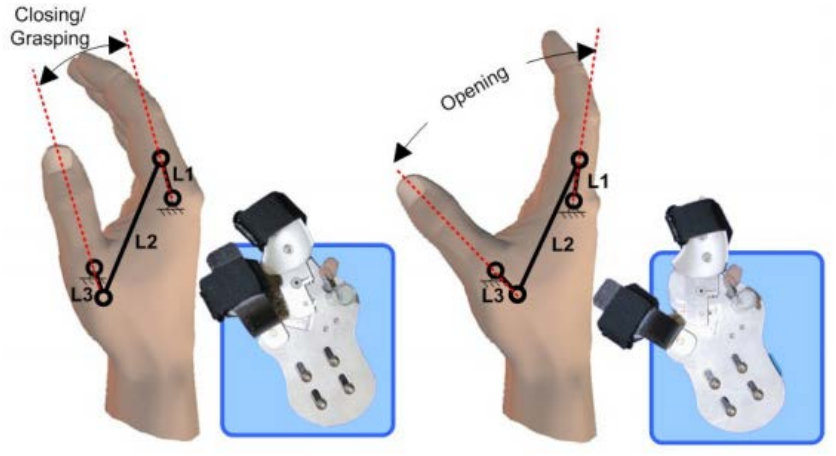

Figure 2-8 Attachment of patient hand to "IntelliArm" flexed and extended finger posture [36]

The motor controls all four fingers while the thumb is driven by the coupled knuckle joint. The intelliarm is capable of quantitative analysis for each joint and DOF, where it can detect and provide data on abnormal passive coupling between joints and abnormal synergy. This is a much more accurate assesment than a therapist would manually be capable of providing. The exoskeleton is also equipped with safety stops to prevent patient specific hyper extension/flexion, resistance based control, and an emergency kill switch, making the device user friendly [36]. The major limitation of this exoskeleton is its lack of hand support. The wrist module only allows one

DOF and stops at the wrist joint, no finger support is provided. It is therefore not capable of manipulating the extremely distinct motions of a regular human hand, making it impractical as a hand therapy device [36].

2.4.2 Pneumatic Actuated Exoskeletons

2.4.2.1 HWARD – the Hand Wrist Assistive Rehabilitation Device

The HWARD hand wrist device was developed by Takahashi et al. in 2008 to aid in hand grasping/releasing motions after stroke based on motor learning theories [37]. The robot is a pneumatically activated exoskeleton capable of three DOF using air cylinders: simultaneous flexion/extension of the four fingers, as well as a separate degree of freedom for the flexion/extension of the thumb about the knuckle and a flexion/extension DOF for the wrist [37]. For this device, the hand is secured to the exoskeleton using three Velcro straps with the ulnar forearm secured inside a padded splint as seen in Figure 2-9 [38]. Each air cylinder and limb is fixed on opposite ends of a lever with a revolute joint in between [38]. The device is actuated by three double-acting air cylinders, with a controlled 4-15N force of air pressure [38]. The palmar portion of the hand is therefore left unobstructed in order to allow patients to experience tactile feedback from real life objects during grasp and release tasks during therapy [37]. The robot is also backdriveable, therefore enabling stoke patients to actively perform movements while the device is not being engaged in active assistance [37].

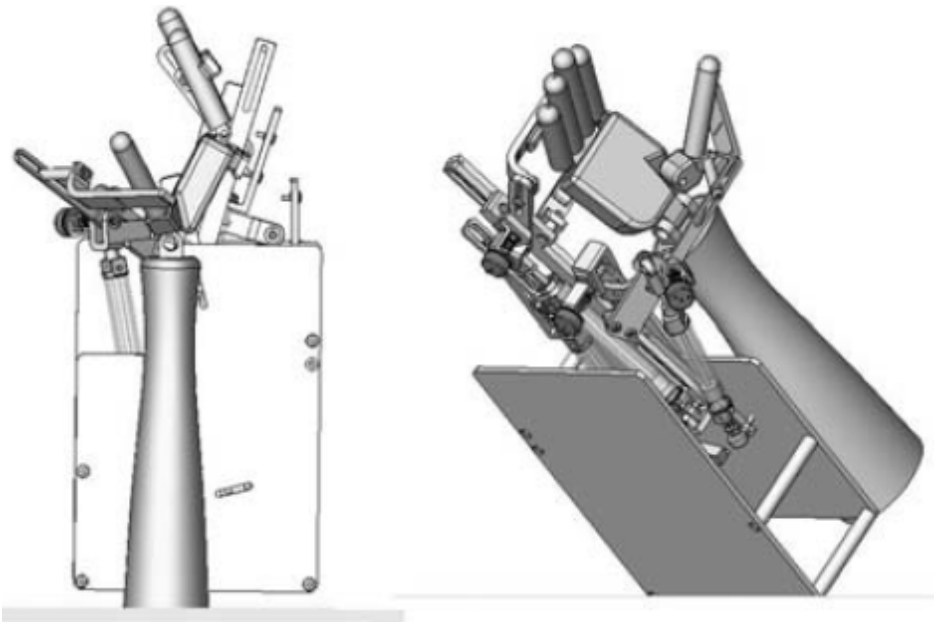

Figure 2-9 HWARD – 3-DOF pneumatically actuated exoskeleton to aid stroke impaired hands [37]

The HWARD makes use of pneumatic muscle actuators which are typically known to be safer and more user-friendly. Another interesting design characteristic which is similar to many that have been seen before is the three Velcro straps and padded splint which are designed so that the ulnar aspect of the lower arm can be held comfortably. This one specifically is also non-portable meaning the patient will have to be sitting down and strapped in in order to wear the device.

2.4.2.2 Hand Mentor

The Hand Mentor is an active repetitive motion therapeutic exoskeleton developed by Kinetic Muscles Inc. in 2004. The device provides the repetitive upper extremity training of reaching and feeding motions, designed to enhance patient quality of life by increasing independence. It is driven by an air-muscle which allows a one degree of freedom extension motion, and records any resistive force resulting from the muscle stiffness of the hand and wrist. The pneumatic muscle creates a pulling force when pressurized resulting in an opposing flexion or assist extension at the

wrist. It has one module to extend the fingers and wrist, as shown in Figure 2-10. However, it does not activate the thumb. This therapeutic design also incorporates sensors that monitor three various feedback responses: hand placement in space, applied force to the hand by the compliant air muscle actuator, and electromyography (EMG) surface electrodes to record patient muscular activity in congruency with an EMG display [39].

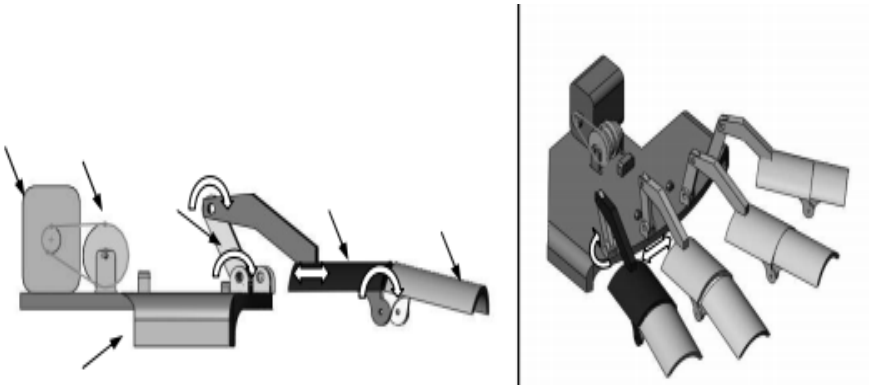

Figure 2-10 (Left) Connection of the links of a finger module (Right) Isometric view of four finger module [39]

The use of finger and wrist components which can be activated simultaneously and separately is very important for exoskeleton design. This allows fingers to move in a more realistic manner similar to that which would occur during ADL.

2.4.2.3 A Wearable Rehabilitation Robotic Hand Driven by a PM-TS Actuator

The wearable rehabilitation robotic device created by Wu et al. proposed a novel actuation method, composed of a pneumatic muscle and torsional spring system (PM-TS) to enable joint drive. Due to the limitations arising from using pneumatic muscles as the sole actuation method (need for

antagonistic pairs), Wu et al. proposed the use of a torsional spring system in congruency with the pneumatic muscle. The pneumatic muscle is arranged on the upper forearm to provide the pulling moment while the torsional spring provides the opposing torque. This system design allows the spring system to provide the extension of the pneumatic muscle, allowing for bidirectional movement, while reducing the exoskeleton's weight, bulkiness, cost, as well as making it a good take home therapy device for repetitive exercises. With this new PM-TS actuation pair (shown in Figure 2-11) the device is capable of two active degrees of freedom (flexion/extension of the joints of the fingers not including the thumb). They also purposed a new and unique control system which is made up of sensors that provide feedback on angle, pressure, and force. Together, this design decreases the amount of actuators that must be controlled, making the device easier to control and quantify [16].

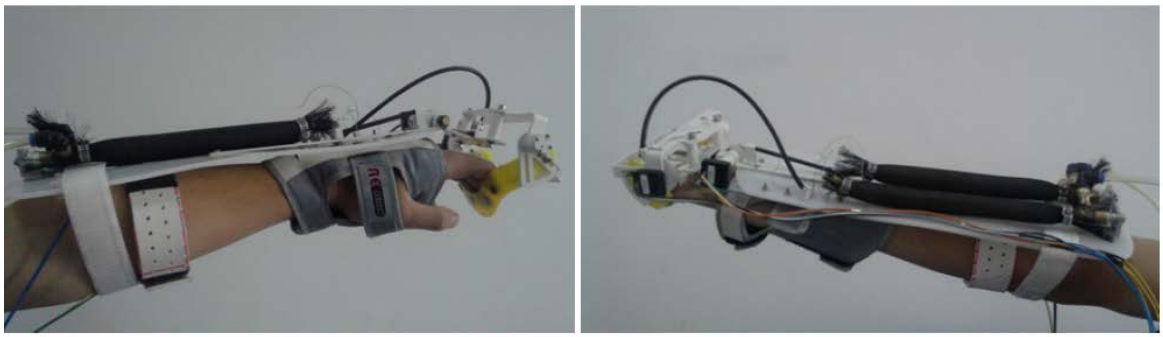

Figure 2-11 Prototype of the wearable rehabilitation robotic hand using PM-TS actuation [16]

This design proposes an innovative actuation method which attempts to decrease the overall "bulkiness" of a common hand exoskeleton. Due to the antagonistic pair design necessary for typical pneumatic muscles, their use of a novel PM-TS design is important. This method decreases the weight and overall size of the exoskeleton making it more portable while still being able to provide the force required for rehabilitation. One of the limitations of this design remains the size

of the single set of pneumatic muscles require for unidirectional motion. Moreover, it is still bulky and complicated to wear, making it difficult to carry around and use without a therapist.

2.4.3 Passive Hand Exoskeletons

In contrast to the "active" upper limb robotics described above, passive orthoses are typically less expensive, more appropriate for individual unsupported use at home, and are safer to use. Due to the above reasons, passive upper limb exoskeletons are typically preferred to more complex actuated devices. Some examples of popular passive devices used currently are described in further detail below. However, these devices have their limitations as well. These include only a few degrees of freedom, which decrease a patient's workspace, a lack of feedback regarding movement recovery, and can be difficult to adjust or modify by the patient alone. By definition, these devices do not include actuators, but provide interesting design concepts which may be useful in the design of high force output, low-cost, lightweight, aesthetically pleasing, low-profile and portable hand rehabilitation exoskeletons.

2.4.3.1 HandSOME

HandSOME is a portable hand exoskeleton for stroke rehabilitation designed in 2011 to perform pinch-pad grasping motions. This device is passive, lightweight, and portable, designed to give an extension moment to the finger joints to compensate for finger flexor spasticity caused by stroke. It uses a four bar linkage system (which can be seen in Figure 2-12) with a passive spring actuation mechanism between the fingers and thumb mechanism comprised of elastic cords to assist with finger and thumb extension [40]. This linkage ensures proper inter-joint coordination during the

grasping motion. Its main function is to follow the normal kinematic trajectory of the hand during pinch-pad grasp in order to provide assistance in the torque profile to best compensate for finger flexion hypertonia, and measure the angle of grasp using an encode [40]. During experimental trials, subjects showed a large increase in their active ROM with the device as well as an increase in the ability to perform functional grasp of objects. This device enables users to perform grasping motion in a natural format. However it is only capable of one DOF.

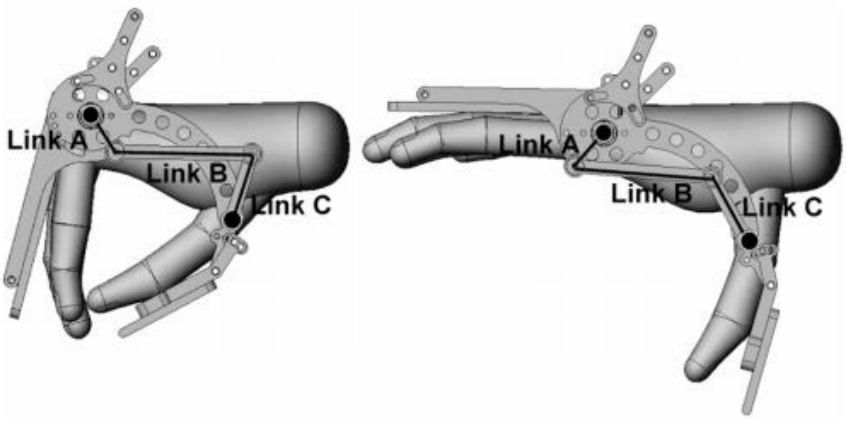

Figure 2-12 HandSOME portable hand exoskeleton linkage system capable of pinch-pad grasp [40]

The limitation of this work is that the device is only capable of pinch pad grasp. It will not provide assistance in overall finger extension which is what is necessary in slowly redeveloping muscle memory for 6 hours a day. It would also be beneficial if each finger module was separately activated making it easier for patients to wear the exoskeleton for a longer duration throughout the day.

2.4.3.2 Saeboflex

The Saeboflex is a therapeutically designed reach and grasp device commercially produced by two occupational therapist [41], [42]. It is a dynamic wrist, hand, and finger exoskeleton developed to aid finger extension in patients with upper limb spasticity caused by stroke [41]. Its design is low profile, simple and portable as seen in Figure 2-13. The Saeboflex is capable of 1 DOF extension. It is designed to be worn as a therapy glove at the maximum recommended intensity of three 45 minute intervals [42]. The mechanical extension springs help position the wrist and fingers into extension in preparation for object manipulation after a patient actively flexes their fingers to grasp [41], [43].

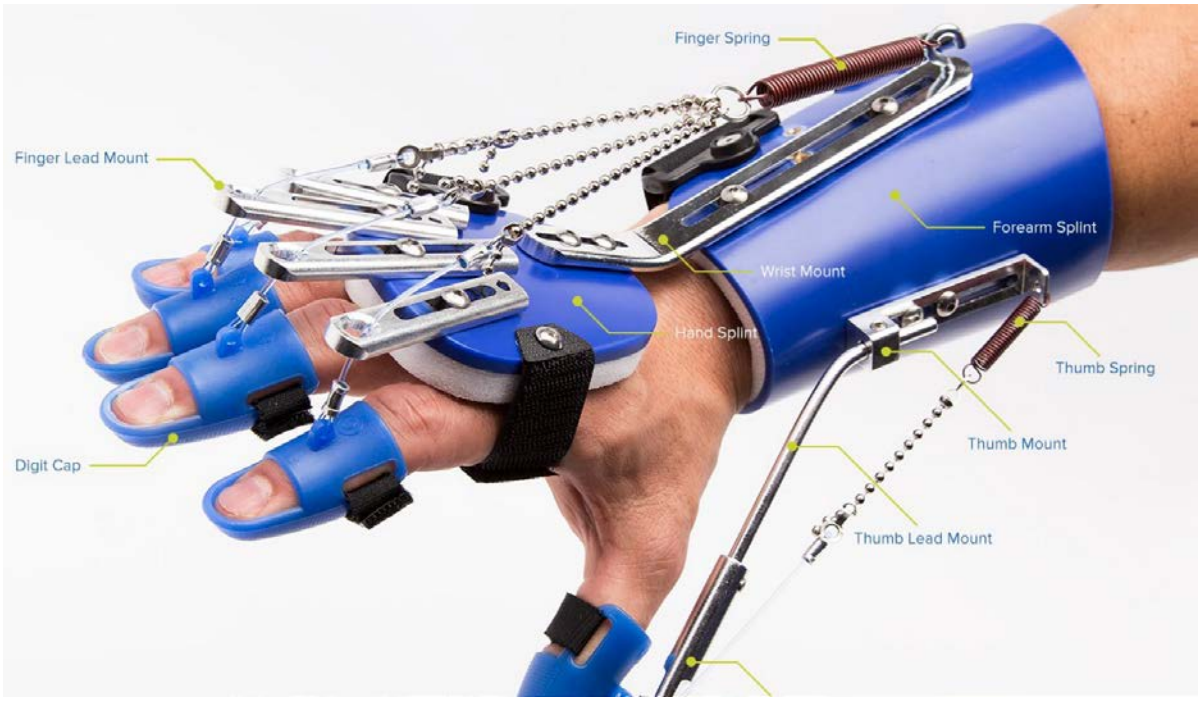

Figure 2-13 Saeboflex Reach design for hypertonicity [41]

This design is innovative because it aids in motor impairment while being the least bulky and the most low profile device on the market. It is also ideal for at home repetitive task practice without

the help of a therapist [42]. This is a significant aid in training without supervision, making it more accessible, cost efficient, and able to maximize therapy options. The major limitation of this design derives from the complexity of the human hand and the inability to move in more than 1 DOF. The only motion Saeboflex is capable of is extension, leaving out many other motions necessary to perform activities of daily living. Moreover, it is designed to be equipped with long chains that run directly above each finger. This design could be made to be much more low-profile and aesthetically pleasing if the mechanism were decreased in size.

2.4.4 Hand Exoskeleton Summary

Current exoskeleton designs actively powered by electrical motors, described above, run into the same common problems associated with electrical actuation mechanisms. Most of these designs are powered by up to 8 motors and attached to a host computer capable of simulating a virtual environment. These are highly complex systems capable of providing quantitative feedback on mechanical quantities such as force output and velocity of the focal limb. Most also require the assistance of a trained therapist to aid the patient with securing their hand in and out of the device. The fact that these systems need electrical motors and are tethered to large host computers makes them bulky, heavy, complicated, and non-portable.

Those that are pneumatically or hydraulically activated also run into similar problems. Both the HWARD and the Hand Mentor are capable of one active DOF per joint due to the unidirectional nature of a pneumatic actuator. In order to increase the number of DOF capabilities and create bidirectional motion, there is a need for pneumatics to be aligned in antagonistic pairs. This consists of a larger and bulkier device and its corresponding tethered systems. The PM-TS actuator

proposed by Wu et al. has many admirable qualities. With the combination of a pneumatic muscle and a torsional spring mechanism, this actuator is capable of bidirectional movement without the weight and costs associated with using two pneumatic muscles per joint. The pneumatic muscle on top provides the pulling motion while the torsional spring provides its opposing torque. This actuation mechanism has many favourable features; however, it could still be made more discrete and aesthetically pleasing.

The Saeboflex is the design most capable of meeting the non-functional customer needs outlined in this thesis. The device is lightweight, portable, capable of 1 extension DOF, and capable of being used without the aid of a therapist. The limitation of the Saeboflex, similar to that of the PM-TS actuator, is their aesthetics and lack of low-profile design. While both designs are much more discrete than their counterparts, there is definitely a possibility of being able to decrease the overall volume of these devices. This work will attempt to not only achieve similar force outputs, but also drastically decrease the overall size and cost of current actuators, which could be used as replacements for those used in the devices describe herein.

2.5 Anatomical Review

To improve the design of a hand exoskeleton, a better understanding of the anatomy and physiology of the upper limb is crucial. While outside the scope of this thesis, a thorough biomechanical analysis would be required. An anatomical review of the bones and muscles of the upper limbs is provided in Appendix A.

Chapter 3

Experimental Testing of Polymer Fibres

3.1 Tested Fibre Types

Based on information gathered from the literature, nylon and polyethylene showed promising results as potential artificial muscle actuators [6]. Most research so far has used light gauge monofilament fishing line and Shieldex conductive sewing yarn (a conductive form of nylon 6,6) as their precursor polymer fibre for actuator fabrication. Haines et al. were the first to propose the use of nylon and polyethylene in the fabrication of twisted and coiled actuators in 2014 [6]. However, their fabrication techniques are ill described and important parameters for optimized actuator performance are non-existent.

The first goal of this thesis is to study numerous low-cost polymers made of nylon and polyethylene in order to understand and define the fabrication process, determine the critical parameters in the fabrication process which provide consistent results and those parameters which can be adjusted for optimal performance of the actuators themselves. Moreover, the different polymer fibres were tested and compared in an attempt to differentiate which were capable of providing the highest percentage of reversible thermal contraction for the highest value of force. Only filaments capable of forming continuous and full coils during the twisting phase were chosen for further experimentation. Coils that wind into continuous, regularly spaced rings adjacent to each other were considered adequate for use throughout the remainder of this thesis. Those found

to be inadequate had areas of irregularly spaced rings or snarls within the fibre which prevented coil formation in those distinct areas.

3.1.1 Nylon Fibres Tested Based On a Literature Review

While attempting to make TCP actuators identical to those fabricated in the work of Haines et al, this research will use the same Shieldex nylon 6,6 conductive yarns (117/17 and 235/34) that are used in their work, as well as regular 10lb nylon 6 monofilament fishing line. Initial nylon filaments which are to be tested are shown in Figure 3-1.

Figure 3-1 Tested Nylon fibres: (A) Shieldex conductive nylon fibre 117/17, (B) Shieldex conductive nylon fibre 235/34, and (C) 10lb nylon 6 monofilament fishing line

3.1.2 Polyethylene and 50lb Nylon Monofilament

In addition to those fibres previously used in the literature, four separate ultra-high molecular weight polyethylene (UHMWPE) fibre types are considered, as well as much stronger 50lb nylon 6 monofilament fishing line. The polyethylene fibres considered for this study are shown in Figure

3-2 (Berkley FireLine fused 30lb test line, SPIDERWIRE camo-braid 30lb test line, Sufix 832 Low-Vis braided 80lb test line with Gore ePTFE fibre, and PowerPro braided 100lb test line). It is important to note that UHMWPE fibres are only available from two manufacturers in the form of Spectra fibres made by Honeywell and Dyneema fibres made by DSM.

Figure 3-2 Polyethylene test fibres (A) Berkley FireLine 30lb test line, (B) SPIDERWIRE camo-braid 30lb test line, (C) Sufix 832 Low-Vis 80lb test line, and (D) PowerPro braided 100lb test line

The high strength nylon 6 monofilament considered in this study is shown in Figure 3-3 (Trilene Big Game 50lb test line).

Figure 3-3 (A) Trilene Big Game 50lb test line (B) 100x optical magnification of this fibre 770 µm

3.2 Methodology

3.2.1 Twisting and Coiling

In order to understand the fabrication process and the critical parameters involved in the performance of TCP actuators, initial testing was conducted in an attempt to mimic the results obtained by Haines et al. Various types of nylon fibres were considered, but two versions of nylon 6,6 Shieldex conductive yarn (117/17 2 ply, Denier 240/34f and 235/34 4 ply, Denier 940/136f) seen in Figure 3-1 (a) and (b) respectively) and 10lb regular nylon 6 monofilament fishing line Figure 3-1 (c)) were the focus of initial testing due to findings presented in this previous work. In order to fabricate the initial conductive nylon TCP actuators, a single 50cm strand of each conductive sewing thread was tied to a paperclip at both ends using a “surgeon’s loop” fishing knot (chosen for its resistance in tension and its minimal impact on line strength). This arrangement was based on previous work found in the literature. After some experimental effort, it was found that four 50cm strands of conductive sewing thread attached together at each end proved to produce

more consistent, equally spaced, and successful coils (Haines et al. only used single strands). Therefore, all subsequent tests were done using four strands twisted all together. For the fishing line, the same procedure was followed, although only one strand of varying lengths was tied to a paperclip at both ends using the same knot. For all nylon fibre types, one paperclip was then attached to a variable speed electric drill (Black & Decker 5.2A, 3/8 in) using a threaded eye hook which was used as the rotational device (twisting mechanism), and the other was attached to a weight (this varied for different fibres) in order to maintain constant tension on the fibre during twisting, as shown in Figure 3-4. The performance of the sewing thread and fishing line fibre is heavily dependent on its payload; therefore, the weight chosen for this step was crucial. It was found that the weight could vary within a small range based on the type and length of fibre used. However, once outside this range the fibre exhibited failure by becoming tangled, showing signs of breakage, or burning during the annealing process as discussed in the literature [6], [44]). Unfortunately, the literature provides very little guidance on the payload range for different fibre types. Therefore, for the purpose of this study, many different payloads were tested until the ideal weight was found for each fibre type. As shown in Table 3-1, the nylon monofilament fishing line was twisted while attached to a weight of 209g. The thinner Shieldex conductive yarn (117/17) underwent the twisting phase using a weight of 268g and the thicker fibre (235/34) was twisted using a weight of 632g.

Table 3-1 – Summary of the experimental parameters of all nylon fibres used in this study

Material	*Diameter (μm)*	*Load during coiling (g)*
Regular monofilament fishing line (10 lb) test)	430	209
Nylon 6,6 Shieldex conductive sewing yarn (117/17)	234	268
Nylon 6,6 Shieldex conductive sewing yarn (235/34)	468	632

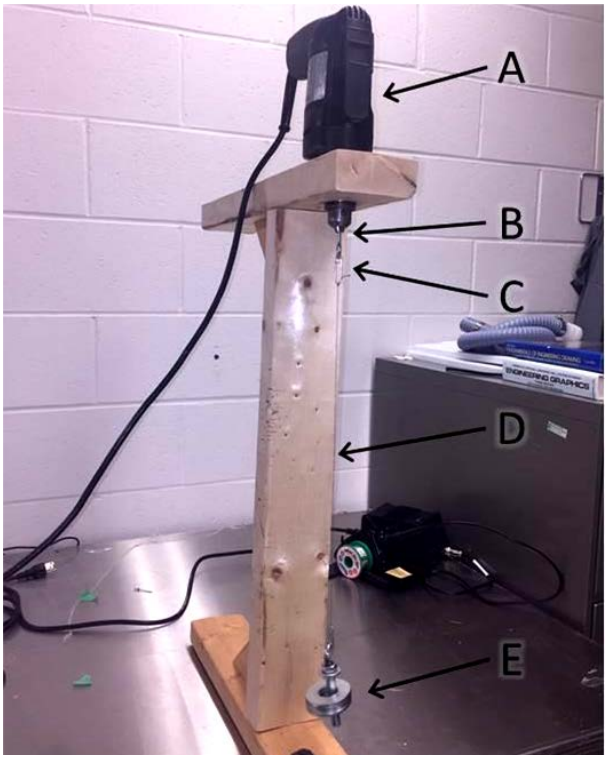

Figure 3-4. The experimental setup demonstrating (A) Black & Decker drill, (B) eye hook, (C) paper clip, (D) four ply 117/17 conductive yarn and (E) weight

The fibres (Figure 3-5) were allowed to hang vertically under the force of gravity provided by their respective weights. The weight is prevented from rotating using a small metal rod projecting out from the middle of the weights and which makes contact with the vertical wooden support. Once the drill is turned on and rotation of the drill begins, twists are slowly inserted into the thread. The

strand(s) of thread begin to shorten until they reach a critical point (the critical twist density) where they become saturated with twists. At this point, tight coils spontaneously start to form along the length of the twisted thread. The fibres can then maintain their coiled configuration when unloaded. However, these coils typically begin to untwist naturally if left to hang freely under load.

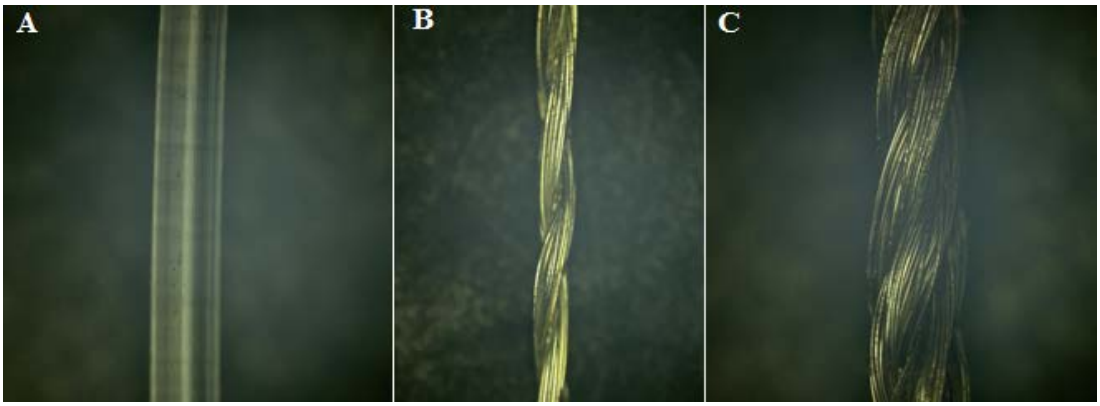

Figure 3-5. Uncoiled nylon fibres, 100x optical magnification of: (A) 430 µm diameter monofilament fishing line, (B) 234 µm Shieldex conductive yarn (117/17 2ply), (C) 468 µm Shieldex conductive yarn (235/34 4ply)

Based on the initial fabrication results obtained from the nylon fibre tests, the procedure was then modified to account for shortcoming in the initial fabrication process. For tests involving polyethylene and the 50lb nylon monofilament, a single 50 cm strand of each fibre was tied to a 5/16" 'S' hook on either end. The smaller weights involved in the fabrication of the early nylon TCP actuators made the use of paperclips sufficient. Conversely, the much higher strength of the polyethylene fibres and 50lb nylon monofilament required the use of much stronger 'S' hooks in order to accommodate more weight. One end of the 'S' hook was then attached to the same rotational device and the remaining end was attached to a heavier weight. Again, a wide range of weights were tested until an ideal weight was found for each fibre type which provided sufficient tension in the formation of continuous and full coils. This newly enhanced experimental setup is shown in Figure 3-6.

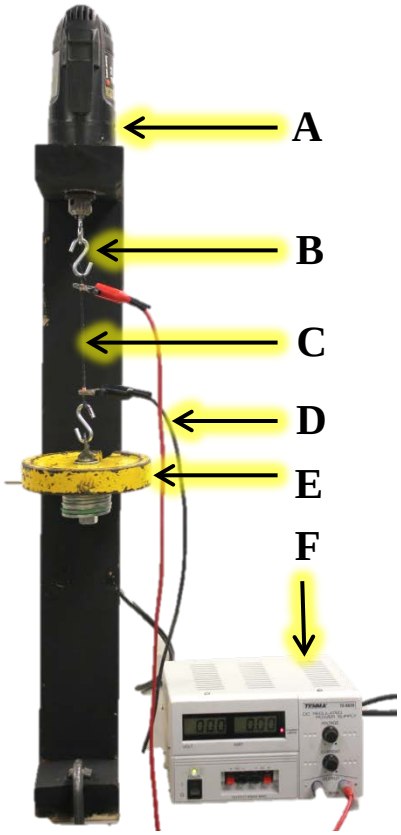

Figure 3-6 Polyethylene TCP twisting and coiling setup ; (A) power drill (B) 'S' hook (C) Polyethylene PowerPro 4-ply filament (D) jumper cables (E) weight (F) power device

Initial polyethylene PowerPro testing began with a weight of 1.13kg and was increased by small increments until reaching a weight of 1.81kg. This weight was found to produce the best coils for a single strand of the fibre. However, no matter how many trials were executed, the fabrication of consistent coils was never achieved. Therefore, due to the relative success of the previous four strand nylon coils, and the lack of consistency in the one strand polyethylene coils, polyethylene coils were then fabricated using four strands exclusively. All four strands of the fibre were attached to the ‘S’ hooks on either end and the weight was incrementally increased from 1.81kg to a final value of 2.68kg, which was found to produce consistent coils.

Based on knowledge gained with the previous fibres, four strand coils were also attempted with the 50lb nylon monofilament. However, it was evident early on that this fibre was not capable of producing continuous and full coils when using four strands. The primary reason is the significantly larger diameter of this fibre which is obtained from a single filament, increasing both its stiffness and the volume it occupies when coiled. For this fibre type, single strand coils were fabricated. The same experimental setup described for the polyethylene fibres was used for the twisting and coiling of these fibres. Using 50cm single strands of the 50lb nylon monofilament, the weight was increased from 209g until an appropriate coiling weight of 706g was found.

A summary of the coiling weights used for the polyethylene and 50lb nylon monofilament fibres is provided in Table 3-2 .

Table 3-2 Summary of the Experimental Parameters of PowerPro Polyethylene and Big Game 50 nylon monofilament

Material	*Diameter*	*Load during Coiling*
Polyethylene PowerPro	460 μm	2680g
Nylon 50lb Monofilament	770 μm	706g

Unlike conductive sewing thread, nylon and UHMWPE fishing line do not contain an imbedded heating element; therefore alternative heating methods are required. While heating of the original 10lb fishing line was done using a heat gun exclusively, a new and unique method of heating the polyethylene and 50lb nylon monofilament was developed which allowed greater control in heating the coils. Once twists were inserted into the fibre(s) and a consistent coil was formed, a 30cm length of 36 gauge Koiler nichrome 80 resistance wire (resistance of 85.3Ω/m) was manually

wrapped around the twisted and coiled precursor fibre as seen in Figure 3-7. The ends of each fibre were also sprayed with Super Shield Nickel Conductive Coating and allowed to dry for a minimum of 5 minutes before wrapping 0.5cm pieces of copper foil tape around each end of the TCP actuator at the electrical connection points. The copper tape was found to not have an effect on contraction, as it was only placed over the knots at each end of the newly formed TCPs. This was done to enhance the positive connection between the power source and the resistance wire within the fishing line.

Figure 3-7 Big Game fishing line twisted and coiled with a manually wrapped Koiler resistance wire

Several nylon fibres were also painted with Thermalcote thermal joint compound. This was done to test the difference between thermal conductive grease (joint compound) and the Supershield

conductive spray coating that was used in all previous trials of Powerpro and nylon 50lb monofilament (shown in Figure 3-8).

Once twisted and coiled, manually wrapped with resistance wire, and covered in some form of conductive coating, the fibres were ready for heat training.

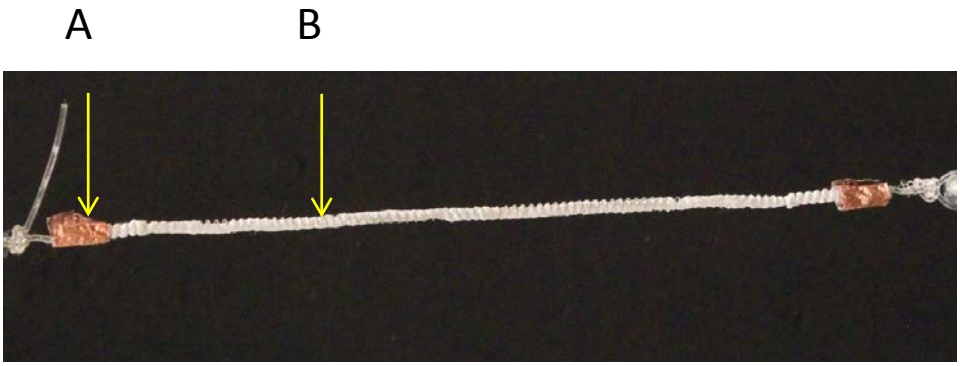

Figure 3-8 Big Game test line with (A) Copper foil tape, and (B) painted with Thermalcote thermal joint compound (white)

3.2.2 Heat Training of Coils

Haines et al. showed that thermally annealing coiled fibres, or "heat training" the coils, can help "set" the polymer's new structure and help prevent end rotation (or untwisting) during actuation [6]. Again, no specific process was described. In this study, nylon conductive sewing threads, as well as fishing line fibres that did not fail (break or tangle) during twisting and coiling were heated with a Wagner (HT3500) heat gun set at 480°C for approximately 10 seconds by continuously moving the heat gun up and down while the newly formed coils remained attached to the drill and payload at each end respectively. This method was found to produce fairly repeatable and

successful results however it was not consistent based on the localization of the temperature. Only fibres with consistent and tight coils after annealing (as in Figure 3-9) were chosen for further processing. Other heating mechanisms were also tested. Several fibres were removed from the fabrication setup and further heated in an oven at 270°C for 45 minutes. Once the oven had been preheated, nylon fibres were placed between two sheets of aluminum foil and placed on the highest oven rack in order to ensure even heat treating of the fibres and verify if this enhanced the contractile response. Once the fibres were deemed of good quality based on visual inspection and properly heat trained (thereby not being able to untwist spontaneously), they were used for experimental measurements and testing using either the heat gun (10lb nylon fishing line) or Joule heating (conductive sewing thread, polyethylene and 50lb nylon fishing line) to provide the heat necessary for contraction.

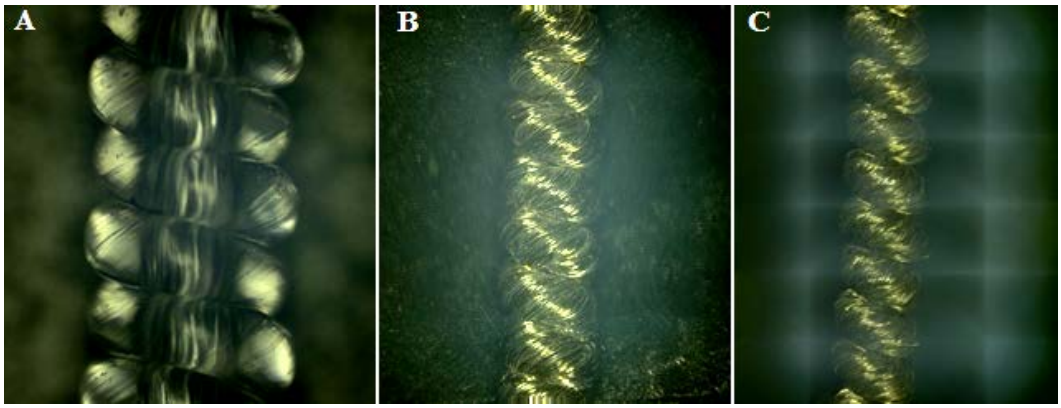

Figure 3-9 Nylon actuator fibres after undergoing a twisting and coiling process, as well as being heat trained. 100x optical magnification of: (A) a single monofilament fishing line fibre, (B) a four fibre coil of Shieldex conductive yarn (117/17 2ply), and (C) a four fibre coil of Shieldex conductive yarn (235/34f 4ply)

Polyethylene proved to be particularly difficult to heat train as it has a much lower melting temperature than that of nylon (refer to Table 3-3).

Table 3-3 Material Properties of Actuator Precursor Polymers [45]–[47]

	Chemical Formula	*Melting Point (°C)*	*Coefficient of Linear Thermal Expansion* $(x10^{-6}K^{-1})$
UHMWPE	$(C_2H_4)_n$	147	100-200
Nylon 6,6	$C_{12}H_{22}N_2O_2$	268	90

When the previously described method of using the heat gun was attempted for the polyethylene, a small contraction was observed. However, it was reversible and inconsistent. This was because the contraction was dependant on the localized temperature provided by the heat gun. Without the heat gun the fibre would immediately cool down and go back to its relaxed state. Moreover, localized melting was observed on the fibre which significantly affected the success of the coils. The heat gun's temperature was thus reduced to 176°C. In this particular case, it was found to be critical that the gun be moved consistently and not held in one spot to prevent hot spots and localized melting of the polyethylene. This step was repeated five times to ensure that the coils had annealed and maintained their new configuration. This heating method was adequate for the heat training phase in order to maintain fibre structure, but in order to move forward to the Joule heating phase a more effective method was necessary to control exact fibre temperatures.

Later heat training of the polyethylene and 50lb nylon fibres was done without the heat gun. Once the resistance wire was wrapped around the coils, the conductive coating had dried and copper foil tape was placed on the fibre ends, the coils were directly heat trained by using the resistance wire heating elements connected to a power supply using Joule heating. This process is described in the next section. Specifically, for the heat training phase of the fabrication process, and in order to

prevent the fibres from burning or failing, Joule heating began at a lower temperature and slowly increased after allowing the fibre to contract for 10 minutes.

3.2.3 Joule Heating

Joule heating is the generation of heat by passing an electric current through a conductive element such as a resistance wire, or conductive sewing thread, therefore producing heat [48]. This is the most convenient way to control actuation heat, without the need for additional equipment [44]. Joule heating also has a coefficient of performance of 1.0, meaning every Joule of electrical energy supplied produces one Joule of heat. This efficiency makes Joule heating an appealing mechanism for heating fibres. The amount of Joule heating that is produced when electrical current flows through a conductor can be calculated using Joule's Law given as:

$$H = I^2 \cdot R \cdot t \tag{6}$$

Where H is the heat produced, I is the current traveling through the resistor or other element in Amps, R is the resistance in Ohms, and t is the duration of current flow in seconds [49]. The performance of the newly twisted and coiled polymer fibres was found to be highly dependent on heat training, as well as ensuring a consistent temperature throughout the fibre during contraction. This is because too much heat during heating burns and melts the fibre, and not enough heat causes a lack of contraction. Moreover, too much heat locally can also be problematic due to locally high fibre temperatures; therefore care must be taken to ensure proper heat distribution throughout the coil.

During initial testing, Shieldex conductive sewing yarn (235/34) was found to produce the most consistent coiled fibres, able to withstand heat training without exhibiting signs of failure. Therefore, these threads were the main focus of most initial Joule heating tests. Nonetheless, a few 10lb nylon monofilaments and 117/17 fibres were also tested. Several of the coiled 235/34 fibres were removed from the coiling apparatus and paired with an identical coiled fibre of the same material. Two twisted and coiled fibres were then plied together to from a helix. This helix was then attached at either end using 4cm copper clamps, as seen in Figure 3-10. Although, helix based actuators were found to produce no advantage over two individual actuators. The conductive sewing yarns are silver plated which can act as a conductive element, allowing Joule heating to occur. Joule heating was the method chosen in previous research for activating contraction of the coiled fibres, as it provided the most control over the heating parameters. However, Cho et al., also applied thermal grease to the precursor fibre to further enhance conductivity between the Shieldex sewing thread TCP actuator and its Joule heating mechanism [44]. For this work, Super Shield Nickel Conductive Coating was applied to the sewing thread fibres where they met the copper clamps, as well as over the length of the fibre. The 10lb monofilament fishing line solely used the heat gun for heating, as it contained no conductive element which would permit Joule heating to occur. The current literature available repeatedly indicates a preference for using Joule heating. However, very little information is available on the parameters used (i.e. current/voltage, resistance, fibre temperature, etc.) or those parameters previously determined for optimal contraction. Many configurations were tested. Based on the system available, 6.4A applied at ~2V worked best, although alternative solutions are possible based on equation 6 above. For this application current is the only parameter that is being changed. Since the wire has a fixed resistance per length and the length remained fairly constant, the voltage needed to change vary little to attain

the ideal current value. The amount of heat produced by this configuration was enough to make the coiled fibres contract without causing them to burn/melt. Only the fibres which sustained the Joule heating process without failing or burning were deemed of adequate quality for use as a TCP actuator.

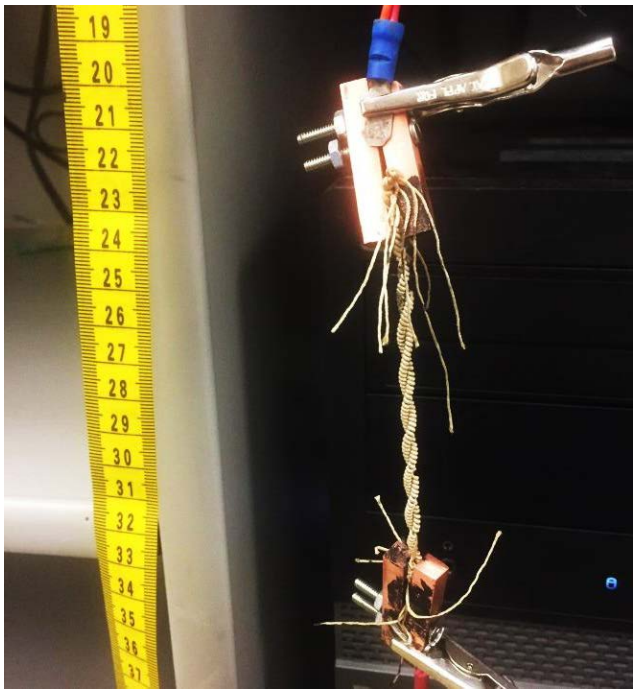

Figure 3-10 Experimental setup used to test Joule heating contraction

Neither nylon nor polyethylene fishing line contains a conductive component. Therefore, to use Joule heating, a conductive element must be incorporated within the coiled fibres in order to be able to control and maintain the temperature. Very little information is provided in the literature on how this can be achieved, so for the purpose of this study, Koiler premium nichrome 80 36 gauge resistance wire was manually wrapped around the formed coils. Initially, 50cm lengths of resistance wire were cut and attached to the 'S' hook alongside the strand(s) of precursor fibre(s) prior to the twisting and coiling phase. However, it was found that when the twisting device began

rotating, the resistance wire coiled inconsistently and was prone to breaking. This is most likely because the conductive wire is much less flexible than the polymer precursor fibres. Slowly and manually wrapping a 30cm long strand of the wire between each individual coil, as shown in Figure 3-11, worked much better once the TCPs were created. This was time consuming but proved to be the most effective way to create consistent conductivity for Joule heating within the polymer fibres at the outset of the study. After testing the first 11 fibres that succesfully made it through all phases of testing, the manual wrapping method was modified by using wire which was cut to match the exact length of the polymer fibre(s) and tying them on the 'S' hook simultaneously. Then, once the fibre(s) and the resistance wire were side by side, the twisting device was turned on at a significantly lower rotational speed and both the fibres and the wire were twisted together, ensuring that the wire coiled at the same rate as the fibre(s). Although the resistance wire broke on occasion due to the reasons described above, the time saving in the fabrication of the actuators was enough to justify the decision to use this process.

Figure 3-11 Twisted and coiled polyethylene actuator with resistance wire manually wrapped along the length of the fibre and kept in place with a small strip of copper conductive tape

Once the fibres were enhanced with their conductive component, they were capable of contraction using the Joule heating method described above. In order to further ensure an adequate connection between the resistance wire and the power supply, small pieces of 0.64cm wide, 2cm long copper conductive foil tape were wrapped around either end of the actuator where the knot was located, forming two copper layers.

The power supply was then turned on for 10 seconds at a time. Once turned on, the copper tape showed the first signs of heating due to its direct contact with the clamps. The resistance wire itself was next to heat, as expected, and after 1 second, the entire fibre was found to be heated to the appropriate temperature, as shown in Figure 3-12. This very quick, but progressive heating mechanism can have a negative impact on the function of the actuator if overheating occurs locally on the fibre due to an ill-spaced resistance wire.

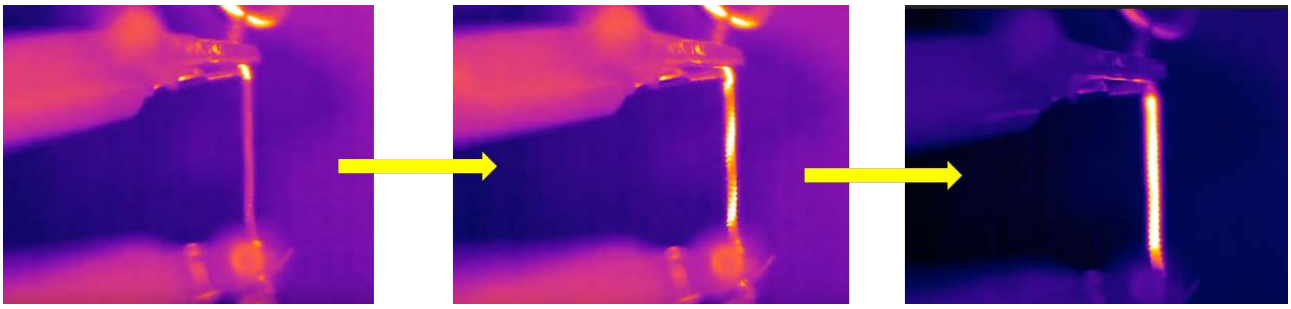

Figure 3-12 Joule heating thermal camera images of TCPs wrapped in resistance wire and with copper taped ends

Once wrapped around the fibre coils, the length of the Koiler resistance wire varied slightly (±1cm) due to the manual nature of the process. This is evidently problematic in maintaining consistency as the length of the resistance wire is directly proportional to its electrical resistance. The heat

generated by the resistance wire is directly proportional to the current flowing through the wire. Therefore, in order to keep the current constant (temperature), either the wire lengths must be the same or the voltage must be adjusted to compensate for the varying lengths.

With the conductive heating element now in place, a range of different currents were tested in order to determine the ideal value for contraction of each polymer. This phase proved to be difficult for the polyethylene fibres because polyethylene has a very low melting point and is very sensitive to temperature fluctuations. Testing began using a similar current as that used for the nylon actuators in order to gauge whether the polyethylene actuator would contract or burn/melt. From there it was easier to increase or decrease the current as needed. In this case, current is the main control parameter for heating since the resistance is fixed based on the length of the wire and accommodated for by varying the voltage (as per equation 6).

Nylon 6,6 has a melting temperature of 268°C (as shown in Table 3-3). Polyethylene, on the other hand, has a much lower melting temperature of 147°C, which means that polyethylene would be much more sensitive to temperature increases due to heating of the resistance while producing an adequate contractile response for producing force [50]. Nylon sewing thread had an optimal contraction current of 6.4A. In order to accommodate the lower melting temperature of polyethylene, Joule-heating for UHMWPE actuators was found to be in the current range of 0.41-0.45A. These lower values take into account the lower melting point of polyethylene, the fibre diameter and internal structure, as well as the higher resistance of the wire. The final ideal current which was used for testing UHMWPE was 0.43A. At this current level, these fibres were actuated with a resistance wire temperature of 238°C, based on the results of the thermal imaging such as

those shown in Figure 3-12. While this temperature is above the melting point of polyethylene, it was found that the 4-strand braided UHMWPE actuators required more heat to contract due to their larger diameter (more fibre material to heat and complex fibre geometry). This, however, likely caused the increase in failure rate for these actuators when compared to nylon, which have a higher melting temperature, due to localised temperature peaks. The 50lb nylon monofilament was heated 5 times at ten second intervals in order to thermally anneal them, where the heat was slowly increased until it reached the optimal heat for contraction. Based on experimental trials this was deemed to be 0.38A, with a resistance wire temperature of 204°C (well below nylon's melting point). In total the fibre was heated ten times from 0.32-0.38A until it was deemed fully heat trained and ready for Instron testing. Overall fibre linear contraction was obtained by manually measuring the relaxed length of the actuator prior to Joule heating with a ruler (given in cm), then comparing the contracted length.

While the actual temperature of the actuator cannot be computed under load, it can be measured experimentally using thermal imaging, as in Figure 3-12. However, as the resistance wire heats up, its resistance also increases, thereby increasing the rate at which the temperature increases. This increase in resistance can be approximated by the following linearized equation:

$$R = R_o[1 + \alpha(T - T_o)] \quad (7)$$

where R is the wire resistance at temperature T, R_o the wire resistance at the reference temperature T_o (where R_o = 85.3Ω/m and T_o = 20°C) and α is the temperature coefficient of resistance (for

nichrome 80, α = 0.00017). Assuming a maximum temperature of approximately 240°C. The maximum percentage change in wire resistance can be calculated as follows:

$$R = 85.3\,\Omega/m\,[1 + 0.00017(240°C - 20°C)] = 88.53\,\Omega/m$$
$$\frac{R - R_o}{R_o} \cdot 100 = \frac{88.53\,\Omega/m - 85.3\,\Omega/m}{85.3\,\Omega/m} \cdot 100 = 3.8\% \quad (8)$$

For the purposes of this study, a wire resistance change of 3.8% can be considered to be negligible.

3.2.4 Contraction Force Measurments

All contraction force testing was done with the use of an Instron Universal Test machine (model 4482) with 1000N load cell in order to obtain the most accurate force data possible. The measurement error for the load cell was ±0.25N, with a displacement error of ±0.02mm. The fibre maintained its configuration attached to the 'S' hook, while each hook was attached to one end of the Instron machine. The experimental setup is shown in Figure 3-13.

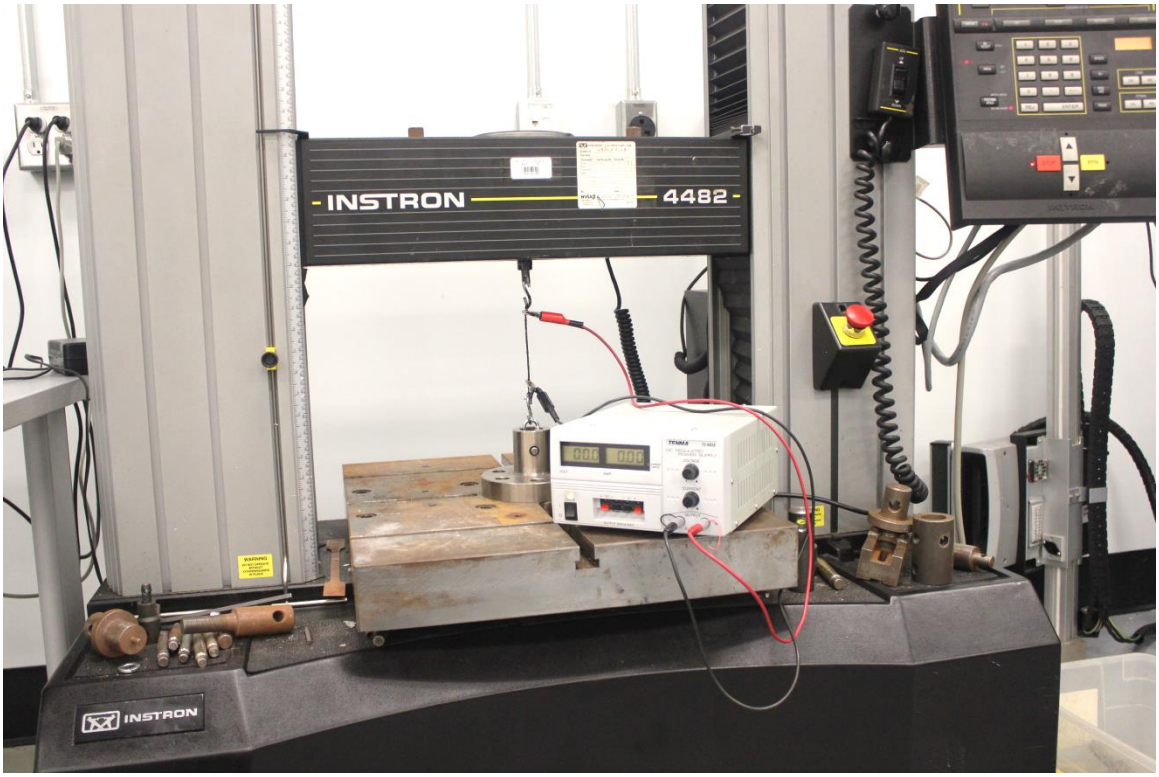

Figure 3-13 Instron testing setup

Chapter 4

Results and Discussion

4.1 TCP Results

Early testing was conducted using 10 lb, 430 µm monofilament fishing line, as this is the most readily available and most similar to that used in previous TCP actuator studies. Testing began by assessing the effect that factors such as fibre length would have on the contractile response. Prior literature had not indicated the exact lengths or contraction ratios clearly. This makes reproducibility of TCP actuator results in the literature very difficult [6]. For the initial tests using the 10lb fishing line only, the contraction percentages were obtained by heating the fibres with a heat gun at 230°C. It was determined that regardless of the initial fibre length; the fishing line only provided an average contractile response of about 8.5% (Table 4-1). For the purpose of using TCPs as lightweight and discrete actuators having a maximum length of 10cm and a contraction of at least 1.5cm or 15% of the maximum length would be required. Therefore, the 10lb nylon fishing line, as initially tested, was deemed to be insufficient. Moreover, nylon monofilament could not make use of Joule heating as is, because it did not contain a conductive element. Therefore, the heat gun had to be used as the heat source for contraction.

While less commonly available, Shieldex nylon conductive yarn (117/17) has also been identified in a number of articles as being the most consistent precursor TCP fibre for strain and force production [6], [28]. To validate the literatures' procedures, one strand actuators were fabricated. However, one strand actuators were found to be too thin for general handling and broke

consistently during twisting and coiling. In an attempt to improve on the fabrication process, four strands of this yarn were tied together at both ends before twisting to produce a larger and stronger form of the fibre. When the yarn is pulled taut, all the fibres have similar stress, and all contribute nearly equally to the overall tensile strength. These 4 strand actuators proved to have a higher overall tensile strength and success rates of twisting without failure than their previous one strand counterparts. The use of four strands of fibre came from the literature consistently referring to the 4 ply nature of the actuators. In fact, "4 ply" actuators in the literature actually relates to the 4 ply fibre construction of the single conductive yarns themselves. Recent work done by Cho et al., however, was also executed with the same 4 strand, '4 ply' TCP actuators, with their results exhibiting similar one strand TCP failures in their initial trials [44]. This once again demonstrates the unclear parameters set out in early work on TCPs. All testing results throughout this work for Shieldex conductive yarns were obtained from actuators made of four strands of these fibres tied together acting as a single fibre, which was found to work better than single strands.

Unfortunately, more than half the conductive sewing thread actuators failed before contraction could be calculated, as shown in Table 4-2. Although many fibres failed during the twisting and coiling process (perhaps due to their thin and delicate nature) and were exempt from the recorded data, many more failed before the Joule heating phase was complete. Of the surviving Shieldex 117/17 fibres that were subjected to Joule heating, only half ended up surviving the process. Inconsistencies and vagueness in the literature with respect to the parameters used in Joule heating made it very difficult to optimize the coiled fibre contraction [8]–[10]. In this study, Joule heating was created by applying a voltage and slowly increasing the current until the coiled fibres showed a reaction. It was observed that many of the fibres did not react before the heat overloaded the

fibres and they burned/melted through. Of the fibres that were properly Joule heated using 6.4A, those that did survive showed similar contractile properties as the 10lb fishing line, with an average contraction of 7% Table 4-1. These fibres, therefore, proved to be too frail and did not contract enough for the purpose of this research and the goal of eventually activating a hand exoskeleton. These results were similar to the work done by Yip et al. in that the "maximum contraction for the 117/17 conductive thread was approximately 10% before the thread burned out" [28].

The 235/34 4 ply Shieldex nylon conductive yarn was also tested. This yarn was double the diameter of the 117/17 yarn. Experimental testing was performed on this fibre in order to account for the inconsistencies observed in the previously tested 117/17 yarn. Of the two Shieldex fibre types tested, the 235/34 was found to be the most consistent which made the production of the TCP actuators out of 235/34 yarn the most reproducible of the previously tested nylon fibres. Most of these fibres made it past the twisting, coiling and heat training processes and were suitable for testing contractile properties using Joule heating. These actuators showed an average contraction of 16% (Table 4-3). Based on the fact that the fibres measured an average of 7.8cm, a 16% contraction would likely be sufficient for use on exoskeletons.

Table 4-1 Nylon 6, 430 µm-diameter 10lb monofilament fishing line contraction values when heated at 230°C

Initial length of fibre (cm)	*Payload (g)*	*Initial coil length (cm)*	*Length of heat trained coil (cm)*	*Length of contracted coil (cm)*	*Contraction percentile (%)*
14.4	209	3.3	2	1.8	10
27.8	209	7.3	8.3	7.7	7
28.3	209	7.1	8.0	7.5	6
30.1	209	7.0	5.6	5.1	9
31.1	209	5.0	3.9	3.6	8
38.0	209	9.0	6.2	5.5	11
50	209	14.2	10.2	9.4	8

Table 4-2 Nylon 6,6 conductive sewing yarn (117/17 2 ply) contraction rates when heat trained at 480°C and heated using 2V at 6.4A

Length of fibre (cm)	*Payload (g)*	*Initial coil length (cm)*	*Baked at 170°C? (Yes/No)*	*Length of heat trained coil (cm)*	*Length of contracted coil (cm)*	*Contraction percentile (%)*
50	180	5.4	Yes	5.7	Failed	-
50	300	3.8	No	4.0	Failed	-
50	300	4.2	Yes	4.4	Failed	-
50	268	6.8	Yes	6.9	6.4	7.23
50	304	7.4	No	7.8	Failed	-
50	268	9.5	No	9.2	8.6	6.52
50	268	10.1	Yes	10.3	9.5	7.76
50	268	7.0	No	7.2	Failed	-
50	268	7.5	No	7.8	7.3	6.41

Table 4-3 Nylon 6,6 conductive sewing yarn (235/34 4 ply) contraction rates when heat trained at 480°C and heated using 2V at 6.4A

Length of fibre (cm)	*Payload (g)*	*Initial coil length (cm)*	*Baked (Yes/No)*	*Length of heat trained coil (cm)*	*Length of contracted coil (cm)*	*Contraction percentile (%)*
50	632	6.6	Yes	5.2	4.0	24
50	632	4.6	No	5.8	4.8	17.24
50	632	9	No	7.8	7	10.26
50	632	8.6	Yes	9.8	8.1	17.35
50	632	5.2	Yes	6.0	Failed	-
50	632	7.3	Yes	7.8	5.1	34.62
50	632	6.8	No	6.4	6.2	3.125
50	632	7.0	No	7.5	6.8	9.33
50	632	6.4	No	6.7	6.0	10.45
50	632	8.1	No	8.4	7.3	13.09
50	632	8.4	No	6.9	5.7	17.39

4.2 Polyethylene and 50lb Monofilament Results

Of the four prospective UHMWPE fibres tested shown in Figure 3-2, only two exhibited favorable results and were further tested in order to determine whether it was possible to make TCP actuators

out of polyethylene. Berkley FireLine uses thermally fused micro fibre technology to create a pseudo monofilament out of UHMWPE braided fibres and Spiderwire Camo-Braid includes a fluorocarbon coating which provides a smooth surface to the conventional UHMWPE braided fibre core. In both cases these fibres were found to be hard to attach to 'S' hooks for the twisting and coiling procedure, and did not coil uniformly or at all when twist insertion was attempted. This is likely due to the increased rigidity of these fibres when compared to the other fibres considered in this study. Power Pro and Sufix 832 UHMWPE braided lines were the only fibres amongst the tested polyethylene that were further tested. It is important to note that the polyethylene fibres considered initially cover the range of polyethylene fibres (and their modified derivatives) currently readily available on the market. Sufix 832 was also eventually eliminated from the testing process after only a few trials due to its lack of contractile response. Although this material was capable of forming mediocre coils, it was not capable of exhibiting the spring like contractile properties that make for an effective actuator. This is likely due to the incompatibility of braided UHMWPE with the included Gore fibre for the proposed use in this study. Therefore, Power Pro was chosen as the sole UHMWPE fibre tested throughout the remainder of this research. PowerPro is a 100lb braided test line with a 460 µm diameter, exhibiting a much higher tensile strength than its nylon counterparts. This work also tested a high strength nylon fibre, Trilene Big Game nylon 6 50lb monofilament.

Early testing of UHMWPE fibres was done with a single strand of polyethylene creating a 1 strand actuator due to the significant increase in strength of the fibres compared to their nylon counterparts. After several trials and testing of various weights, it was noted that the 1 strand actuators were not capable of creating continuous and full coils and, therefore, could not proceed

to the next level of testing. Previous nylon actuators were found to be more effective using a 4-ply configuration. For this reason, the second series of polyethylene actuators were fabricated using a methodology similar to the initial conductive nylon TCPs using 4 separate fibre strands. Again this configuration was much more effective and produced 4 strand actuators that formed uniform and concise coils that could be used for further testing. Once a significant amount of fibres were fabricated and coiled (as seen in Table 4-4) without failing, experimental testing moved on to Joule heating.

Table 4-4 UHMWPE 4-ply actuators fabricated (length presented in centimeters)

Trial	*Initial length*	*Length while attached to 'S' hook*	*Length after twisting and coiling*
1	50	34	10
2	50	39	9
3	50	36	10
4	50	38.1	8.4
5	50	37.3	9.2
6	50	37.2	9.7
7	50	35.4	9.4
8	50	37	9
9	50	39.2	9.7
10	50	36.9	9.4

Trilene Big Game, on the other hand, proved impossible to produce using 4 strands of fibres, so these actuators were created using single strands only. In this case the fibre diameter prevented the meshing of multiple strands into consistent coils.

Both Power Pro and Big Game actuators started out as 50cm strands, and varied in length once they were attached to their respective 'S' hooks. This is because of the manual procedure currently used for attaching the fibres to the 'S' hooks. Therefore, it was difficult to match the actuators with a consistent (25 or 30cm) length of resistance wire. Wrapping the resistance wire manually was

problematic and led to inconsistency in the heating phase. This was due to the wire not being long enough in some cases or excess wire being cut off to accommodate the fishing line length. Since resistance wire length relates directly to the wire's resistance value and affects the ability of current to flow through the wire, inconsistencies in the coiled fibre lengths made it difficult to control the heating throughout the resistance wire. This problem was enhanced by the natural variation (noise) of the variable voltage power supply used. In fact, in order to keep the current required to generate adequate heat for contraction, the voltage must be adjusted in each case. It is clear based on the results of the 50lb nylon actuators shown in Table 4-6 that the length of resistance wire is crucial in obtaining consistent contractile properties. This is demonstrated by the fact that actuators 12-16 were fabricated by paying particular attention to initially cutting these fibres to the same approximate length (37.8-39.6cm) and ensuring that the length of resistance wire was all matched at 30cm, with both being twisted together. It is clear that this produced more consistent contractile percentages without the threat of failure.

As discussed, resistance wire used to create Joule heating in UHMWPE and 50lb nylon actuators were initially cut in equal lengths of 50cm, which was added in with the 4 strands of UHMWPE fibres or 1 strand of nylon fibre and twisted together to form coils. This, however, proved difficult in fabricating successful actuators because of the difference in fibre stiffness. Frequently, the resistance wire broke or failed at locations where twisting or coiling occurred too rapidly and caused localised stress on the wire It was found to be easier and more effective to wrap a 30cm long strand of the resistance wire manually around the TCP actuators once it had already been twisted and coiled for testing purposes. The problem with this approach is that the fibres (although all having an equal initial length), once twisted and coiled, were no longer of equal length. The act

of manually wrapping the resistance wire also created actuators with varying lengths of resistance wire due to the inconsistencies involved in manual procedures.

All nylon fibres were also either sprayed with conductive spray or painted with thermal grease. This was done to further enhance the conductivity and ensure a good connection between the resistance wire and the electric elements used for Joule heating. Only a few fibres ended up being painted with conductive grease because the thermal grease on the pre-coiled actuators was found to cause the nylon actuators to relax after the heating phase more than previous testing had shown. In essence, the length between coils was seen to consistently relax after each contraction, similar to the creep results seen in polyethylene described below. “Creep is a time-dependent deformation process at a stress less than the tensile strength of the material” [51]. Conductive spray, however, seemed to have no negative effects on actuator relaxation.

With a Joule heating element available in each actuator, a variable voltage power supply was used to create the heat for contraction. Many trials were performed in an attempt to produce consistent results. It was crucial to watch the variable voltage power supply to ensure no variations in the current occurred, which could overheat the fibre being tested such as the one shown in Figure 4-1.

Figure 4-1 Overheated polyethylene TCP actuator failure in numerous locations

Once the correct current was determined for each actuator type, the measurement of contraction on multiple actuators was performed. Contraction was determined by accurately measuring the relaxed length of the actuator with a ruler in cm, then subtracting the contracted length taken from the same point of reference on the actuators. UHMWPE based actuators were heated using a current of 0.43A, thereby producing a temperature of 238°C, and results of these tests are shown in Table 4-5. Contraction lengths were measured manually with a ruler after one cycle of contraction, performed once the heat training phase was completed. Conversely, 50lb nylon based actuators were initially heated using a current of 0.32A and slowly increased to 0.38A, subsequently producing a temperature of 204°C, after ten trials beause nylon was found to be extremely sensitive to localised temperature fluctuations. Since nylon fibre contraction was optimized close to the nylon's melting temperature of 220°C, small variations in current could lead to fibre failure. In fact, actuators that provided heat by a current even slightly above these values, such as 0.4A, failed as shown in Figure 4-2, and were not included in the results portion of this work. Contraction results of the 50lb nylon Big Game based actuators are shown in Table 4-6. In this case, the first eleven trials were completed with 30cm long strands of resistance wire, where trials 12-16 were done with a length that matched that of the nylon fibre attached to the 'S' hook.

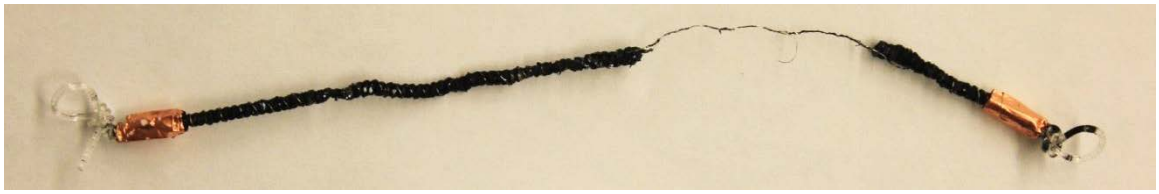

Figure 4-2 Nylon actuator 0.4A

Along with its significantly higher strength, Table 4-5 demonstrates the positive contractile characteristics of those UHMWPE that did not fail. UHMWPE actuators are capable of producing an average single contraction which is similar or better than the other fibres in this study, while producing the largest contractile force, making them a potential candidate for TCP actuator fabrication.

Table 4-5 UHMWPE TCP contraction results while heating at 0.43A

Trial	*Length while attached to 'S' hook (cm)*	*Length after Twisting and Coiling (cm)*	*Length after Heat Training (cm)*	*Contraction (%)*
1	48.2	11.91	14.2	7.7
2	49.7	11.9	13.3	10.2
3	46.2	11.12	13.2	10.6
4	47.2	13.3	13.7	8
5	46.2	10.3	12.3	fail
6	44.1	10.7	fail	-
7	47.8	10.5	12.6	8.7
8	48.4	10.13	12.1	13.2
9	47.9	10.0	13.2	9.8
10	47.9	10.3	12.1	13.2
11	48.1	10.4	11.4	fail
12	48.4	10.8	12.4	fail
13	48.8	10.2	13.2	10.6
14	46.8	10.6	fail	-
15	46.9	10.1	13.1	10.7
16	48.9	10.7	fail	-
17	47.6	10.4	11.8	10.2

Unfortunately, UHMWPE fibres demonstrated a large amount of relaxation after each heating and contraction cycle. The problem is that polyethylene exhibits creep, which is further discussed in in section 4.3. After each contraction cycle the fibre would relax and the length of the actuator would increase by an average of approximately 0.21cm. These results are shown in Figure 4-3 where a single polyethylene TCP actuator was taken and repetitively contracted ten times, after having completed heat training, in order to determine whether the creep found in these fibres had a reasonable limit.

Table 4-6 Nylon Big Game 50lb 1-ply TCP actuator results while heating at 0.38A

Trial	*Length while attached to 'S' hook (cm)*	*Length after Twisting and Coiling (cm)*	*Length after Heat Training (cm)*	*Contraction (%)*
1	35.6	8.8	fail	-
2	32.1	8.8	9.9	11.3
3	31.6	8.4	9.3	14
4	35.1	fail	-	-
5	34.1	8.7	9.1	9.8
6	35.9	9.2	fail	-
7	35.6	8.7	10.9	10.1
8	33.1	8.8	fail	-
9	34.4	8.7	9	13.3
10	37.1	9.3	11.2	11.6
11	37.7	9.2	11.6	12
12	39.2	9.6	11.2	10.7
13	38.7	9.4	10.5	10.5
14	39.6	9.5	10.7	10.2
15	38.4	9.6	11.2	10.7
16	37.8	9.2	11.1	10.3

Repetitive contraction measurements were, therefore, difficult to measure. For this reason, the contractile results given in Table 4-5 are from a single contraction, directly executed after the end of the heat training phase. Moreover, it would be difficult to implement these UHMWPE actuators into an exoskeleton due to their constantly changing length. Their continued relaxation (creep) after each contraction would prevent them from being a suitable material candidate for further actuator fabrication.

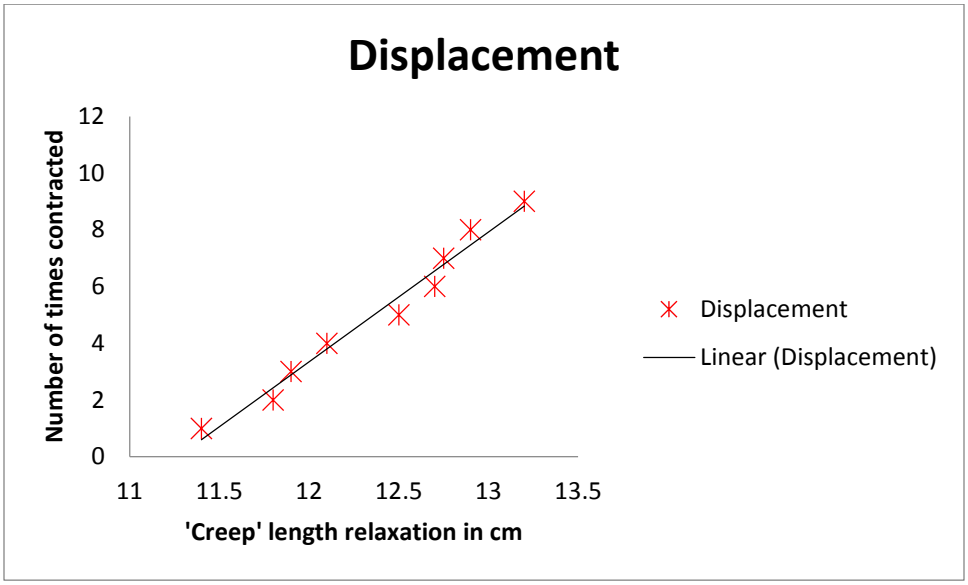

Figure 4-3 'Creep' data for repetitive contraction of a single polyethylene TCP actuator

In an attempt to make up for this drastic shortcoming, numerous adjustments were attempted to keep UHMWPE TCP actuator lengths constant. One variation was placing wires in the oven after twisting and coiling to produce consistent annealing of the coils throughout. This seemed to make no difference in contraction potential. Another variation was spraying the actuators with a conductive coating spray prior to contracting. The conductive spray was applied in an attempt to harden the polyethylene into its coiled configuration while still maintaining its contractility. Heat shrink wrap was also used, which seemed to help at first, but overtime, the coils would slip within

the casing allowing creep to occur. Despite the many attempts to account for this creep behavior, nothing seemed to elongate the service life of these actuators and keep the length of the TCP actuators consistent enough for repeated use. This creep demonstrates the difficulty of using such fibres in biomimetic applications.

To further quantify the contractile force results and solidify the conclusions drawn above, all successful fibre samples (Shieldex conductive yarn (117/17), nylon 10lb monofilament, PowerPro UHMWPE filament, and nylon Big Game 50lb monofilament) were tested on an Instron Universal Testing machine to compare contractile responses and actuation force results for each. Since only 50lb nylon based actuators seemed to produce results which would lend themselves to be useful in a hand exoskeletons, these actuators were thoroughly tested for maximum contraction force capacity on the Instron machine. This was done to determine whether they would be useful in activating a spastic hand exoskeleton.

During testing with the Instron machine, fibres remained attached to their ‘S’ hooks, while the ‘S’ hooks were hooked onto either end of the machine. The Instron machine was used to record force and displacement values while the variable voltage power supply (or in the case of the nylon 10lb monofilament, the heat gun) was used to provide the heat for heating the fibre, as before. All tests began with a 2N preload, prior to heat activation.

Nylon 10lb monofilament was tested while being heated by manually moving the heat gun up and down along the length of the fibre. This caused a cyclical contraction, where the actuator would relax when cooled and produce a contraction force when heated, as seen in Figure 4-4. Upon

cooling, the actuator would relax slightly below the pretension load. However, during heating, the actuator exhibited a peak contraction force of 1.3N above the pretension value.

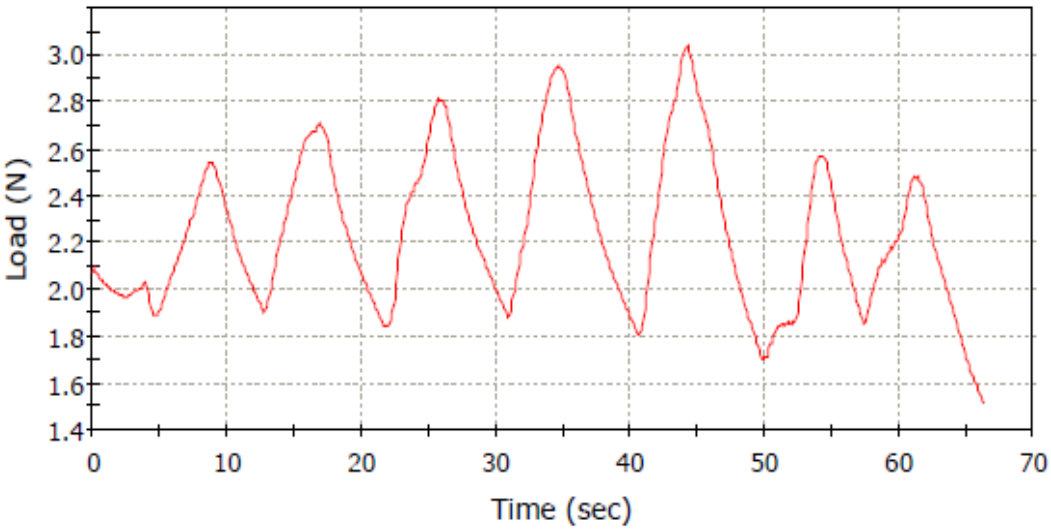

Figure 4-4 Instron testing peak force output for a nylon 10lb monofilament actuator

Shieldex conductive yarn (117/17) also exhibited a cyclical contraction force due to the fact that it is very sensitive to burning and failure. In order to prevent overheating these fibres, the power supply was turned on at 6.4A for a few seconds at a time to demonstrate peak force output without failure, as seen in Figure 4-5. These fibres demonstrated a peak contraction of 0.9N once settled.

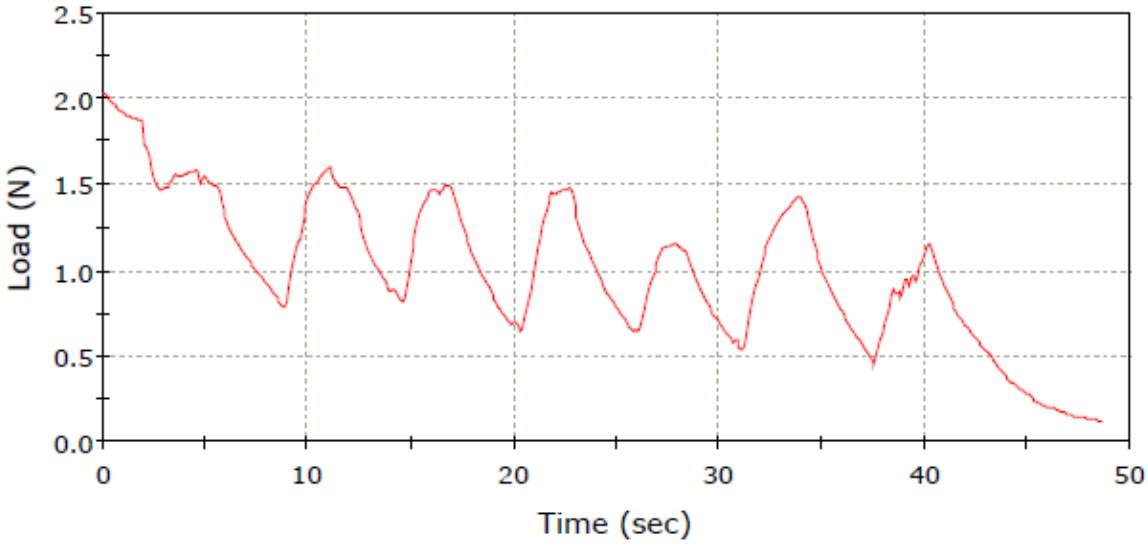

Figure 4-5 Instron testing peak force output for a Shieldex conductive yarn actuator

PowerPro UHMWPE fibres were by far the most successful in producing a large contraction force. Throughout UHMWPE force testing, only one contraction of each fibre was examined. This is because the creep in the fibre did not allow for continuous results. It is seen in Figure 4-6 that this actuator fibre was capable of producing a peak force of 11.1N above the pretension value. These results are much higher than any other polymer tested in this study.

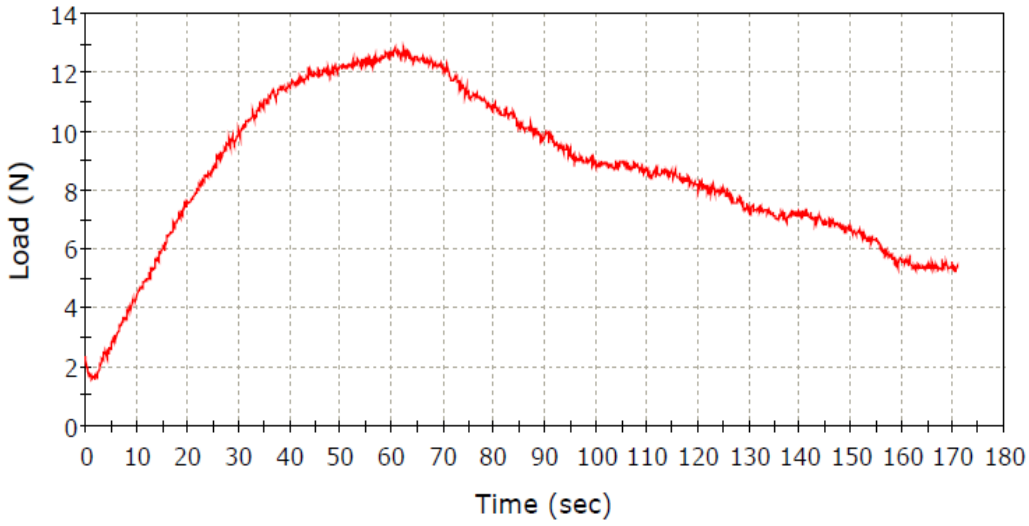

Figure 4-6 Instron testing peak force output for a PowerPro polyethylene actuator

Nylon 50lb monofilament demonstrated a peak force production of approximately 2.4N above the pretension value with a steady decline over time. Figure 4-7 is representative of all nylon 50lb actuator testing that was done using the Instron. All other corresponding graphic results are presented in Appendix C. Heating of the fibre to peak contraction (as demonstrated in Figure 4-7 took an average of 45-50 seconds using the described setup. All fibres steadily began to decline in their contractile force response after the peak value until eventually dropping down to their pre-stretched state. This is likely due to their peak internal heat allowance, which would cause most polymers to stretch under load over time and is to be expected. Under normal conditions, heating would not be expected to occur past the peak load. Activation occurred at temperatures slightly below the melting point of the individual fibres. In certain tests, due to a very sensitive dial, the power supply increased on its own past 0.38A and led to certain fibres failing within seconds.

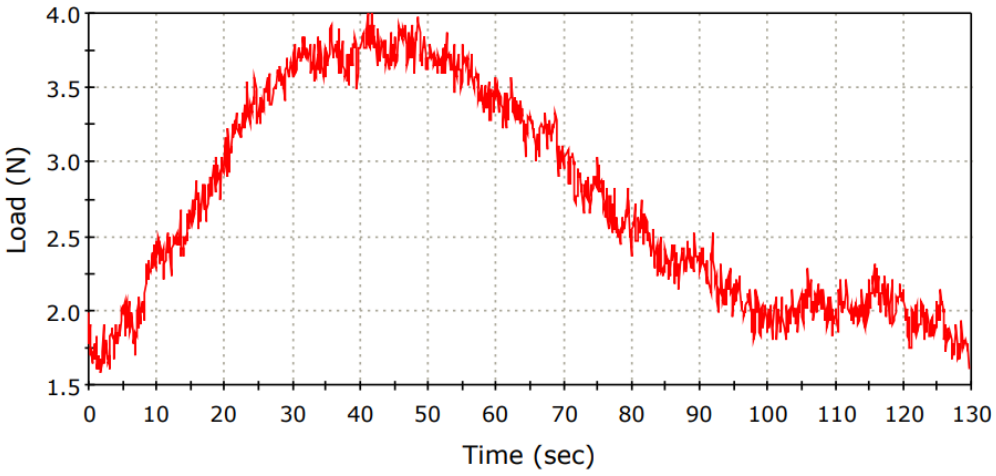

Figure 4-7 Instron testing peak force output for a nylon 50lb monofilament actuator

As an interesting attempt to improve on the contractile force properties of TCP actuators, three 50cm nylon actuators that were approximately of the same length (Table 4-7) were also taken after their individual twisting, coiling and heat training phases and placed side by side and twisted together to form a helix, using a strip of copper foil tape to attach them together at either end, as seen in Figure 4-8. This was done to see if placing three individually fabricated actuators together would allow this 'super' actuator to produce significantly more force in comparison to a single TCP actuator. Testing for this 'super' actuator was performed using 1013g of weight.

Figure 4-8 Three nylon TCP actuators attached together with copper foil tape

Table 4-7 'Super' 3-ply actuator lengths

Trial	*Length while attached to 'S' hook (cm)*	*Length after Twisting and Coiling (cm)*	*Length after Heat Training (cm)*
1	38.8	9.5	11.0
2	38.3	9.9	10.9
3	37.5	9.2	10.7

The three actuator helix configuration that was created was also tested on the Instron machine. In this case, the results (shown in Figure 4-9) indicate that the 'super' actuator only produced slightly more force than its single counterparts. However, heating took longer to achieve peak contractile force. This is because the 3-strand helical configuration may possibly prevent linear displacement

of individual fibres based on the spring like nature of TCPs and the newly formed helical bias angle of the fibres. The ‘super’ actuator may also be affected by inconsistent Joule heating because of the nature of the helical configuration which distributes heat from the resistance wire differently than in a single TCP.

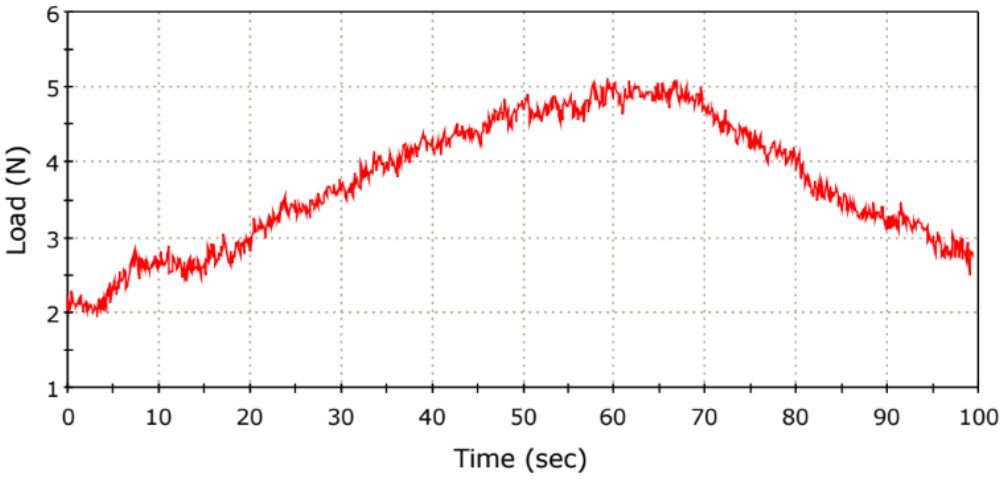

Figure 4-9 Instron testing peak force output for the 3 actuator helix configuration

Table 4-8 below summarizes the fabrication parameters necessary to fabricate the most successful TCPs of each fibre type.

Table 4-8 Summary of Fabrication parameters for all fibre types (all force tests were done with a 2N preload)

Fibre Type	*Force (N)*	*Contraction (%)*	*Configuration*	*Current*	*Temperature*
Nylon 10lb monofilament	1.3N	8.5%	1 ply	-	230℃
Nylon 6,6 Shieldex 117/17	0.9N	7%	4 ply	6.4A	-
Nylon 6,6 Shieldex 235/34	-	16%	4 ply	6.4A	-
UHMWPE PowerPro 100lb braided	11.1N	10.26%	4 ply	0.43A	238℃
Nylon 50lb monofilament	2.4N	11.21%	1 ply	0.38A	204℃

4.3 Discussion

The results obtained in this study demonstrate a crucial need for proper measurement of parameters and maintaining adequate quality control of various fabrication steps. These results indicate that the fabrication parameters for TCP actuator development set out by previous research were not clear and reproducible. The vague experimental setup and fabrication parameters provided in these studies led to inconsistencies in actuator performance.

Prior to initiating the twisting and coiling phase, the amount of precursor actuator fibres must be chosen (i.e. 1, 2, or 4 strands). Throughout the twisting and coiling of the polymer fibres it is very important to maintain consistency in the initial length of actuator fibre, the amount of strands used to create the actuators, the payload used to create tension in the fibres, the number of rotations necessary to fully twist and coil a fibre of chosen length, and a consistent temperature throughout

the entire actuator during contraction. Minute variances in these parameters can drastically alter fabrication and contractile results. Further instrumentation and automation would need to be developed to better control these parameters during the fabrication process, such as a rotation device capable of controlling the total number of turns and its speed of rotation. Based on this research, an automatic coiling device has been developed which is capable of creating TCP actuators of exact length, providing significantly more consistent results. These actuators also demonstrated improvement in contractile force results. This device is shown in Figure 4-10.

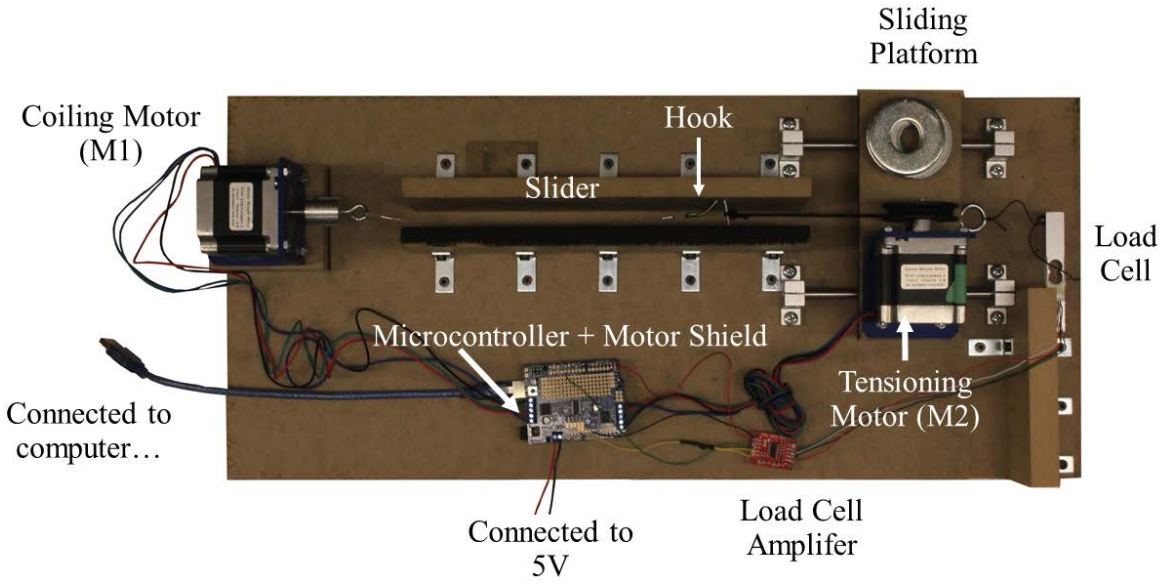

Figure 4-10 Consistent twisting and coiling device [52]

As discussed above, the tension payload weight during fabrication is adjustable within a narrow range for each fibre type and configuration. However, it must be enough to hold the fibre taught while not overloading the fibre to the point of breakage [6]. Each fibre combination proved to have a “critical point”, (i.e. a weight that was ideal for twisting and coiling without causing failure). Another inconsistent variable that needs to be better controlled is the heat emitted from the heat

gun during the heat training process of initial nylon testing. Although the heat gun was moved up and down manually at a constant rate, it is hard to ensure that all fibres were heated consistently. Perhaps for future work, fibres can be heated in an inert environment (such as hydrothermal actuation in water) at a constant temperature [6]. This work attempted to account for this by placing several Shieldex and polyethylene fibres chosen at random in an oven after initial heat training. However, in comparison these fibres showed identical contraction rates to those heat trained using only the heat gun.

A number of variables must also be controlled throughout the Joule heating process of these TCP actuators. To ensure all fibres are actuated similarly, the same power supply was used for all fibre testing. Both conductive sewing yarns were heated with a consistent initial current of 5.0A that was slowly increased until the actuators began to contract at 6.4A. For UHMWPE fibres, a current of 0.43A was established as being critical to generate the heat required for contraction. However, the actual temperature at any given point along the actuator may have varied, causing failure in some cases. The precise control of temperature throughout the actuator is a critical requirement in the global success of the actuator. In future work, contact-typed temperature sensors such as a thermistors within the fibres themselves, could be used in a control loop to accurately track the temperature of the actuator, similar to the temperature control mechanisms used in the work by Cho et al. [44]. These sensors work well because they are small and easy to use.

The initial contraction of UHMWPE TCP actuators showed great promise for future work in hand exoskeletons due to their high force, low profile contraction, which demonstrated greater results than any previously tested TCP actuators. The most crucial limitation observed throughout the

testing of UHMWPE based actuators was creep, or the relaxation its polymer chains within the fibre itself. Polyethylene fibres are susceptible to an irreversible extension along the length of the actuator when placed under long-term static or dynamic loads [53]. This level of elongation is proportional with time and dependent on the type of polymer, operating temperature, melting temperature, mean load, and loading time" [53], [54]. Creep is enhanced at higher temperatures which proved to be a major limitation on the potential service life of UHMWPE fibres throughout actuator fabrication. After each contraction the fibre exhibited major deformation and produced less force until ultimately losing its "spring-like" formation and returning to a long, uncoiled linear fibre. This would make the implementation of UHMWPE fibres as exoskeleton actuators very difficult. Specific testing regarding the contraction force of these actuators would be necessary to assess their use in future designs.

Contraction force of Shieldex conductive yarns as well as 10lb nylon polymer fibres was shown to be insufficient in actuating exoskeletons. The mean maximum voluntary grip force of a standard healthy individual is 245±178N during power grip tested with a standard size dynamometer [55]. The typical grip force in a stroke patient suffering from spasticity in their hand is 55±14.7N [55]. A great deal of mechanical advantage would be necessary to power a device capable of overcoming these values. Therefore, the exoskeleton would be unable to open the fingers of a patient with a spastic hand using the fibres as actuators.

Throughout the process of TCP development many other fibres were considered. After numerous trials using UHMWPE, which later proved to be unsuccessful due to creep, a survey of other high strength fibres was conducted. Kevlar (para-aramid synthetic fibre), a man-made organic fibre

which is part of the polyamide family, was also initially considered as a possibility. This fibre has a very high strength and high thermal stability in comparison to previously tested fibres (as shown in Table 4-9), and does not melt, rather it begins to decompose at high temperatures [56], [57]. Carbon fibre was also considered in search of the perfect precursor fibre for TCP actuator development. Carbon fibre has a composition of at least 92% carbon atoms. It has an incredibly high melting point and anisotropic properties that made it an interesting precursor option [58]. The problem with these materials is their low coefficient of linear thermal expansion, especially in comparison to that of nylon ($90x10^{-6}K^{-1}$), or polyethylene (100-200$x10^{-6}K$), as shown in Table 4-9. A high coefficient of linear thermal expansion is the key parameter which allows a coiled structure such as those described above to contract when heat. Nonetheless, these two fibres were briefly tested with the same methodology as that used for UHMWPE. However, it was quickly evident that they were not good candidates for TCP fabrication. Kevlar was capable of making it past the twisting and coiling phase, as well as the implementation of resistance wire. However, as expected, it showed no contraction when heated (seen in Figure 4-11A). Carbon fibre, on the other hand, was not even capable of forming coils. The fibres broke upon twist insertion (as seen in Figure 4-11B).

Table 4-9 Material properties of Kevlar and carbon fibre [56]–[58]

	Chemical Formula	*Melting Point (°C)*	*Coefficient of Linear Thermal Expansion* ($x10^{-6}K^{-1}$)
Kevlar	$C_{14}H_{14}N_20_4$	Does not melt, begins to decompose at 427-482	3 or less
Carbon Fibre	Long chains of Carbon atoms	3700	2.25

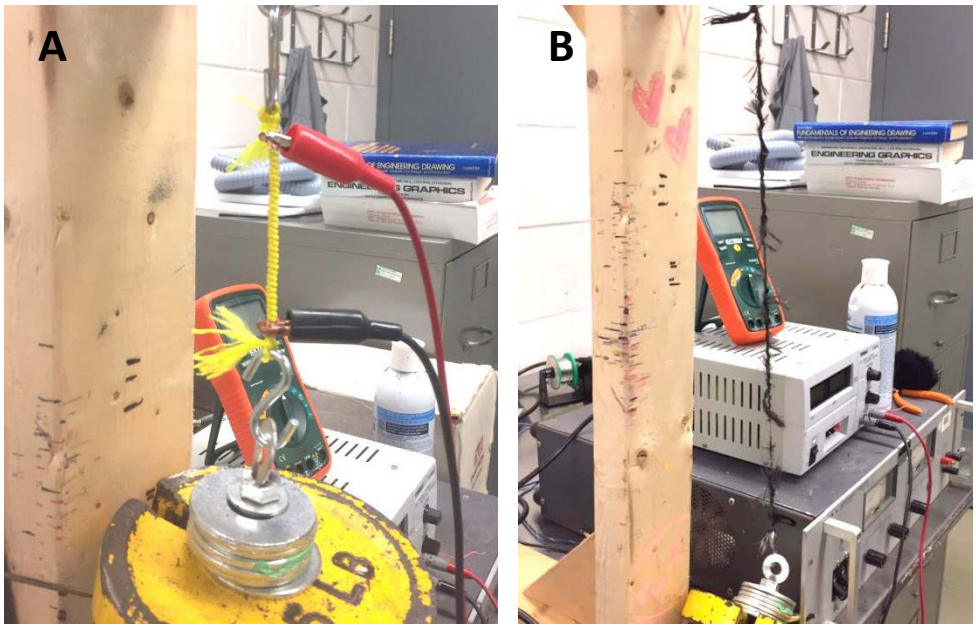

Figure 4-11 (A) Kevlar coiled polymer with no contraction (B) broken carbon fibre

Trilene Big Game 50lb nylon monofilament was found to be the most reproducible and consistent of all fibres that were tested throughout this research. They were able to twist and coil with ease, and capable of Joule heating with minimum failure. These fibres were also capable of repeated contractions by turning the power supply on and off without demonstrating creep or large levels of relaxation. Once the fibres were attached to the Instron, they were preloaded equally at a load of 2N. When the Instron machine indicated the 2N preload, the power supply was turned on and a current of 0.38A was applied for 2 minutes. Throughout these two minutes the Instron machine collected force data from the fibre. Throughout the Instron testing it was found that each actuator was capable of producing approximately 2N of force when subtracting the preload force that was initially introduced. A different configuration using multiple actuators or a significant mechanical advantage could be used to achieve the requires force of 40-70N to overcome the force of a spastic hand [55]. However, the alternative 3 actuator helix configuration discussed above produced only

a slightly higher force of a little over 5N. This small increase may not justify the extra complexities of fabrication, or the time necessary to reach the peak contractile force.

The contributions of this work are emphasized in the results presented in Table 4-10 compared to the actuation devices used to power several commercially available designs described in section 2.4. These tables also demonstrate the vast difference between the weight of conventional actuators and their force outputs compared to TCP actuators.

Table 4-10 Comparison of exoskeleton device actuators

Exoskeleton Design	*Actuator Weight*	*Force (N)*	*Portability*	*Weight of Device (g)*
HWARD (pneumatic)	2 McKibben pneumatic ~ 400g	Can produce up to 122N, but regulated at 4-15N	No	~**2000g** without air compressor
Wu et al. (pneumatic)	1 McKibben pneumatic ~ 200g	10-12N	Yes	~**800g** without air compressor
HANDEXOS (electric)	1 DC motor/finger 28g x 5 = 140g	63-147N/finger	Yes	595g device + 200g actuation block → **795g**
HEXORR (electric)	2 brushless motors 320g → fingers 220g → thumb 4 bar linkage	33N	No	**2400g** without virtual environment
Mistry et al. (hydraulique)	120g	12N per finger	No	**2620g** glove + 120g hydraulic module
Nylon 50lb monofilament based device	0.19g	2.4N x 4 = 9.6N	Yes	Can be as small as 200g Exoskeleton + 0.19g x 4= .76g →**200.76g**
UHMWPE based device	0.34g	11.1N	Yes	Can be as small as 200g Exoskeleton + .34g → **200.34g**

Haines et al. achieved a maximum contractile force of 0.44N with 127μm nylon 4lb monofilament. Instron testing was used to verify whether the novel actuation devices developed in this work were capable of producing more force with larger contractile strokes than those presented by Haines et al. The fibres that were tested in this work consisted of 430μm nylon 10lb monofilament, 234μm Shieldex conductive yarn (117/17), 468μm Shieldex conductive yarn (235/34), 460μm PowerPro UHMWPE braided filament and 770μm nylon 50lb monofilament. The thinner more delicate nylon fibres (conductive yarn and 10lb monofilament) demonstrated a small force output of 0.9N and 1.3N respectively. These values were too low and inconsistent to be able to overcome the spastic force of a human hand. The UHMWPE actuators exhibited the greatest amount of force, with a peak contraction of 11.1N. These results would be favorable if polyethylene did not exhibit creep, thereby hindering its ability to be used in biomimetic applications. The nylon 50lb monofilament actuators demonstrated the most promising results. It was found that each muscle was capable of 2.4N of contraction force per cycle. Since a force of at least 40N is necessary to extend all fingers of a spastically closed hand, the strength of independent actuators for each digit would be necessary in an exoskeleton design, along with the help of a system which could provide a mechanical advantage. A summary of the results is provided in Table 4-11.

Table 4-11 Summary of actuator contractile force results

Precursor Fibre	*Diameter (μm)*	*Cross-Sectional Area ($\times 10^{-8} m^2$)*	*Contractile Force (N)*
Nylon 4lb monofilament (Haines et al.)	127	1.27	0.44
Nylon 10lb monofilament	430	14.5	1.3
Nylon 6,6 Shieldex 117/17	234	4.30	0.9
Nylon 6,6 Shieldex 235/34	468	17.2	-
UHMWPE PowerPro 100lb braided	460	16.6	11.1
Nylon 50lb monofilament	770	46.6	2.4

Chapter 5

Contributions, Conclusions, and Future Work

5.1 Contributions

The goal of this thesis was to investigate the work by Haines et al. on twisted and coiled nylon fibres which undergo linear deformations as a result of changes in temperature. The work by Haines et al. is extended by improving the function and contractile force properties of these twisted and coiled polymer actuators in an attempt to verify whether it would be feasible to implement TCPs as the contractile power source in an upper limb therapeutic exoskeleton. The research performed by Haines et al. was the first to propose the manipulation of these fibres into light-weight, high power actuation devices. The problem, however, is that no consistent fabrication process was defined in their work, making it difficult to mimic their results. Since the development of TCP actuators is still in its infancy, further investigation was required of experimental parameters that allow for predictable fabrication. This information was required in order to test fibre contractile and force properties in determining whether they are capable of powering a hand exoskeleton device.

To address the problems mentioned above, this thesis investigated current fabrication parameters and processes and proposed novel methodology. The particular contributions of this thesis are as follows:

1. Determined reproducible fabrication parameters to create TCP fibre actuators made of nylon and UHMWPE.
2. Determined ways to increase the force output of the actuators.
3. Determined ways of increasing contraction to maximize linear displacement.
4. Determined ways of controlling the heating/activation of the actuators.
5. Investigated ways of limiting creep.
6. Investigated options for making therapeutic hand exoskeleton devices low-cost, lightweight, aesthetically pleasing, low-profile and portable.

5.2 Conclusions

An exhaustive literature review was conducted to understand the current state of TCP actuator research, as well as broaden the understanding of current actuation devices used to power upper limb exoskeletons and their associated advantages and limitations. This research analysis led to the clarification that there are evident shortcomings in actuation devices currently capable of powering such an exoskeleton in a discrete, portable, and aesthetically pleasing manner. Actuator technologies are currently not capable of producing large force outputs without the need for bulky and non-portable instrumentation such as pressure systems and air compressors. Therefore, in an attempt to decrease the overall volume, weight, and cost of a hand exoskeleton, this work proposes a novel mode of actuation, in the form of TCP actuators. This work provided an experimental understanding of parameters for the fabrication and contractile properties of low-profile polymer actuators by developing and testing twisted and coiled polymer fibres to asses the feasibility of their use in upper limb, hand exoskeletons.

The experimental procedures used by Haines et al., were redeveloped and a comprehensive experimental evaluation of nylon 6 and two nylon 6,6 fibres was conducted. Initial TCP fabrication consisted of 10lb nylon monofilament, as well as four strands per actuator composed of Shieldex conductive sewing yarn (117/17 2 ply, and 235/34 4 ply). Work was also done on high strength UHMWPE fibres as well as much stronger 50lb nylon monofilament. Upon twisting and coiling of nylon 6 and nylon 6,6 fibres, it was evident that these fibres were frail and highly susceptible to failure without hope of providing much contractile force. On the other hand, UHMWPE was capable of twisting, forming continuous and full coils, and generating a large contractile force. The problem, however, was that polyethylene demonstrates significant creep characteristics which would relax the TCPs by up to 0.21cm after each contraction cycle. This hindered its use as a consistent actuator. Other polymers such as Kevlar and carbon fibre were also tested. However, due to their small coefficient of linear expansion, they also proved to be ineffective actuators. The fibre considered to be most appealing for TCP actuator development was 50lb nylon monofilament, which provided the most consistent contractile results. With the implementation of Koiler conductive wire for conductivity, and Joule heating, these fibres showed the most promising properties.

This research has demonstrated that properly selected and fabricated TCPs could likely be used to power hand exoskeletons, but further work would be required in the design of the exoskeleton to use TCPs to their full potential.

5.3 Recommendations for Future Work

The scope of this thesis mainly revolved around the fabrication and preliminary prototyping of linear TCP actuators in order to test the feasibility of their implementation into a spastic hand exoskeleton.

The experimental results of TCP fabrication and contraction proved to be valuable in assessing the feasibility of polymers as actuators in hand exoskeletons. There are, however, numerous changes and improvements that can be made to the experimental setup used throughout actuator fabrication in order to further enhance results and improve consistency. TCP development is currently unreliable, leading to many inconsistencies throughout contraction. In order to greatly advance actuator development, many manufacturing parameters must be better monitored for consistent results. Throughout the twisting and coiling of the TCP fabrication it will be important to create a device capable of generating the same number of rotations at a controlled speed of rotation for every single fibre. This will allow all polymer actuators to uniformly rotate without causing failure by over rotation. A method to measure the exact temperature within the polymer fibre would also greatly improve the actuator fabrication process. This could be controlled using an embedded contact-type temperature sensor such as a thermistor, within the fibres themselves, in order to accurately track the temperature of the actuator at any given time, similar to the temperature control mechanisms used in the research by Cho et al. [63]. Another method of temperature regulation that must be controlled, which is imperative to the success of the actuator, is the output of current from the variable voltage power supply. A mechanism must be applied to ensure that the current running through the resistance wire does not increase or decrease spontaneously, but rather stays the same throughout operation.

Due to the large amount of manual labour involved in fabricating and testing these TCP actuators, few testing repetitions were possible. Many more repetitions would be required to validate the positive results obtained herein if these actuators are to be used commercially. Automated fabrication procedures such as those shown in Figure 4-10 would be necessary to increase the number of actuators available for testing.

References

[1] A. D. Pandyan, “Spasticity: Clinical perceptions, neurological realities and meaningful measurement,” *Disabil. Rehabil.*, vol. 27, no. 1–2, pp. 2–6, Jan. 2005.

[2] P. Brown, “Pathophysiology of spasticity.,” *J. Neurol. Neurosurg. Psychiatry*, vol. 57, no. 7, pp. 773–777, Jul. 1994.

[3] R. W. Bohannon and M. B. Smith, “Interrater Reliability of a Modified Ashworth Scale of Muscle Spasticity,” *Phys. Ther.*, vol. 67, no. 2, pp. 206–207, Feb. 1987.

[4] C. P. Phadke, C. K. Balasubramanian, A. Holz, C. Davidson, F. Ismail, and C. Boulias, “Adverse Clinical Effects of Botulinum Toxin Intramuscular Injections for Spasticity,” *Can. J. Neurol. Sci.*, vol. 43, no. 2, pp. 298–310, Mar. 2016.

[5] A. T. Helal, “Material Characterization of a Dielectric Elastomer for the Design of a Linear Actuator,” Thesis, Université d’Ottawa / University of Ottawa, 2017.

[6] C. S. Haines *et al.*, “Artificial Muscles from Fishing Line and Sewing Thread,” *Science*, vol. 343, no. 6173, pp. 868–872, Feb. 2014.

[7] C. S. Edgren, R. G. Radwin, and C. B. Irwin, “Grip Force Vectors for Varying Handle Diameters and Hand Sizes,” *Hum. Factors*, vol. 46, no. 2, pp. 244–251, Jun. 2004.

[8] H. C. Fischer, K. Stubblefield, T. Kline, X. Luo, R. V. Kenyon, and D. G. Kamper, “Hand Rehabilitation Following Stroke: A Pilot Study of Assisted Finger Extension Training in a Virtual Environment,” *Top. Stroke Rehabil.*, vol. 14, no. 1, pp. 1–12, Jan. 2007.

[9] P. Polygerinos, Z. Wang, K. C. Galloway, R. J. Wood, and C. J. Walsh, “Soft robotic glove for combined assistance and at-home rehabilitation,” *Robot. Auton. Syst.*, vol. 73, pp. 135–143, Nov. 2015.

[10] P. M. Aubin, H. Sallum, C. Walsh, L. Stirling, and A. Correia, “A pediatric robotic thumb exoskeleton for at-home rehabilitation: The Isolated Orthosis for Thumb Actuation (IOTA),” in *2013 IEEE International Conference on Rehabilitation Robotics (ICORR)*, 2013, pp. 1–6.

[11] F. Chen Chen, S. Appendino, A. Battezzato, A. Favetto, M. Mousavi, and F. Pescarmona, “Constraint Study for a Hand Exoskeleton: Human Hand Kinematics and Dynamics,” *J. Robot.*, vol. 2013, p. e910961, Sep. 2013.

[12] P. Heo, G. M. Gu, S. Lee, K. Rhee, and J. Kim, “Current hand exoskeleton technologies for rehabilitation and assistive engineering,” *Int. J. Precis. Eng. Manuf.*, vol. 13, no. 5, pp. 807–824, May 2012.

[13] H. I. Krebs, J. Celestino, D. Williams, M. Ferraro, B. Volpe, and N. Hogan, “24 A Wrist Extension for MIT-MANUS,” in *Advances in Rehabilitation Robotics*, Z. Z. Bien and D. Stefanov, Eds. Springer Berlin Heidelberg, 2004, pp. 377–390.

[14] B. Siciliano and O. Khatib, *Springer Handbook of Robotics*. Springer Science & Business Media, 2008.

[15] P. Lochmatter, “Development of a shell-like electroactive polymer (EAP) actuator,” Doctoral Thesis, ETH Zurich, 2007.

[16] J. Wu, J. Huang, Y. Wang, and K. Xing, “A Wearable Rehabilitation Robotic Hand Driven by PM-TS Actuators,” in *Intelligent Robotics and Applications*, H. Liu, H. Ding, Z. Xiong, and X. Zhu, Eds. Springer Berlin Heidelberg, 2010, pp. 440–450.

[17] A. J. Veale and S. Q. Xie, “Towards compliant and wearable robotic orthoses: A review of current and emerging actuator technologies,” *Med. Eng. Phys.*, vol. 38, no. 4, pp. 317–325, Apr. 2016.

[18] L. Hs and X. Sq, “Exoskeleton robots for upper-limb rehabilitation: state of the art and future prospects.,” *Med. Eng. Phys.*, vol. 34, no. 3, pp. 261–268, Apr. 2012.

[19] R. A. R. C. Gopura, D. S. V. Bandara, K. Kiguchi, and G. K. I. Mann, “Developments in hardware systems of active upper-limb exoskeleton robots: A review,” *Robot. Auton. Syst.*, vol. 75, pp. 203–220, Jan. 2016.

[20] “Smart materials | Article about Smart materials by The Free Dictionary.” [Online]. Available: http://encyclopedia2.thefreedictionary.com/Smart+materials. [Accessed: 05-Aug-2017].

[21] M. Schwartz, *Smart Materials*. CRC Press, 2008.

[22] F. K. Straub and D. J. Merkley, “Design of a smart material actuator for rotor control,” in *Smart Structures and Materials 1995: Smart Structures and Integrated Systems*, 1995, vol. 2443, pp. 89–105.

[23] W. M. Huang, Z. Ding, C. C. Wang, J. Wei, Y. Zhao, and H. Purnawali, “Shape memory materials,” *Mater. Today*, vol. 13, no. 7, pp. 54–61, Jul. 2010.

[24] M. A. Ward and T. K. Georgiou, “Thermoresponsive Polymers for Biomedical Applications,” *Polymers*, vol. 3, no. 3, pp. 1215–1242, Aug. 2011.

[25] D. C. Lagoudas, *Shape Memory Alloys: Modeling and Engineering Applications*. Springer, 2008.

[26] A. Cherubini, G. Moretti, R. Vertechy, and M. Fontana, “Experimental characterization of thermally-activated artificial muscles based on coiled nylon fishing lines,” *AIP Adv.*, vol. 5, no. 6, p. 067158, Jun. 2015.

[27] J. Hu, *Shape Memory Polymers and Textiles*. Elsevier, 2007.

[28] M. C. Yip and G. Niemeyer, “High-performance robotic muscles from conductive nylon sewing thread,” in *2015 IEEE International Conference on Robotics and Automation (ICRA)*, 2015, pp. 2313–2318.

[29] C. S. Haines, N. Li, G. M. Spinks, A. E. Aliev, J. Di, and R. H. Baughman, “New twist on artificial muscles,” *Proc. Natl. Acad. Sci.*, vol. 113, no. 42, pp. 11709–11716, Oct. 2016.

[30] S. M. Mirvakili and I. W. Hunter, “Bending artificial muscle from nylon filaments,” in *Electroactive Polymer Actuators and Devices (EAPAD) 2016*, 2016, vol. 9798, p. 97981L.

[31] N. Hogan, H. I. Krebs, J. Charnnarong, P. Srikrishna, and A. Sharon, “MIT-MANUS: a workstation for manual therapy and training. I,” in *, IEEE International Workshop on Robot and Human Communication, 1992. Proceedings*, 1992, pp. 161–165.

[32] C. N. Schabowsky, S. B. Godfrey, R. J. Holley, and P. S. Lum, “Development and pilot testing of HEXORR: Hand EXOskeleton Rehabilitation Robot,” *J. NeuroEngineering Rehabil.*, vol. 7, p. 36, 2010.

[33] A. Chiri *et al.*, “HANDEXOS: Towards an exoskeleton device for the rehabilitation of the hand,” in *2009 IEEE/RSJ International Conference on Intelligent Robots and Systems*, 2009, pp. 1106–1111.

[34] J. Iqbal, H. Khan, N. G. Tsagarakis, and D. G. Caldwell, “A novel exoskeleton robotic system for hand rehabilitation – Conceptualization to prototyping,” *Biocybern. Biomed. Eng.*, vol. 34, no. 2, pp. 79–89, 2014.

[35] J. Li, R. Zheng, Y. Zhang, and J. Yao, “iHandRehab: An interactive hand exoskeleton for active and passive rehabilitation,” in *2011 IEEE International Conference on Rehabilitation Robotics (ICORR)*, 2011, pp. 1–6.

[36] H. S. Park, Y. Ren, and L.-Q. Zhang, “IntelliArm: An exoskeleton for diagnosis and treatment of patients with neurological impairments,” in *2008 2nd IEEE RAS EMBS International Conference on Biomedical Robotics and Biomechatronics*, 2008, pp. 109–114.

[37] C. D. Takahashi, L. Der-Yeghiaian, V. Le, R. R. Motiwala, and S. C. Cramer, “Robot-based hand motor therapy after stroke,” *Brain*, vol. 131, no. 2, pp. 425–437, Feb. 2008.

[38] C. D. Takahashi, L. Der-Yeghiaian, V. H. Le, and S. C. Cramer, “A robotic device for hand motor therapy after stroke,” in *9th International Conference on Rehabilitation Robotics, 2005. ICORR 2005.*, 2005, pp. 17–20.

[39] A. H. Ab Rahim, M. N. A. Bin Ab Patar, A. T. M. Amin, and J. Mahmud, “The Development of Finger Rehabilitation Device for Stroke Patients,” *Appl. Mech. Mater.*, vol. 393, pp. 604–610, Sep. 2013.

[40] E. B. Brokaw, I. Black, R. J. Holley, and P. S. Lum, “Hand Spring Operated Movement Enhancer (HandSOME): A Portable, Passive Hand Exoskeleton for Stroke Rehabilitation,” *IEEE Trans. Neural Syst. Rehabil. Eng.*, vol. 19, no. 4, pp. 391–399, Aug. 2011.

[41] “SaeboFlex / SaeboReach Details,” *Saebo*, 20-Jul-2015. [Online]. Available: https://www.saebo.com/saeboflex-saeboreach-details/. [Accessed: 25-Jul-2017].

[42] R. A. Stuck, L. M. Marshall, and R. Sivakumar, “Feasibility of SaeboFlex upper-limb training in acute stroke rehabilitation: a clinical case series,” *Occup. Ther. Int.*, vol. 21, no. 3, pp. 108–114, Sep. 2014.

[43] L. Andriske, D. Verikios, and D. Hitch, “Patient and Therapist Experiences of the SaeboFlex: A Pilot Study,” *Occup. Ther. Int.*, 2017.

[44] K. H. Cho *et al.*, "Fabrication and modeling of temperature-controllable artificial muscle actuator," in *2016 6th IEEE International Conference on Biomedical Robotics and Biomechatronics (BioRob)*, 2016, pp. 94–98.

[45] "Plastics Properties Table | Sort, Compare, Select | Curbell Plastics," 30-Jun-2017. [Online]. Available: https://www.curbellplastics.com/Research-Solutions/Plastic-Properties. [Accessed: 30-Jun-2017].

[46] "MatWeb - The Online Materials Information Resource," 30-Jun-2017. [Online]. Available: http://www.matweb.com/. [Accessed: 30-Jun-2017].

[47] R. Welgos, "Nylon 6 and 6,6 aren't always the same," *Mach. Des. Clevel.*, vol. 66, no. 22, p. 55, Nov. 1994.

[48] S. M. Mirvakili *et al.*, "Simple and strong: twisted silver painted nylon artificial muscle actuated by Joule heating," *SPIE*, Mar. 2014.

[49] "December 1840: Joule's abstract on converting mechanical power into heat." [Online]. Available: https://www.aps.org/publications/apsnews/200912/physicshistory.cfm. [Accessed: 21-Apr-2018].

[50] "Honeywell Spectra® 1000 Fiber." [Online]. Available: http://www.matweb.com/search/DataSheet.aspx?MatGUID=c3ffe4ecc48246cd94dd2f214b752962&ckck=1. [Accessed: 03-Aug-2017].

[51] R. F. Landel and L. E. Nielsen, *Mechanical Properties of Polymers and Composites, Second Edition*. CRC Press, 1993.

[52] S. Horton and P. Dumond, "The Design of a Consistent Manufacturing Device for Coiled Polymer Actuators," in *Proceedings of the The Engineering in Medicine and Biology Conference*, 2018, pp. 1–7.

[53] M. Vlasblom, J. Boesten, S. Leite, and P. Davies, “Creep and stiffness of HMPE fiber for permanent deepwater offshore mooring,” in *2012 Oceans - Yeosu*, 2012, pp. 1–7.

[54] S.-S. Yeo and Y. G. Hsuan, “Evaluation of creep behavior of high density polyethylene and polyethylene-terephthalate geogrids,” *Geotext. Geomembr.*, vol. 28, no. 5, pp. 409–421, Oct. 2010.

[55] I. J. Baguley, M. T. Nott, and H. L. H. Barder, “The Use of Computerised Dynamometry to Quantify Functional Grip and Release in People Post Stroke: A Pilot Study,” *Open Rehabil. J.*, vol. 3, no. 1, 2010.

[56] G. Ventura and V. Martelli, “Thermal conductivity of Kevlar 49 between 7 and 290K,” *Cryogenics*, vol. 49, no. 12, pp. 735–737, Dec. 2009.

[57] G. B. Guimaraes and C. J. Burgoyne, “Thermal expansion behaviour of Kevlar 49 yarns,” in *Non-Metallic (FRP) Reinforcement for Concrete Structures*, Sapporo, Japan, 1997, vol. 2, pp. 171–178.

[58] D. D. L. Chung and D. Chung, *Carbon Fiber Composites*. Butterworth-Heinemann, 2012.

[59] G. Tortora and B. Derrickson, *Principles of anatomy and physiology*. John Wiley \\\\& Sons, 2005.

[60] A. Freivalds, *Biomechanics of the Upper Limbs: Mechanics, Modeling and Musculoskeletal Injuries, Second Edition*. CRC Press, 2011.

[61] T. Cl and S. Rj, “The anatomy and mechanics of the human hand.,” *Artif. Limbs*, vol. 2, no. 2, pp. 22–35, May 1955.

[62] D. Elliot and D. A. McGrouther, “The Excursions of the Long Extensor Tendons of the Hand,” *J. Hand Surg. Br. Eur. Vol.*, vol. 11, no. 1, pp. 77–80, Feb. 1986.

[63] C. A. Moran, “Anatomy of the Hand,” *Phys. Ther.*, vol. 69, no. 12, pp. 1007–1013, Dec. 1989.

[64] G. J. Loren, S. D. Shoemaker, T. J. Burkholder, M. D. Jacobson, J. Fridén, and R. L. Lieber, “Human wrist motors: Biomechanical design and application to tendon transfers,” *J. Biomech.*, vol. 29, no. 3, pp. 331–342, Mar. 1996.

[65] M. A. C. Craigen and J. K. Stanley, “Wrist Kinematics: Row, Column or Both?,” *J. Hand Surg.*, vol. 20, no. 2, pp. 165–170, Apr. 1995.

[66] R. A. Berger, “The Anatomy and Basic Biomechanics of the Wrist joint,” *J. Hand Ther.*, vol. 9, no. 2, pp. 84–93, Apr. 1996.

[67] D. A. Neumann, “Chapter 7: Wrist,” in *Kinesiology of the Musculoskeletal System: Foundations for Rehabilitation*, Elsevier, 2016.

[68] M. J. Rainbow, A. L. Wolff, J. J. Crisco, and S. W. Wolfe, “Functional kinematics of the wrist,” *J. Hand Surg. Eur. Vol.*, vol. 41, no. 1, pp. 7–21, Jan. 2016.

[69] J. Coupier, S. Hamoudi, S. Telese-Izzi, V. Feipel, M. Rooze, and S. Van Sint Jan, “A novel method for in-vivo evaluation of finger kinematics including definition of healthy motion patterns,” *Clin. Biomech.*, vol. 31, pp. 47–58, Jan. 2016.

[70] R. A. Berger, “The radioscapholunate ligament: A gross and histologic description,” *Anat. Rec.*, vol. 210, no. 2, pp. 393–405.

[71] T. P. Crowley, “The Flexor Tendon Pulley System and Rock Climbing,” *J. Hand Microsurg.*, vol. 4, no. 1, pp. 25–29, Jun. 2012.

[72] P. R. M. D. Manske and P. A. B. S. Lesker, “Histologic Evidence of Intrinsic Flexor Tendon Repair in Various Experimental Animals An In Vitro Study,” *Clin. Orthop.*, vol. 182, pp. 297–304, Feb. 1984.

[73] “Climber Problems: The A2 Pulley Strain – Crux Crush.” [Online]. Available: http://cruxcrush.com/2013/10/24/climber-problems-the-a2-pulley-strain/. [Accessed: 09-Aug-2017].

[74] B. Hirt, H. Seyhan, M. Wagner, and R. Zumhasch, *Hand and wrist anatomy and biomechanics: a comprehensive guide*. 2017.

[75] K. N. An, F. C. Hui, B. F. Morrey, R. L. Linscheid, and E. Y. Chao, “Muscles across the elbow joint: A biomechanical analysis,” *J. Biomech.*, vol. 14, no. 10, pp. 659–669, 1981.

[76] J. W. Garrett, “Anthropometry of the Hands of Male Air Force Flight Personnel,” Mar. 1970.

[77] S. R. Habib and N. N. Kamal, “Stature estimation from hand and phalanges lengths of Egyptians,” *J. Forensic Leg. Med.*, vol. 17, no. 3, pp. 156–160, Apr. 2010.

[78] S. Cobos, M. Ferre, M. A. S. Uran, J. Ortego, and C. Pena, “Efficient human hand kinematics for manipulation tasks,” in *2008 IEEE/RSJ International Conference on Intelligent Robots and Systems*, 2008, pp. 2246–2251.

[79] “Physical Therapy Management Of Colles Fracture - Morphopedics.” [Online]. Available: http://morphopedics.wikidot.com/physical-therapy-management-of-colles-fracture. [Accessed: 29-Aug-2017].

[80] Y. Ren, H. S. Park, and L. Q. Zhang, “Developing a whole-arm exoskeleton robot with hand opening and closing mechanism for upper limb stroke rehabilitation,” in *2009 IEEE International Conference on Rehabilitation Robotics*, 2009, pp. 761–765.

Appendix A

Anatomy and Biomechanical Analysis

A.1 Anatomy of the Human Hand

In order to create an effective and precise hand exoskeleton that allows for safe and easy operation, a thorough understanding of hand anatomy and biomechanics is required. In fact, the exoskeleton will need to mimic the exact motion of the human hand when worn by the patient. Several key components to consider when designing the exoskeleton are the degrees of freedom (DOF) as well as the range of motion (ROM) of each joint to ensure a safe and operable device. Hand motion is also complexly related to the intrinsic and extrinsic muscles of the hand and forearm as well as the connective tissue surrounding the area [12].

Some basic anatomical terminology that must be understood is the usage of the words ‘proximal’, and ‘distal’. The term proximal refers to the part of an appendage that is closest to the center of the body, where distal refers to the part furthest away from the body.

A.2 Bones of the Hand and Wrist

Each upper limb is made up of 30 bones located in three locations, (1) the *humerus* in the arm; (2) the *ulna* and *radius* in the forearm; and (3) the 8 carpals in the *carpus* (wrist), the 5 *metacarpals* in the *metacarpus* (palm), and the 14 *phalanges* (bones of the digits) of the fingers which can be seen in Figure A-1 [59]:

- The *humerus*, or the arm bone, is the largest and longest bone of the upper limb. It articulates with the *scapula* on the proximal end and with the *radius* and *ulna* on the distal end where the elbow is located.
- The *ulna* is located on the medial aspect of the forearm (pinky side). At the proximal end of the *ulna* is the *olecranon* which forms the prominence of the elbow. The distal end of the *ulna* is made up of a head that is separated from the wrist by a disc of fibrocartilage.
- The *radius* is the smaller bone of the forearm and is located on the lateral aspect of the arm (thumb side). This bone is narrow at its proximal end and widens at its distal end. The proximal end of the *radius* has a head that articulates with the *humerus* and the *radial notch* of the *ulna*. The shaft of the radius widens distally to form the styloid process on the lateral side, an attachment site for many of the arms muscles and ligaments.
- The *carpus* (wrist) is the proximal region of the hand and is made up of eight small bones, the *carpals*, which are connected to one another by ligaments. These carpal bones are aligned in two transverse rows, made up of four carpals each. The carpal bones in the proximal row are the *scaphoid, lunate, triquetrum, and pisiform*. These four bones articulate with the distal end of the *ulna* and *radius* to form the *wrist*

joint. The carpal bones located in the distal row are made up of the *trapezium, trapezoid, capitate,* and *hamate*. The anterior concave space made by the *pisiform* and *hamate* (on the ulnar side), and the *scaphoid* and *trapezium* (on the radial side), along with several fibrous bands of fascia make up what is known as the *carpal tunnel*.

- The *metacarpus*, or palm, is the intermediate region of the hand and is made up of five bones called the *metacarpals*. These bones are numbered I to V, starting with the thumb from lateral to medial. The base of the *metacarpals* articulates with the distal row of the *carpal* bones, and the head articulates with the proximal *phalanges* to form the *metacarpophalangeal joints* (seen readily as knuckles).
- The *phalanges*, or the bones of the fingers, make up the very most distal part of the upper limb. There are 14 phalanges in the five digits of each hand.

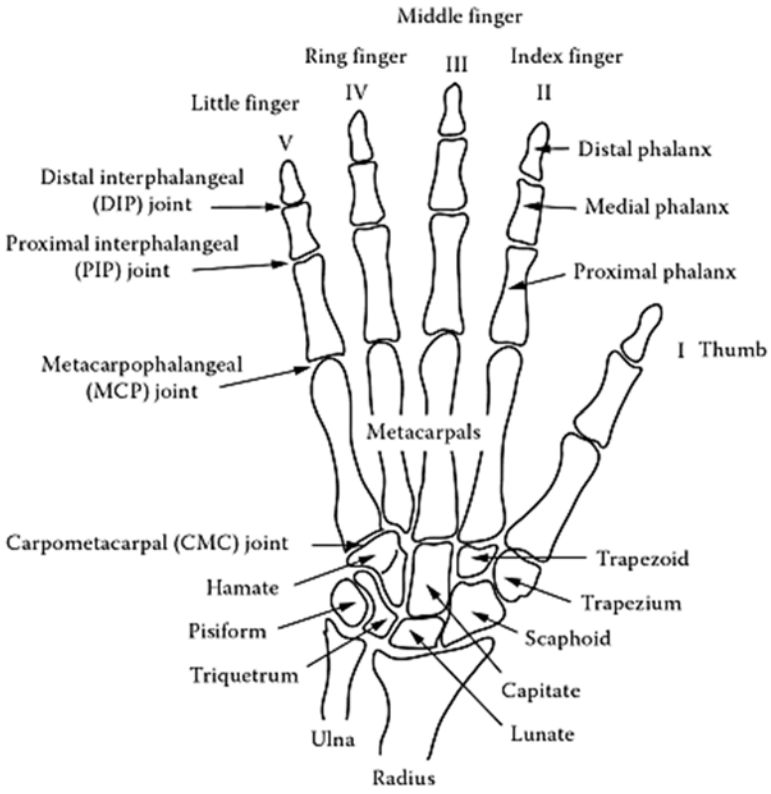

Figure A-1 Palmar View of the Bones of the Hand & Wrist [60]

A.3 Joints of the Hand and Wrist

There are four joints in each finger, in sequence from the proximal to distal: (1) *carpometacarpal* (CMC), (2) *metacarpophalangeal* (MCP), (3) *proximal interphalangeal* (PIP), and (4) *distal interphalangeal* (DIP). The CMC joint is formed by the base of the 4 metacarpals and the distal carpal bones. This join t is stabilized by a strong interosseous ligament in order to form a relatively immobile, stationary joint. The CMC joint forms the hollow of the palm and functions to allow the hand and digits to conform to the shape of the objects being grasped [60]. The MCP joint is formed by the articulation of the convex metacarpal head and the concave base of the proximal phalanx [60]. These joints are stabilized by a joint capsule and ligaments which allow flexion of approximately 90° and extension of 20°-30° from a neutral position in the sagittal plane[60]. At

the MCP there is also a wide range of flexion which ranges from the smallest angle of about 70° for the index finger, and a much larger angle of 95° with the little finger [60]. There is also a radial and ulnar deviation possible at the MCP joint of 40°-60°, which allows the movement in the frontal plane with the index showing up to 60° of abduction and adduction, while the middle and ring fingers can exhibit 45° of flexion [60]. The range of motion at the MCP joint decreases as the flexion angle increases due to the bicondylar metacarpal structure. The MCP joint also exhibits axial rotation of the fingers from the pronated to the supinated position as the fingers are extended [60]. The IP joints (PIP and DIP) are hinge joints present in each finger (thumb only has one IP joint), and are only capable of flexion and extension of the finger [60]. Volar and collateral ligaments, connected with expansion sheets of the extensor tendon, prevent side to side motion at the joint [60]. These IP joints however can still exhibit 100°-110° of flexion in the PIP, and 60°-70° in the DIP [60].

A.4 Major Muscles of the Forearm, Hand, and Wrist

There are many muscles of the forearm which act on the wrist, hand, thumb, and fingers. These muscles are divided into two categories: extrinsic and intrinsic, based on the origin of the muscle. The muscles that originate primarily in the forearm are known as the extrinsic muscles of the hand because they originate outside the hand and insert themselves within it, and the muscles that originate primarily in the hand are known as the intrinsic muscles [60]. The extrinsic muscles are therefore larger in size and provide strength, while the intrinsic muscles are small and provide precise coordination for the fingers [60]. The extrinsic muscles can also be further classified into two categories based on location and function: the (1) anterior compartment muscles and (2) posterior compartment muscles [59].

A.5 Extrinsic Muscles of the Hand

a) **Anterior Muscles:** The muscles originate on the humerus, and typically insert on the carpals, metacarpals, and phalanges as shown below in Figure A-2 [59]. These muscles are further grouped into the *superficial anterior compartment of the forearm,* and the *deep anterior compartment of the forearm* and all function as flexors. These are the muscles that are responsible for forearm supination [61]. The superficial muscles consist of the *flexor carpi radialis* which flexes and abducts the hand at the wrist joint, the *palmaris longus* which weakly flexes the hand at the wrist joint, the *flexor carpi ulnaris* which flexes and adducts the hand at the wrist joint, and the *flexor digitorum superficialis* which flexes the middle phalanx of each finger, the proximal phalanx of each finger, as well as the hand at the wrist joint [59]. The deep flexor muscles consist of the *flexor pollicis longus* which works to flex the phalanx of the thumb at the interphalangeal joint, and the *flexor digitorum profundus* which flexes the distal and middle phalanges, the proximal phalanx of each finger, and the hand at the wrist joint [59].

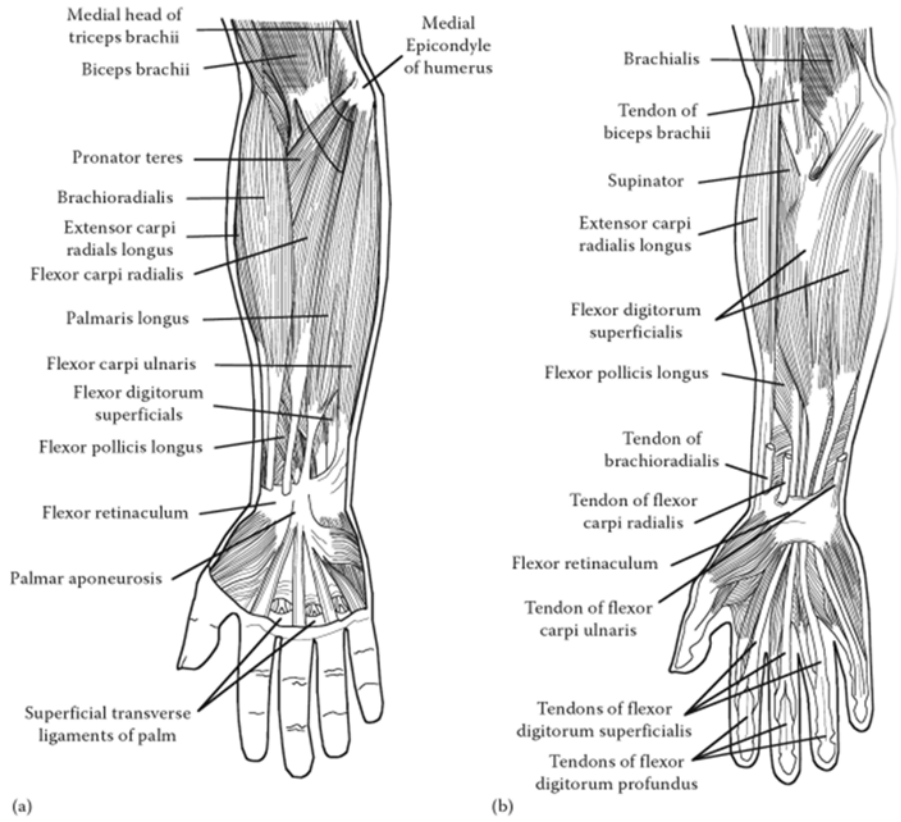

Figure A-2 Anterior Muscles of the right hand (a) superficial layer and (b) middle layer [60]

The posterior compartment muscles of the forearm

b) **Posterior Muscles:** This group of muscles originate on the humerus, and insert on the metacarpals and phalanges. These muscles are further grouped into the *superficial posterior compartment of the forearm,* and the *deep posterior compartment of the forearm* and all function as extensors. The superficial muscles in this group consist of the *extensor carpi radialis longus* and the *extensor carpi radialis brevis* which extend and abduct the hand at the wrist joint, the *extensor digitorum* which extends the distal and middle phalanges of each finger and also helps extend the hand at the wrist joint, the *extensor digiti minimi* which extends the proximal phalanx of the little finger and the hand at the wrist joint, and the *extensor carpi ulnaris* which extends and adducts the hand at the wrist joint

[59]. The deep extensor muscles consist of: *abductor pollicis longus* which abducts and extends the thumb and abducts the hand at the wrist joint, the *extensor pollicis longus* which extends the proximal phalanx of the thumb and hand at the wrist joint, the *extensor pollicis longus* which extends the distal phalanx of the thumb at the interphalangeal joint and abducts the hand at the wrist joint, and the *extensor indicis* which extends the distal and middle phalanges of the index finger at the interphalangeal joint as well as the hand at the wrist joint [59].

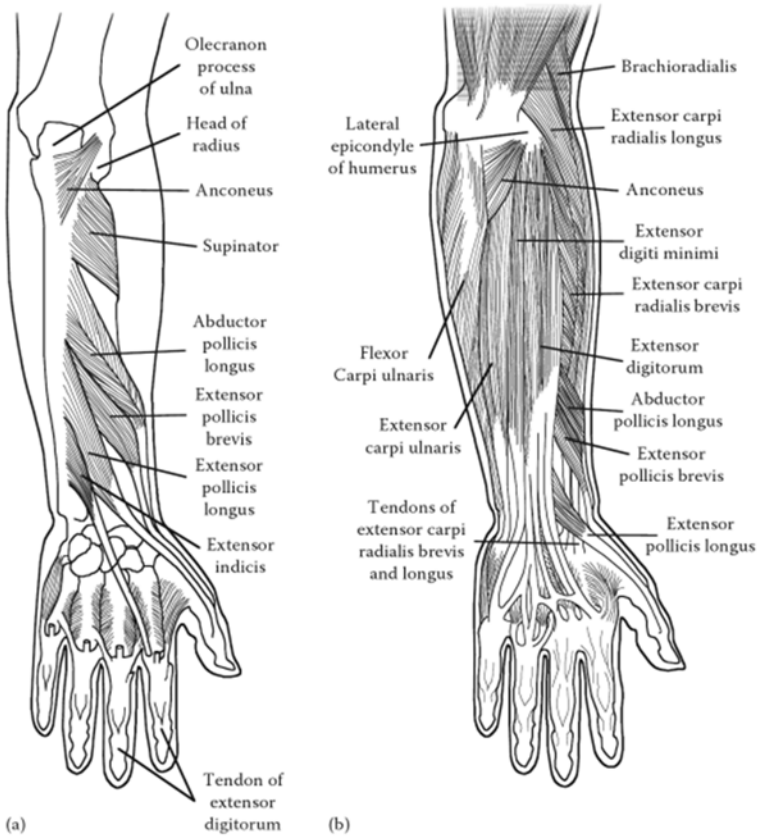

Figure A-3 Posterior Muscles of the right hand: (a) deep layer and (b) superficial layer [60]

Intrinsic Muscles of the Hand

Just like the extrinsic muscles of the hand which were responsible for moving the digits in certain ways in order to provide strength, there is also a grouping of muscles commonly referred to as the intrinsic muscles of the hand seen below in Figure A-4. The muscles of this group have their origin and insertion located within the hand in order to perform the weak but intricate and precise movements of the digits [59]. The intrinsic muscles of the hand are sub grouped into three categories: (1) thenar, (2) hypothenar, and (3) intermediate.

- **The thenar muscles** (located on the lateral part of the palm) consist of the *aductor pollicis brevis* which is in charge of abducting the thumb at the carpometacarpal joint, the *opponens pollicis* which moves the thumb across the palm in order to meet the remaining fingers at the carpometacarpal joint, the *flexor pollicis brevis* which flexes the thumb at the carpometacarpal and metacarpophalangeal joints, and the *adductor pollicis* which adducts the thumb at the carpometacarpal and metacarpophalangeal joints [59].
- **The hypothenar muscles** (located on the medial part of the palm) consist of the *abductor digiti minimi* which abducts and flexes the little finger at the metacarpophalangeal joint, the *flexor digiti minimi brevis* which flexes the little finger at the carpometacarpal and metacarpophalangeal joint, and the *opponens digiti minimi* which moves the pinky finger across the palm to meet the thumb at the carpometacarpal joint [59]. Of these three muscles, it is important to note that the *abductor digiti minimi* is the most superficial of the hypothenar muscles and is a very powerful muscle that plays an important role in grasping objects with outspread fingers [59].

- **The intermediate muscles** (midpalmar) act on all the digits. These muscles consist of the *lumbricals* which are responsible for finger flexion at the metacarpophalangeal joints, as well as extension at the interphalangeal joints, the *palmar interossei* adduct and flex the fingers at the metacarpophalangeal joints and extend the finger at the interphalangeal joints, while the *dorsal interossei muscles* which abduct and flex fingers A-4 at the metacarpophalangeal joints [59]. The *interossei muscles* are important in skilled activities such as writing and typing.

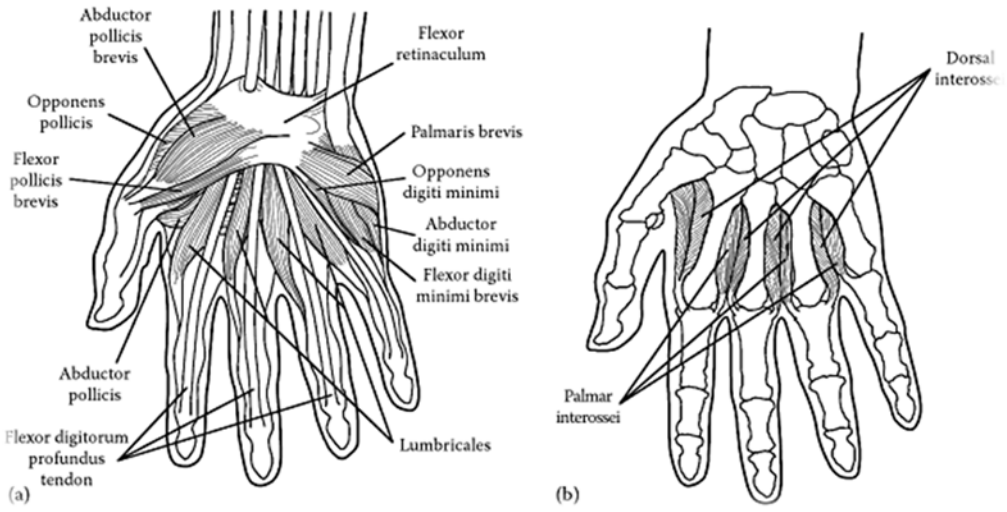

Figure A-4 Intrinsic Muscles of the right hand: (a) palmar view, and (b) dorsal view [60]

Tendons and Ligaments of the Hand

The tendons and ligaments in the hand are very important because tendons function to transfer the pull of muscles to surrounding bones, and ligaments connect one bone to another [59]. As the finger moves, each corresponding tendon (the extensor and flexor simultaneously) slide a certain distance [62], [12]. Studies done by D. Elliot et al. show that the relationship between the sliding excursion of the finger tendons and the angular displacement of the MCP, PIP, and DIP joints are

both linear and non-linear [62]. The distance moved by these tendons is also larger in the more proximal joints of the hand. It is also important to note for design mechanics that the flexor tendons tend to slide a greater distance than their extensor counterparts and the excursion of the extrinsic muscle tendons is greater than the intrinsic muscle tendons [12].

There are also many important ligaments in the hand, such as the extracapsular and capsular ligaments that function to provide stability and support to the hand. Extracapsular ligaments lie outside the articular capsule, while capsular ligaments lie within the articular joint capsule [59]. One of the most important extracapsular ligaments to note is the transverse intermetacarpal ligament or the ligament most commonly referred to as the TIML. This ligament attaches to and runs between the volar plates at the level of the metacarpal heads along the entire width of the hand. Full extensibility of this ligament is necessary for grasping and prehensile activities. Capsular collateral ligaments on the other hand provide very crucial joint stability to all finger and thumb joints. Some examples of capsular joint ligaments are the MCP joint ligaments, the PIP joint ligaments, and the DIP joint ligaments. The MCP joint collateral ligaments have dual attachment points: the bony and glenoid. The glenoid portion arises from the metacarpal head and attaches to the volar plate, and the collateral portion arises from the metacarpal head and attaches to the base of the phalanx [12], [63]. In contrast to the MCP joint collateral ligaments, the PIP and DIP joint collateral ligaments attachment point is completely bony. The ligaments of these two joint types are concentrically placed and are of equal length [63]. Therefore, these ligaments are maximally taught throughout their range of motion [12], [63].

A.6 Hand and Wrist Biomechanics

There are three main properties that can facilitate the understanding of the biomechanics of the wrist. These three properties consist of: (1) the kinematics of the wrist joint, which involves wrist motion analysis without looking at the internal and external forces, (2) the material properties of the carpal ligaments such as the yield strength, stress, and strain, in isolated bone-ligament-bone preparations, and (3) wrist kinetics which look at the forces across the wrist joint and the way these three aspects interact with one another [64].

A.7 Wrist (Carpal Bone) Kinematics

The wrist is a composite joint meaning that it is the site of union for several bones of the body. When the carpal bones of the wrist move, there is a complex amount of motion which occurs at numerous different levels such as the muscles, ligaments, tendons, and bones. These components must all interact with one another to provide a displacement. In order for the wrist to reach its optimal and maximum ranges of motion, it is necessary for all the joints along the carpus to collaborate together in order to enable a good rotation [65]. From a functional standpoint, the carpal bones all work together at the wrist joint and can be divided into two rows, the distal row and the proximal row, and the scaphoid which acts as an anatomical bridge [65]. However, upon closer investigation, it is seen that the carpal bones act differently and perform different actions based on what row they are located in, especially those of the proximal carpal row [66].

The distal carpal-row bones consist of the trapezius, trapezoid, capitate, and the hamate shown in Figure A-5 [67]. These bones move together as a functional unit, are tightly bound to the

metacarpals, and mimic the behavior of the second and third metacarpal bones [68]. This congruency between the bones of the distal row of carpals and the base of the metacarpal bones is in part due to the "interlocking of articular surfaces and the dense ligamentous connections" [66]. The relationship these bones share holds true for not only the direction of motion but also for the magnitude of motion [66].

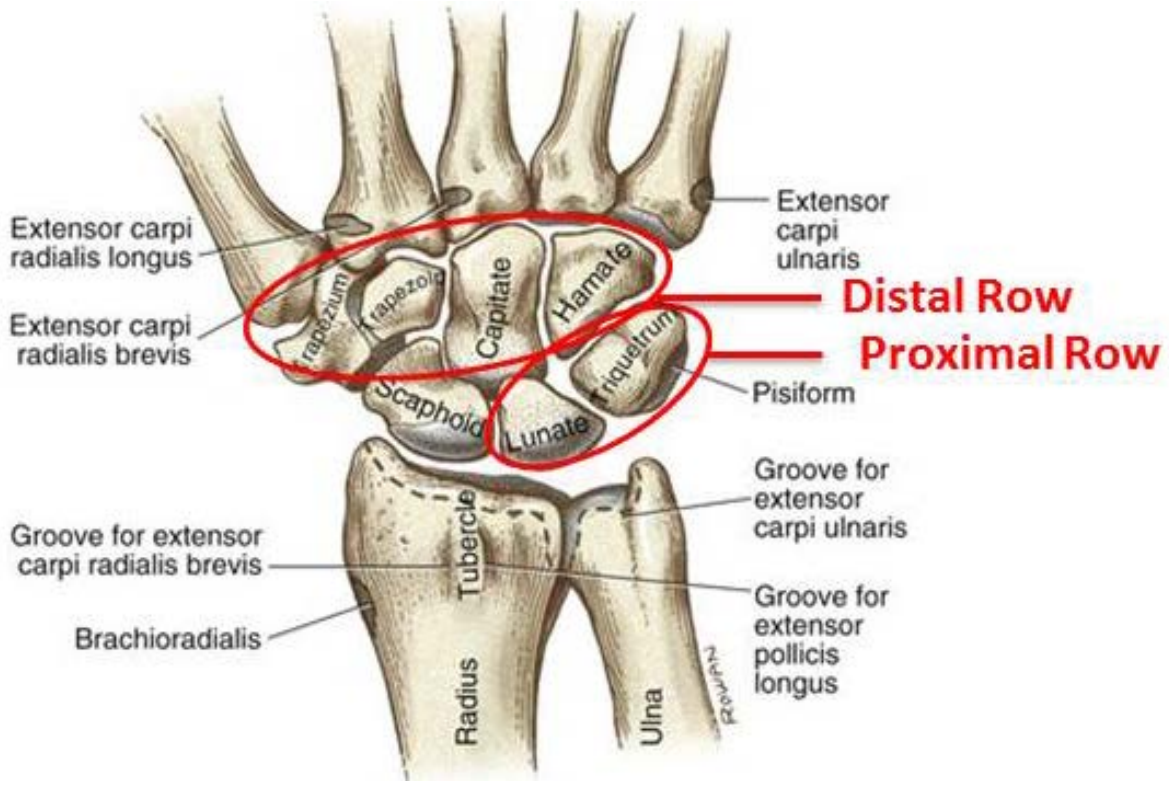

Figure A-5 Dorsal view of the Carpal rows [67]

The proximal row of the carpus consists of the lunate and the triquetrum [68]. These bones are a bit different in the sense that they have more freedom of movement between the individual bones. Although they still function as a general unit, the individualized inner movements allow for the large range of motion as well as the stability seen uniquely in the wrist joint. Their motion is indirectly related to the primary mechanical signals from the distal row [68].

The scaphoid bone acts as a connection rod between the two rows to aid in coordination of motion between the two rows [68]. Radial and ulnar deviation occurs when the scaphoid slides down the slope of the distal radius [65]. However, from a more generalized perspective, one could say that the proximal-row carpus bones move with the distal-row carpus bones as a functional unit at the mid carpal joint to flex and extend the wrist [66], [68].

A.8 Finger Kinematics

A wearable assistive device such as an exoskeleton is physically coupled with the human hand. Therefore, the device's design must be based off of the kinematic and biomechanical model of the hand in order to mimic its exact motion [33]. The skeleton of the human hand contains 27 bones. These bones consist of the 8 carpal bones mentioned above, as well as 14 phalanges and 5 metacarpal bones [69]. Due to the complexity of the hand's structure, its motion becomes very challenging to replicate. Each finger allows four DOF: from the distal phalanx there is one DOF per DIP and PIP joint allowing their flexion/extension, and two DOF at the MCP (metacarpo-phalangeal) allowing for both flexion/extension and abduction/adduction. The thumb, however, allows for six DOF and the opposition motion that is fundamental to human dextrous manipulation. In addition to the thumbs IP (interphalangeal) and MCP joints that allow for the flexion/extension, there is also the CM (Carpometacarpal) joint that allows the flexion/extension, the abduction/adduction, and the thumb opposition motions simultaneously.

A.9 Material Properties of the Carpel Ligaments

It has been previously shown that the ligaments of the wrist are similar to other joint systems found in the human body based on their material properties. The *radioscaphocapitate* and the *long radiolunate* ligaments (Figure A-6) of the wrist, both belonging to the grouping referred to as the *palmar capsular* ligaments, are common viscoelastic structures that exhibit failure at approximately 100N [66]. The grouping of ligaments found between the bones of the proximal carpal row is referred to as *the intrinsic* (interosseous) ligaments, and is generally stronger than the previously mentioned palmar capsular ligaments. This group of ligaments exhibit failure at a much higher value of 300N and has a strain at failure of more than 50%, which is much larger than that of the palmar capsular ligaments which exhibit strain of approximately 10-35% [66]. The ligaments mentioned above, however, are much stronger than the *radioscapholunate ligaments*, which requires much less force to produce failure at only 50N based on previously reported distraction testing [70]. This ligament is much more elastic than the interosseous and palmar ligaments, with little collagen and a much lower tensile yield point and elastic modulus [66],[70].

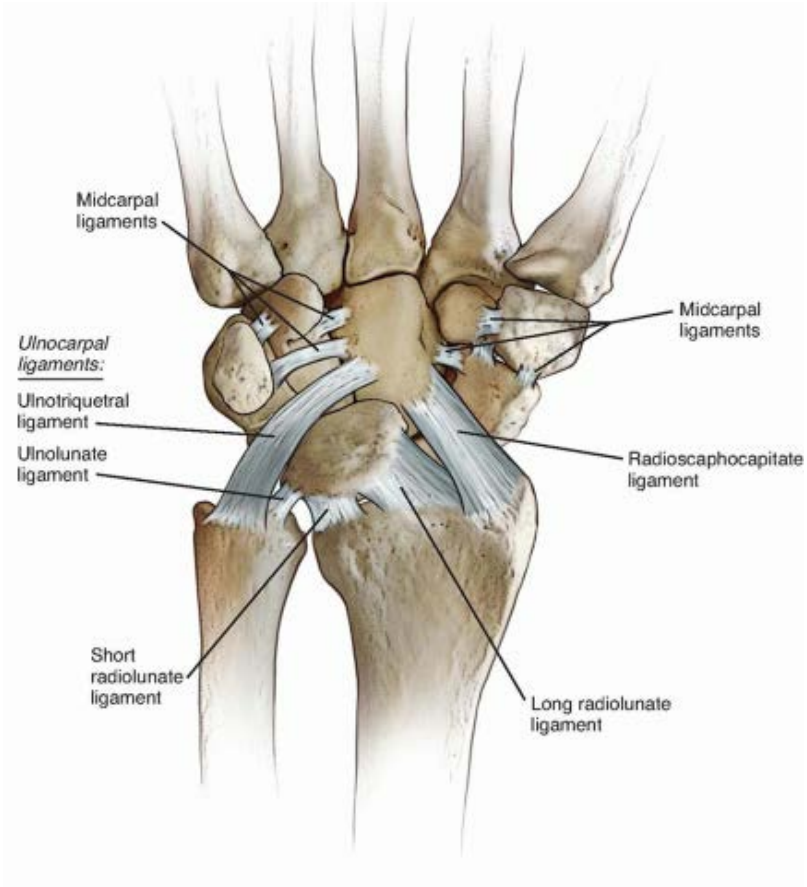

Figure A-6 Palmar view of the ligaments of the wrist [59]

The *scapholunate* and *lunotriquetral* ligaments also have a wide range of important material properties that allow for optimal wrist motion. The dorsal region of the *scapholunate* ligament requires up to 250N of force in order to fail, making it the stronger region of the ligament, with the palmar region failing at only 125N [66]. The *lunotriquetral* ligament is similar to the *scapholunate* in material properties, however the palmar region for this ligament is stronger, followed by the dorsal region [66].

A.10 Flexor Tendon Sheath Pulley System

The tendon sheath is a complex structure surrounding the tendons which contains synovial fluid, through which the flexor tendons of the digits run. The synovial fluid found in the sheath acts as both a lubricant for the joint in order to facilitate low-friction gliding, as well as a nutritional environment for the flexor tendons. This sheath is essential for the optimal functioning of the flexor tendons. Its primary purpose is to ensure the tendons stay close to the bone in order to "turn the corner" with ease, and transfer the force developed in the muscle-tendon unit into movement at the phalanges. It originates at the base of the metacarpal bone, ends at the distal interphalangeal (DIP) joint, and is held against the phalanges by a group of pulley systems [60]. These pulleys act to prevent bow-stringing of the tendons and allow the transfer of the necessary forces for pinch and grasp [71]. The pulley component of the flexor tendon sheath can be divided into three distinct categories based on their location (as demonstrated in Figure A-7): (1) a palmar aponeurosis pulley, (2) five annular (ring-shaped) pulleys (A1, A2, A3, A4, and A5), and (3) three cruciate (cross-like) pulley, (C1, C2, and C3) [60]. The A2 and A4 pulleys are located on the proximal and middle phalanges, and are true fibro-osseous pulleys [60]. These two act as the strongest pulleys withstanding the greatest forces during pinch and grasp functions, as well as maintaining a stable joint [71]. The other annular pulleys (A1, A3, A5) are located at the palmar surface of the MCP, PIP, and DIP joints. These pulleys are more flexible and allow for compression during flexion without impinging on the tendons, they typically come into use when the A2 and A4 have been damaged [72].

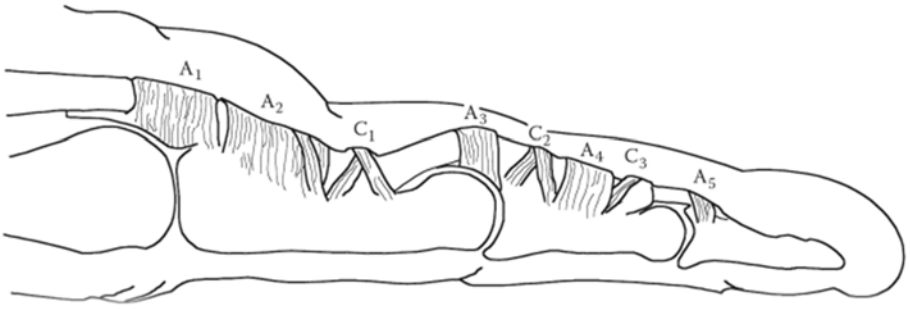

Figure A-7 Finger Pulley System: A, annular, C, cruciate[73]

A.11 Wrist Mechanics

Kinematic understanding of the human wrist joint is complex due to its large range of motion and dextrous capabilities. The structure of the various joint articulations plays a major role in the efficiency of wrist motion. During muscle contraction the carpal bones, radioulnar joint, proximal and distal carpal articulations, as well as numerous ligaments all work together in order to stabilize the wrist. An understanding of the osteokinematic movement of the joints with help from these components is therefore crucial in counteracting the shifts in the carpal bones during contraction [74].

The seven major muscles involved in wrist and hand motions are the: *flexor carpi radialis (FCR), flexor carpi ulnaris* (FCU), *flexor digitorum profundus* (FDP), *flexor digitorum* superficialis (FDS), *extensor carpi radialis brevis* (ECRB), *extensor carpi radialis longus* (ECRL), and the *extensor carpi ulnaris* (ECU). The FCR, FCU, ECRB, ECRL, and ECU are the main muscles whose primary function is to move the wrist, while the FDP and FDS are secondary wrist movers [60]. These muscles and tendons, involved in wrist movements, are described based on function below [75]:

- Flexion: FCR and FCU
- Extension: ECRB, ECRL, and ECU
- Radial Deviation: FCR, ECRB, and ECRL
- Ulnar Deviation: FCU and ECU

The characteristics typically used in order to describe the muscles are muscle fibre length (FL) and physiological cross sectional area (PCSA). The length of a muscle is directly related to the muscles mechanical potential for tendon excursion (the distance a tendon travels upon movement of a joint), and the maximum tension of the muscle to its physiological cross sectional area [75]. Upon wrist movement, each tendon slides across the wrist joint a certain distance to execute the motion, and the distance the tendon moved across the joint as well as the moment arm at various wrist joint angles can be measured and derived through experimentation [60].

A.12 Anthropometric Data

Mean Finger Lengths and Measurements

Dimensions of the fingers and of the palm and their respective range of motion are critical components in the analysis of kinematics and dynamics of the human hand and exoskeleton design. In Table A-1 and Table A-2, the results of Garrett's studies are shown where measurements were taken from the right hand of 148 men and 211 women who were Air Force Flight (USAF) personnel in 1968 [76]. In Table A-1, *crotch to tip* is the distance along the axis of the digit from the midpoint of its tip to the level of the corresponding webbed crotch between two digits; and *wrist crease to tip* is the distance along the axis of the digit from the midpoint of its tip to the wrist crease baseline [11], [76].

Table A-1 Mean finger length and palm dimensions of USAF male (M) and female (F) flying personnel in cm [11], [76]

	Finger Length (crotch to tip)				*Finger Length (wrist crease to tip)*			
	Mean	s.d.	<5%	<95%	Mean	s.d.	<5%	<95%
M								
Thumb	5.87	0.45	5.07	6.57	12.70	1.13	11.05	14.68
Index	7.53	0.46	6.83	8.19	18.52	0.88	17.33	20.06
Middle	8.57	0.51	7.82	9.74	19.52	0.92	18.10	21.04
Ring	8.0	0.47	7.44	8.93	18.72	0.91	17.52	20.28
Little	6.14	0.47	5.44	6.99	16.61	0.91	15.11	18.10
F								
Thumb	5.37	0.44	4.68	6.12	11.05	1.00	9.51	12.83
Index	6.90	0.52	6.10	7.80	16.67	0.89	15.21	18.14
Middle	7.79	0.51	7.01	8.68	17.65	0.87	16.22	19.05
Ring	7.31	0.52	6.52	8.22	16.76	0.94	15.28	18.20
Little	5.46	0.44	4.80	6.24	14.64	0.92	13.11	16.12

Table A-2 Average hand dimensions of USAF male (M) and female (F) flying personnel in cm [11], [76]

Measurement	*Mean length*
Hand Length	
M	19.72
F	17.93
Hand Breadth	
M	8.96
F	7.71
Hand Circumference	
M	21.59
F	18.71
Hand Thickness	
M	3.29
F	2.76
Hand Depth	
M	6.19
F	5.17

It is also important to note the individual length of each phalanx separately which was recorded in a study performed by Habib and Kama [77]. The results of their study is presented in Table A-3, where each phalanx of the index, middle, ring, and little fingers are recorded (I1 means distal phalanx, I2 middle phalanx, and I3 proximal phalanx of the index finger as well as the other fingers) [76], [77].

Table A-3 Mean length of the hand and of the phalanges of the index, middle, ring, and little fingers in cm [76], [77]

	Hand	*I1*	*I2*	*I3*	*M1*	*M2*	*M3*	*R1*	*R2*	*R3*	*L1*	*L2*	*L3*
Male Right hand	19.29	2.32	2.37	2.65	2.60	2.78	2.80	2.29	2.56	2.76	1.96	1.92	2.51
Male Left Hand	19.36	2.32	2.39	2.61	2.60	2.82	2.75	2.30	2.59	2.78	1.95	1.98	2.49
Female Right Hand	17.60	2.23	2.24	2.45	2.44	2.55	2.56	2.12	2.34	2.52	1.79	1.74	2.26
Female Left Hand	17.62	2.20	2.24	2.35	2.24	2.43	2.53	2.13	2.36	2.49	1.77	1.77	2.26

This data provides us with an understanding of the mean values of measurements for each individual component of the human hand. With these parameters, we are then able to compose a model for a novel hand exoskeleton that is better able to accommodate the exact dimensions of a standard adult hand.

Biological Ranges of Motion and Constraints

The natural function of the arm below the elbow involves various distinct movements at the wrist, thumb, and fingers. In the fingers, the metacarpophalangeal (MCP) joint permits flexion/extension,

as well as rotation, and the interphalangeal (IP) joints permit flexion/extension of the proximal, middle, and distal phalanges [11]. In the thumb, the metacarpophalangeal joint permits flexion/extension, abduction/adduction; the interphalangeal joint permits flexion and extension [11].

The normal range of motion (ROM) of the human hand joints correspond to static constraints on joint angles in the model. The main static constraints were collected by Cobos et al. [78], and can be seen in Table A-4 which presents the normal ranges of motion. A healthy human wrist is capable of moving in a large ROM in order to perform activities of daily living. A description of the terminology for the ROM of the wrist can be found in Table A-5.

Table A-4 Statics Constraints of finger joints [78]

Finger	*Flexion*	*Extension*	*Abd./Add.*
Thumb			
TMC	50°-90°	15°	45°-60°
MCP	75°-80°	0°	5°
IP	75°-80°	5°-10°	5°
Index			
CMC	5°	0°	0°
MCP	90°	30°-40°	60°
PIP	110°	0°	0°
DIP	80°-90°	5°	0°
Middle			
CMC	5°	0°	0°
MCP	90°	30°-40°	45°
PIP	110°	0°	0°
DIP	80°-90°	5°	0°
Ring			
CMC	10°	0°	0°
MCP	90°	30°-40°	45°
PIP	120°	0°	0°
DIP	80°-90°	5°	0°
Little			
CMC	15°	0°	0°
MCP	90°	30°-40°	50°
PIP	135°	0°	0°
DIP	90°	5°	0°

Table A-5 Range of Motion Terminology for the Wrist [79]

Terminology	*Definition*	*Range of Motion (mean)*	*Diagram [76]*
Extension (Dorsiflexion)	Bending motion of the wrist that causes the palm to face upward	0°-70°	
Flexion (Palmar flexion)	Bending motion of the wrist that causes the palm to face downward	0°-75°	
Abduction (Radial deviation)	Side motion of wrist towards the thumb and midline of the body	0°-20°	
Adduction (Ulnar deviation)	Side motion of the wrist away from the thumb and midline of the body	0°-35°	
Supination	Forearm rotation of the hand so that the palm faces upward	0°-85°	
Pronation	Forearm rotation of the hand so that the palm faces downward	0°-70°	

Appendix B

Current Hand Exoskeleton Summaries

Table B-1 Current hand exoskeletons driven by electric actuators

Reference	*Force Transmission*	*DOF*	*Rotation Points:*	*Attachment:*
MIT Manus (Hogan et al.) [13]	Brushless motors	3 at wrist	No finger extension/flexion. Wrist pronation/supination, flexion/extension, and abduction/adduction	Patients wrist is attached to a curved slider, actuators are mounted on the sides, and connected to a two spur gear train that meets at a differential mechanism (figure below)
HEXORR (Schabowsky et al.)[32]	4 bar linkage	2	Driver link base is aligned with MCP joints and the driver-coupler joint is aligned with the PIP joints. All 4 fingers have coupled MCP and PIP rotations, with a separate, similar but simplified, module for the thumb that rotates about the CMC joint	Patients forearm is placed on a resting bar and strapped onto the bar with two Velcro straps. The hand is attached to the exoskeleton on the dorsal side at 3 locations with the palm left unrestricted.
HANDEXOS (Chiri et al.) [33]	Cable, crank-slider	5	➢ 5 independent finger modules Each module is composed of 3 links for the phalanges, where COR of each is matched with corresponding finger joints. Flexion/extension of the MCP joint is driven by a slider-crank mechanism, while the PIP and DIP joints are driven by Bowden cable transmission	5 independent finger modules. Exoskeleton is composed of an external backing element applicable on the dorsal aspect of the wearers hand and shell like elements on each phalange, connected to one another by translational and rotational joints. Six

				pulleys (2 for each joint) are placed on both sides of the exoskeletons independent finger modules
iHandRehab (Li et al.) [35]	Cable	8	Only consists of finger modules for the index finger and thumb. All activated joints (index finger MCP (2DOF), PIP (1DOF), and DIP (1DOF)) (thumb CMC (2DOF), MP (1DOF), and IP (1DOF)) driven by 2 cable transmission mechanism for each joint. Each finger exoskeleton consists of 4 joint modules; DIP, PIP, MCP1, and MCP2.	The thumb and index finger module are fixed on a palmar base at locations fixed by the human hand. The palmar base, thumb, and index finger exoskeletons are mounted with Velcro on the dorsal aspect of the hand
IntelliArm (Ren et al.) [80]	Linkage	1 at wrist	Drives hand open at MCP and thumb joint attached to the end of the robotic arm. Makes use of the same four bar linkage with a single motor system. The motor will rotate the link L1 to open MCP joints of all four fingers; link L3 will push the thumb away synchronously. Therefore, MCP joints of all 4 fingers are driven by one motor while the thumb is driven by a coupled MCP joint motion.	The thumb of the patient is strapped into an arch shaped support, with an adjustable soft band. In order to guide the MCP joint, another brace is mounted and holds the remaining 4 fingers with a soft adjustable strap. Attached to a virtual environment

Table B-2 Current Hand Exoskeletons Driven by Pneumatic Actuators

Reference	*Force Transmission*	*DOF*	*Rotation Points:*	*Attachment:*
HWARD (Takahashi et al.) [38]	Linkage	3	Device composed of four fingers rotating as a single unit about the MCP joint. The thumb moves out of plane of the palm and fingers independently. And the wrist is capable of flexion/extension. Robot movement is achieved with a single lever design and a revolute joint in between. Device is pneumatically actuated with the use of 3 double-acting air cylinders which are each regulated to provide 4-15N of Force.	-palmar aspect of the hand is left unobstructed. The right hand is positioned in the device with the MCP joint and the wrist COR aligned with the robots finger and wrist joint axes. The dorsal aspect of the patients' fingers, hand and thumb contact the device, and are secured in place with the use of narrow padded Velcro straps. The subjects forearm rests inside a padded splint mounted to the surface of a platform.
Hand Mentor (Kinetic Muscles) [39]	Linkage	1 Per joint	-flexion/extension ROM in 5 independent finger modules. Each module has 2 shell-like links, one for the proximal phalange (PP), and one for the distal phalange (DP). The DP link is connected to one end of the PP link, with the other end of the PP link connected to the main base. The connection point of the links is placed at the joints of the fingers. →actuated by a stepper motor connected to the	The joint for the DP link is located at the fingers side, while the MP & PP links are above the metacarpal joint. All links are coupled with a pulley like design connection as the cable will use those pulleys as its canal

			main pulley which is connected to 5 different sized pulleys, with a clockwise rotation resulting in finger extension	
Wu et al. [16]	Cable, Linkage	2 per finger	In order to transform the translation into rotation, a pulley mechanism is designed and arranged above the joints. Wu et al. proposed a new PM-TS actuator structure with one pneumatic muscle and a torsion spring. The PM is arranged in a suitable place to provide the pulling motion, while the torsion spring provides the opposing torque	Patients hand is strapped to the device using a glove and three adjustable Velcro straps on the dorsal aspect of the hand and forearm. The PMs are arranged on top of the forearm attachment, and the torsion springs are mounted on the joints. Steel wires are used to connect the PMs & the pulleys, which result in rotation of the finger joints

Table B-3 Overview of Passive Hand Exoskeletons

Reference	*Force Transmission*	*DOF*	*Rotation Points:*	*Attachment:*
HandSOME (Brokaw et al.) [40]	Linkage	1	The finger MCP and thumb CMC joint positions were used as the rotation centers of the device. Device makes use of a 4 bar linkage to force the thumb and fingers in a coordinated grasp motion. Design uses elastic cords as springs to assist with finger & thumb extension and provide assistance profiles that emulate the torque vs. extension angle profiles for passive movement. The ground point of the spring is located at the end of a lever arm that can be rotated to change the assistance profile. When the lever arm is in its normal position, the spring path goes through the center of rotation of the finger MCP when the hand is in full finger flexion (0° of finger extension). Theta is defined as the angle of the lever arm relative to this normal position. By rotating the lever arm away from this normal position, the therapist is able to change the shape of the assistance profile and increase the amount of assistance	Padding and support straps are placed on the device on the back of the hand to maintain ideal positioning as well as added comfort throughout the movement. Velcro straps were positioned distally to prevent fingers from curling around straps. One strap was aligned with the distal phalanx of the pinky and another at the PIP joint of the pointer finger. If needed, a third strap was used across the distal phalanges of the middle three digits. A single Velcro strap was used at the IP joint of the thumb. Therefore, the straps restricted movement of the thumb IP joint, finger DIP, and finger PIP joints. The main movement is about the MCP of the fingers and the

			applied in the fully closed position. This allows individuals with no extension ability to use the device by simply relaxing their hand, causing the device to open their hand for them, whereas the setting will require some ability to extend volitionally from the fully closed position.	CMC joint of the thumb. A wrist brace was used for subject testing to maintain neutral wrist posture in the device and to ensure proper orientation of the HandSOME device on the subject's hand
Saeboflex [41]	Cable/spring	1	The saeboflex aids in finger extension at the MCP, PIP, DIP joints. The ground point of the spring is located on the forearm and helps pulls the fingers open in an extension motion during grasp and release tasks	Equipped with padding on the dorsal aspect of the hand and around the forearm exoskeleton connection point. Adjustable Velcro straps keep hand mounted in place. Also embodies 5 soft gel caps on the end of each digit. The finger caps prevent flexion at the fingertip and enhance comfort.

Appendix C

Instron Testing of Nylon 50lb and UHMWPE Actuators

Instron testing peak force output of nylon Big Game 50lb monofilament fibres

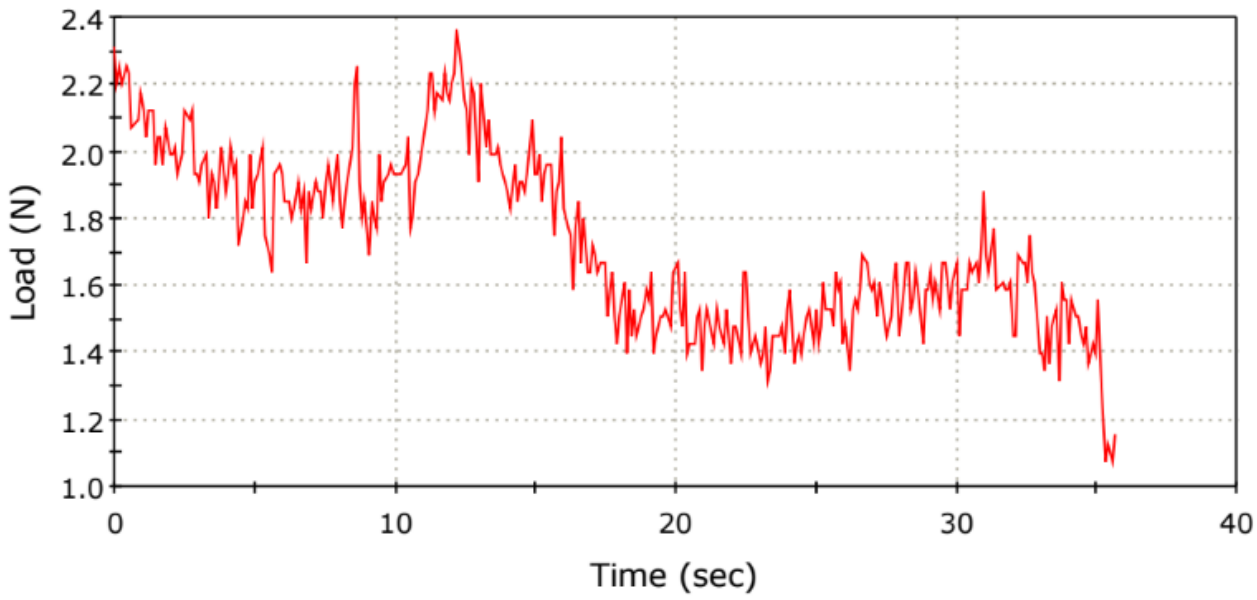

Initial tests began by turning the power supply on at a preloaded tension of 2N, and was turned off after the force output exhibited by the actuator began to decline. In order to not cause the first fibre to fail and determine whether it was contracting at all, this test was conducted with a slightly lower current.

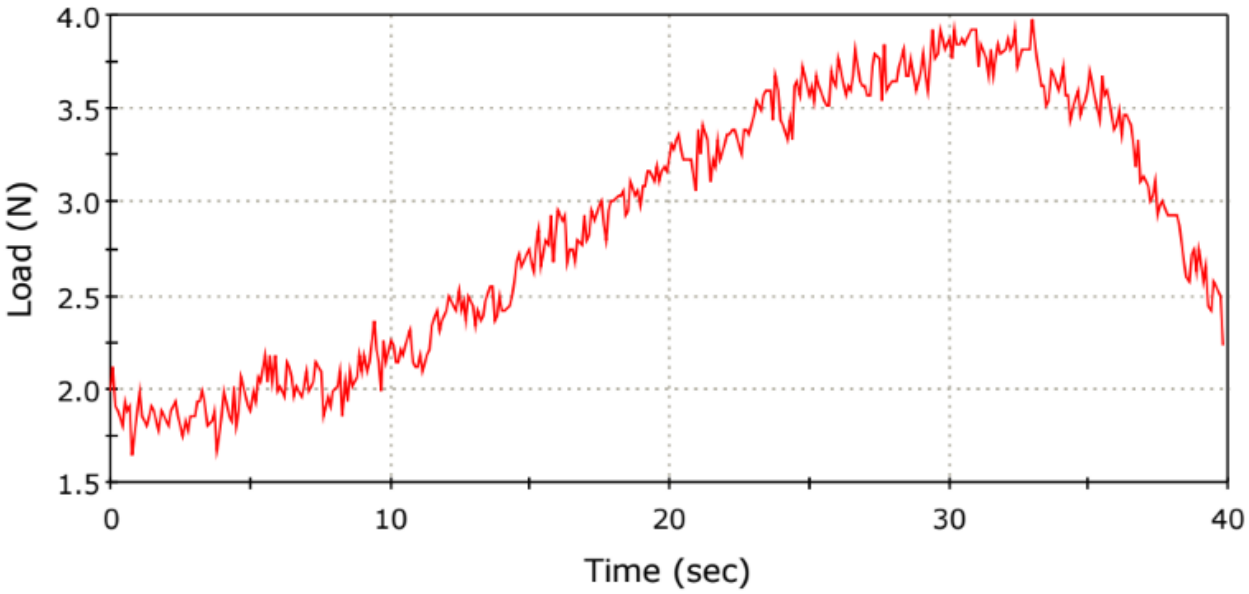

Now the power supply was turned on once the preloaded tension was at 2N, and turned off once the force output was recorded and began to decline. The peak force output here was approximately 4N.

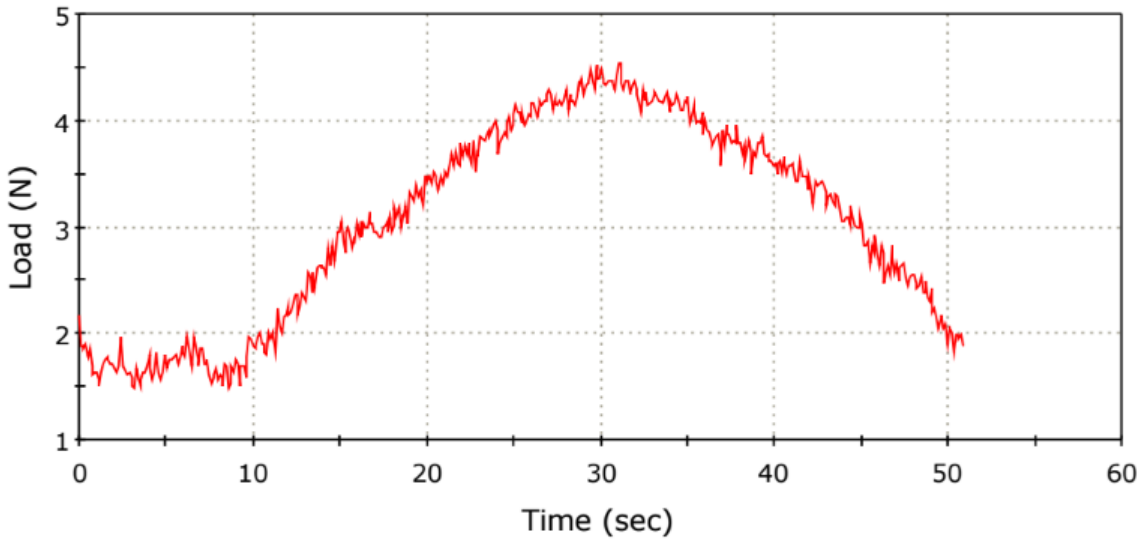

Again, the power supply was turned on once the preloaded tension was at 2N, and turned off once the force output began to decline. Here the peak was slightly higher at approximately 4.5N.

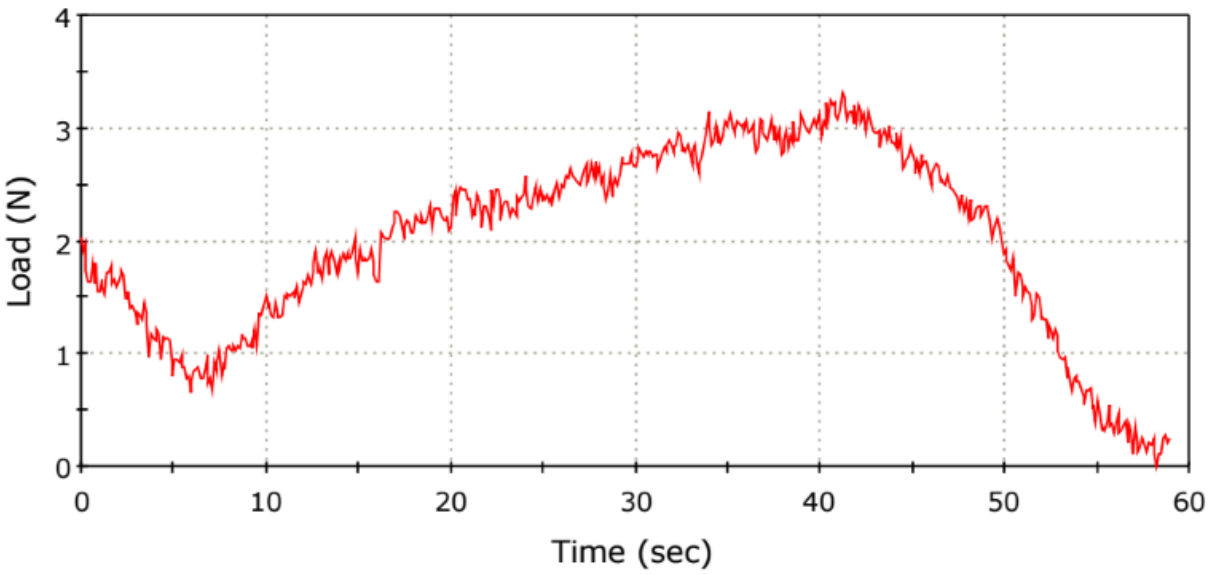

Now, at the preloaded tension of 2N, the power supply was turned on and remained on for a duration of 60 seconds to observe the force characteristics of the curve. This actuator exhibited a slightly lower peak force at 3.2N.

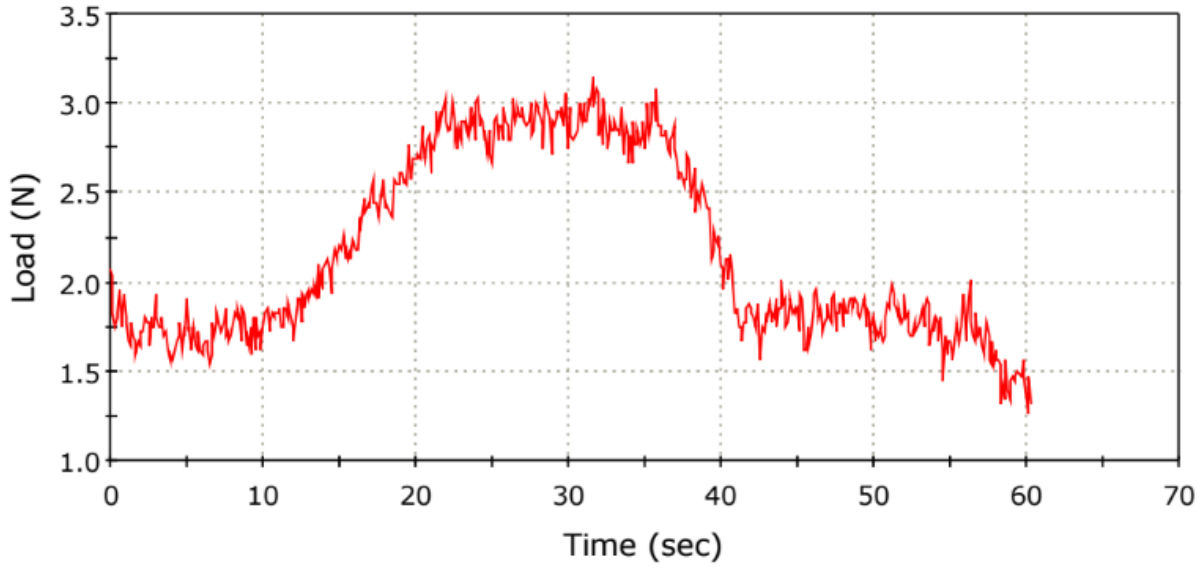

Again, at the preloaded tension of 2N, the power supply was turned on and remained on for a duration of 60 seconds to observe the force characteristics of the curve. This actuator exhibited similar force output as the previous with a peak of 3.1N.

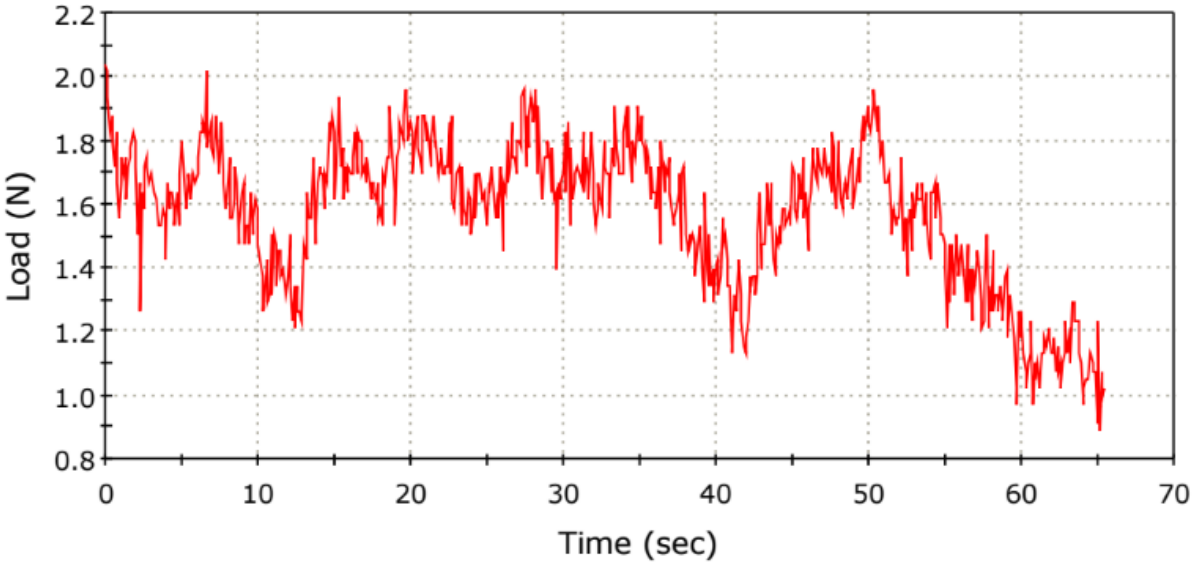

Again, at the preloaded tension of 2N, the power supply was turned on and remained on for a duration of 60 seconds to observe the force characteristics of the curve. The current for this actuator was increased to establish the highest force output, however, instead it resulted in failure.

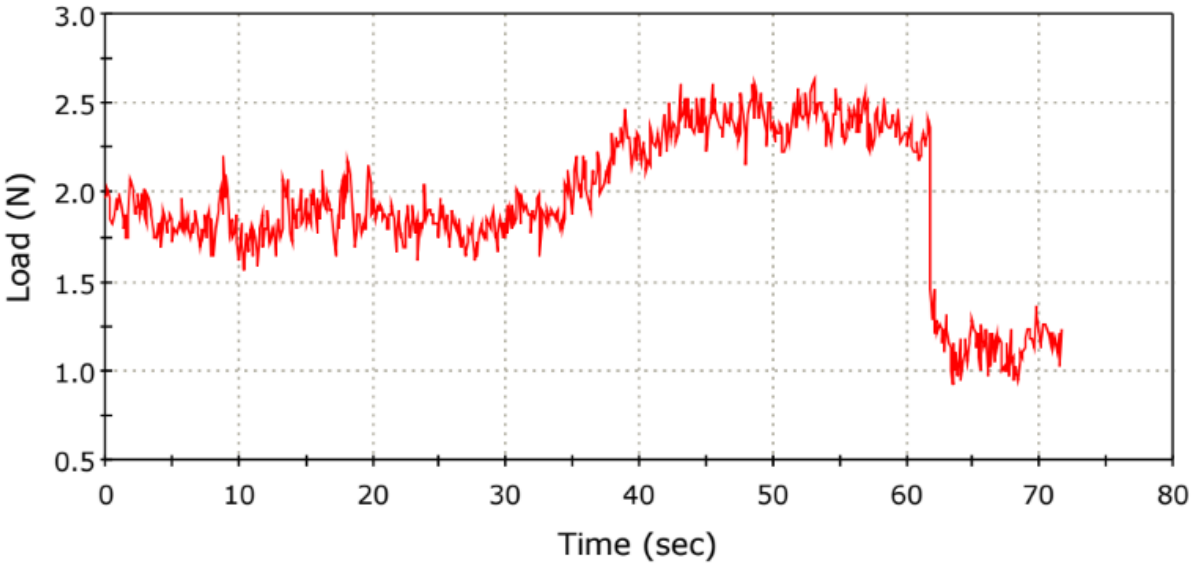

As seen above, testing began at the preloaded tension of 2N. The power supply was turned on and remained on for three minutes or until the actuator exhibited signs of failure. The current spontaneously increased during testing, resulting in the actuator failing at 62 seconds.

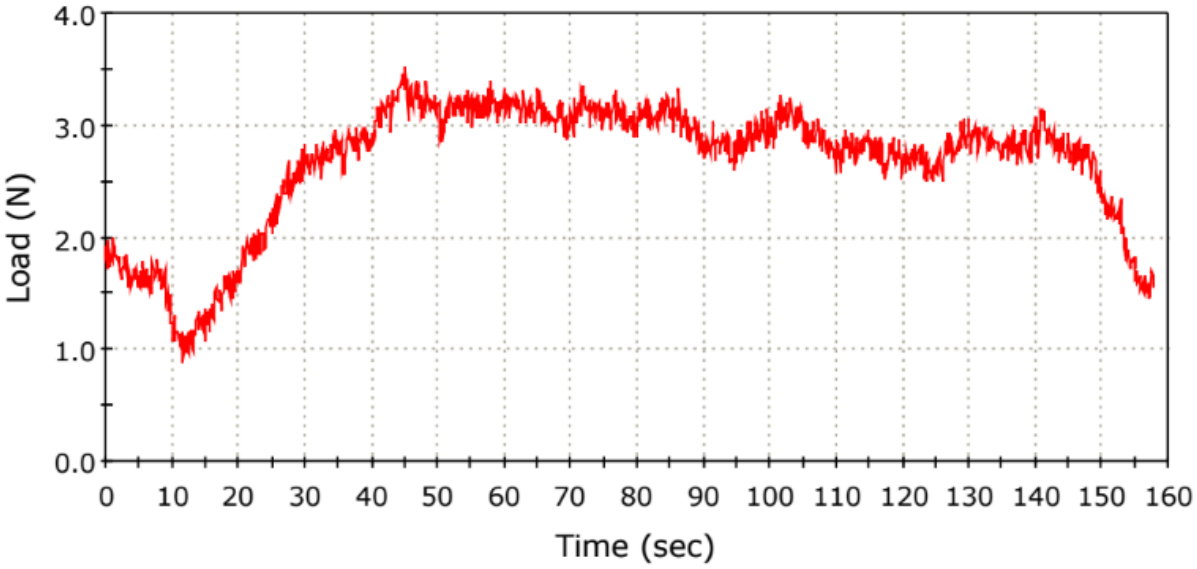

Testing began at the preloaded tension of 2N. The power supply was turned on and remained on for three minutes or until the actuator exhibited signs of failure. Results indicated that this actuator exhibited a peak force output of 3.5N.

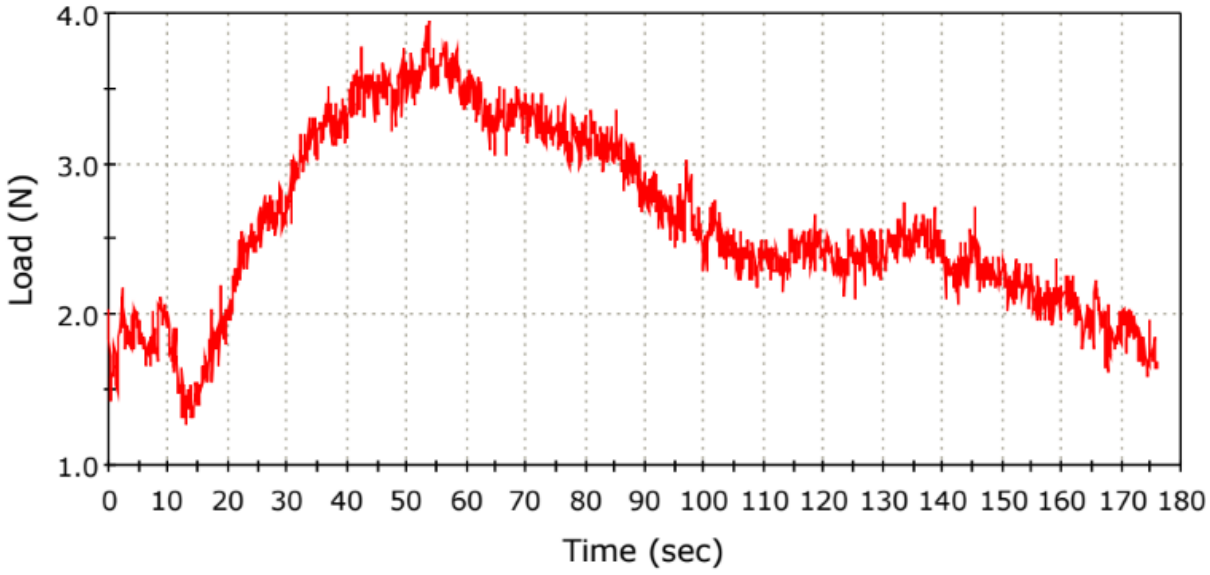

Testing began at the preloaded tension of 2N. The power supply was turned on and remained on for three minutes or until the actuator exhibited signs of failure. Results indicated that this actuator was capable of a slightly higher peak force output just short of 4N, with a very gradual decline.

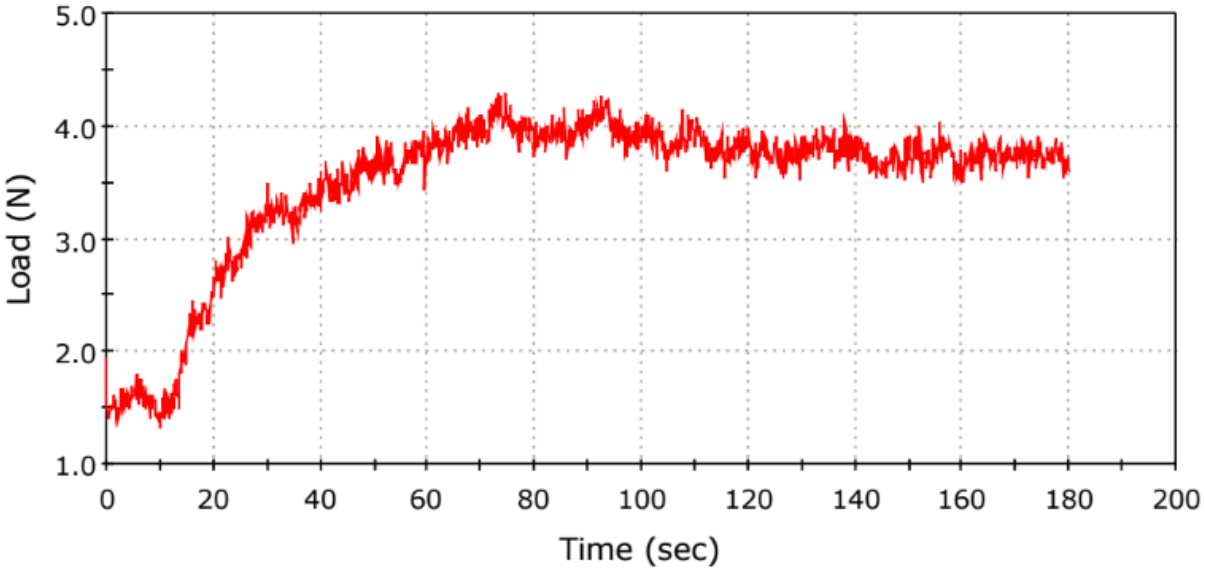

Testing began at the preloaded tension of 2N. The power supply was turned on and remained on for three minutes or until the actuator exhibited signs of failure. The peak force output seen in this graph was in the same range of results derived from other TCP actuators at approximately 4.1 N.

Instron testing peak force output of Polyethylene PowerPro fibres

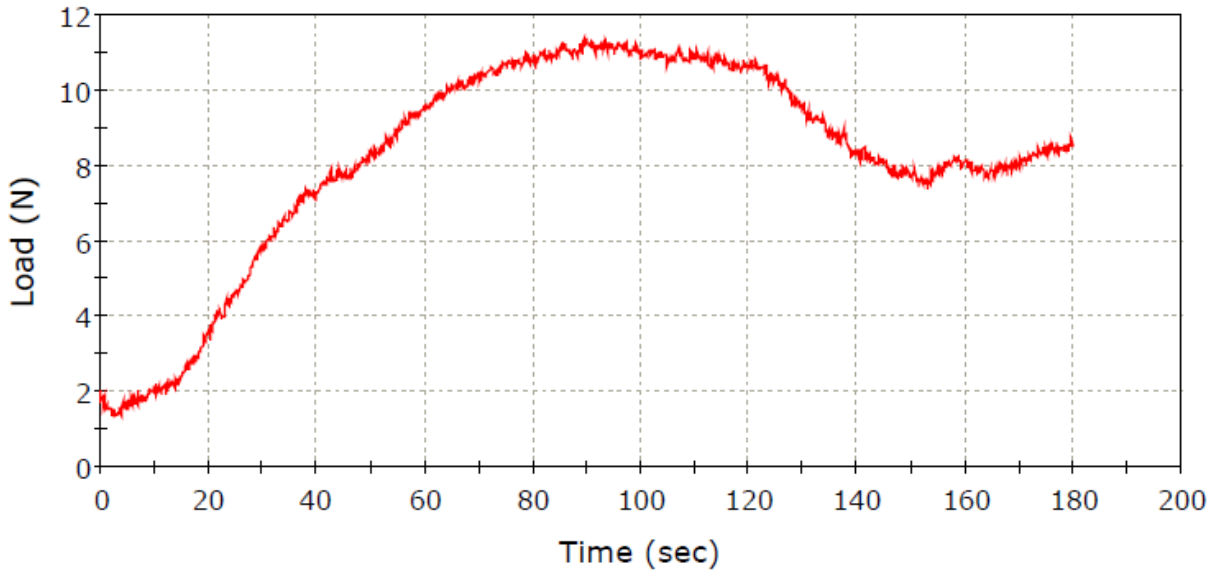

Polyethylene tests also began at a fibre pretension force of 2N. This graph shows the performance of the actuator when the power source was left on for a 3 minute time interval. The peak force output was similar to results obtained throughout this work of approximately 11N. This graph indicated that the polyethylene fibres are capable of maintaining their first contraction for a long period of time without exhibited signs of failure.

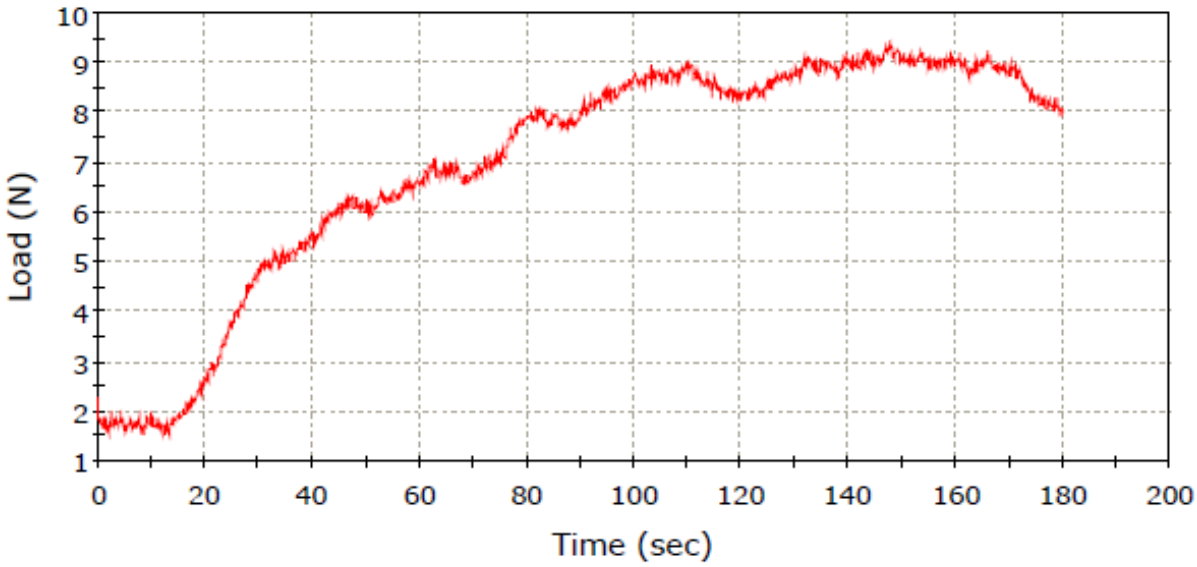

This test was done on a polyethylene fibre after it had already been exposed to Joule heating and had contracted one time. The substantial decrease in force output of approximately 7N is due to the creep that polyethylene exhibits. The fibre relaxed to a longer length than its original length; therefore it remained at the pretensioned 2N for about 20 seconds until it began to tighten on the machine. It then started to exhibit a force output that was much less than its initial test.